

Technische Universität Dortmund
Faculty of Electrical Engineering & Information
Technology

**Study and Implementation of Perpendicular
Magnetic Recorder for Automatic Magnetization of
Pole Tab**



MASTER THESIS

Bijna Balan
July 27, 2015

Supervisors:

Prof. Dr.-Ing. Andreas Neyer, (Technische Universität Dortmund)
Dr. Axel Bartos, Andreas Voss (TE Connectivity, Dortmund)

CONTENTS

1	INTRODUCTION	9
2	FUNDAMENTALS OF MAGNETISM	11
2.1	Magnetism	11
2.2	Permanent magnet	13
2.3	Electromagnetism	13
2.4	Hysteresis curve	15
2.4.1	Magnetic hysteresis loops for soft and hard materials	17
2.5	Magnetoresistive sensors	19
2.5.1	Anisotropic magneto resistive effect	20
2.5.2	Magnetic length sensors	22
3	MAGNETIC RECORDING	27
3.1	Typical magnetic recording system	27
3.2	Longitudinal magnetic recording	28
3.3	Perpendicular magnetic recording	29
4	MAGNETIC TAPE	33
4.1	Structure of the magnetic tape	33
4.2	Magnetization of the magnetic tape	35
4.3	Requirements of a pole tab	40
5	SYSTEM DESIGN	41
5.1	Design of write head	41
5.1.1	G-Head design	46
5.1.2	M-Head design	54
5.1.3	Comparison of G-Head and M-Head designs	59
5.2	Design of read head	60
5.2.1	Sensor system	60
5.2.2	Mechanical modeling and structure	60
5.3	Co-ordinate system	61
5.3.1	Position reference measurement system	63
5.3.2	Mechanical modeling and structure	65
5.4	Design of control program	66
6	SIGNAL PROCESSING AND ANALYSIS	77
6.1	Write process	77
6.2	Read process	79

7 EXPERIMENTS AND ANALYSIS	85
7.1 Effect of electric current on magnetization	85
7.2 Effect of air gap on magnetization	86
7.3 Analysis of magnetization effects on 5mm pole pitch	88
7.3.1 Effect of positioning error by KOSY3 stage	90
7.3.2 Effect of positioning error by PI stage	91
7.4 Analysis of error correction on 5mm pole pitch	93
7.5 Fourier analysis of signals	94
8 CONCLUSION	101

LIST OF FIGURES

Figure 2.1.1	Magnetic field or lines of flux of a moving charged particle.	13
Figure 2.3.1	Figure explaining the Biot-Savart's law	15
Figure 2.4.1	Figure explaining the formation of a B-H curve	17
Figure 2.4.2	Hysteresis Loop	18
Figure 2.4.3	(a) Magnetic hysteresis loop of hard magnetic materials (b) Magnetic hysteresis loop of soft magnetic materials	19
Figure 2.5.1	The geometry of a Hunt element. Image based on [AB12]	20
Figure 2.5.2	Physical origins of AMR (a) M is perpendicular to i and (b) M is parallel to i. The ovals represent the scattering cross-sections of the bound electronic orbits. When the orbits (and applied field) are perpendicular to the current direction, the electron scattering cross-section is reduced, giving a low resistance state. Conversely, when the orbits (and applied field) are parallel to the current direction, the electron scattering cross-section is comparatively high, giving a high resistance state.	21
Figure 2.5.3	Barber pole construction. Image based on [AB12]	21
Figure 2.5.4	Characteristic transfer curves for MR elements, (a) without and (b) with barber poles. Image based on [AB12]	22
Figure 2.5.5	The MLS sensor sliding over a magnetic pole tab.	23
Figure 2.5.6	Principle function of the MLS sensor. Image based on [Mei] . .	24
Figure 2.5.7	Principle function of the MLS5000 sensor. Image based on [Mei15]	25
Figure 3.1.1	Principle of magnetic recording	28
Figure 3.2.1	Longitudinal magnetic recording	28
Figure 3.3.1	Perpendicular magnetic recording	29
Figure 4.1.1	Structure of a magnetic tape	34
Figure 4.1.2	Comparison of isotropic-anisotropic materials (a) barium ferrite isotropy (b) strontium ferrite anisotropy (c) Magnetic domains oriented along the desired direction	35
Figure 4.2.1	Perpendicular magnetization of a pole tab	36
Figure 4.2.2	Incremental measuring system	37
Figure 4.2.3	Track system in absolute measuring system	38
Figure 4.2.4	Vernier coding scales	39

Figure 4.2.5	Gray code measurement system	40
Figure 4.3.1	Different pole pitches in magnetic tape	40
Figure 5.0.2	Block diagram of the overall system	42
Figure 5.1.1	Guided flux design of magnetic core	43
Figure 5.1.2	Comparison between guided flux and non-guided design of magnetic core (a) Guided flux design (b) Non-guided flux design	43
Figure 5.1.3	FEMM Simulation	46
Figure 5.1.4	The geometry design of G-Head	47
Figure 5.1.5	Simulation results of G-Head design. The figure on the right shows the magnetic flux distribution chart corresponding to the simulation result shown on the left.	49
Figure 5.1.6	Detailed view of the write tip of G-Head	49
Figure 5.1.7	The magnetic flux density at the write tip of G-Head	51
Figure 5.1.8	The magnetic field intensity at the upper layer of magnetic tape	51
Figure 5.1.9	The magnetic field intensity at the lower layer of magnetic tape	52
Figure 5.1.10	3D model of the write head	53
Figure 5.1.11	The prototype of the write head	53
Figure 5.1.12	The geometry design of M-Head	54
Figure 5.1.13	Simulation results of M-Head design. The figure on the right shows the magnetic flux distribution chart corresponding to the simulation result shown on the left.	55
Figure 5.1.14	Detailed view of the write tip of M-Head	55
Figure 5.1.15	The magnetic flux density at the write tip of M-Head	56
Figure 5.1.16	The magnetic field intensity at the upper layer of the magnetic tape	56
Figure 5.1.17	The magnetic field intensity at the lower layer of the magnetic tape	57
Figure 5.1.18	3D model of the M-head	58
Figure 5.2.1	Block diagram showing the working of the read head	61
Figure 5.2.2	3D model of the Read Head	61
Figure 5.2.3	Prototype of the Read Head (a) Complete read head assembly (b) Arrangement of MLS5000 sensor on the read head (c) MLS5000 sensor PCB	62
Figure 5.3.1	KOSY3 paltform (a) CAD drawing of the KOSY3 coordinate system (b) KOSY3 platform	63
Figure 5.3.2	CAD design of the system with the position reference system comprising of two linear encoders and corresponding scales for evaluation.	64

Figure 5.3.3	Linear magnetic encoder with magnetic scale	65
Figure 5.3.4	Linear optical encoder with stainless steel scale	66
Figure 5.3.5	3D model of the entire system. Figure on the left shows the front view and the figure on the right shows the side view of the 3D model.	67
Figure 5.3.6	Apparatus used for write and read process	68
Figure 5.4.1	Front panel and Block Diagram of a LabVIEW program	68
Figure 5.4.2	Control panel of the LabVIEW program	69
Figure 5.4.3	Manual control of the KOSY3 platform	69
Figure 5.4.4	Information and global control	70
Figure 5.4.5	Control of the translational stage on Y-axis	70
Figure 5.4.6	Control of the translational stage on Z-axis	71
Figure 5.4.7	Sensor Output Display	72
Figure 5.4.8	Automatic sequence display	72
Figure 5.4.9	Script Generator	73
Figure 5.4.10	Flowchart of the program flow	75
Figure 6.1.1	The write process explained in detail (a) shows the start position of the write head on a non-magnetized tape (b) shows the following stage in which the write head has written a pole pitch of 5mm with a particular polarity (denoted in red color) (c) shows the next stage in which the write head has written another pole pitch of 5mm with reversed polarity (denoted in green color)	78
Figure 6.2.1	Output from linear encoder	79
Figure 6.2.2	Block diagram showing the basic functioning of MLS5000 sensor	80
Figure 6.2.3	Raw values from MLS5000 sensor	80
Figure 6.2.4	Offset corrected output of the MLS5000 sensor with the inverse tangent values.	81
Figure 6.2.5	Lissajous figure of the sine and cosine output signals. The plot with raw sensor values does not form a perfect circle due to the difference in the amplitude of sine and cosine values. Offset corrected values gives a perfect circle.	82
Figure 6.2.6	Pole length determination from the inverse tangent values. The red arrows in the figure shows the start and end position of the pole pitch marked in green on top of the graph.	83
Figure 6.2.7	Pole pitches determined with respect to the alternating south and north poles in a magnetized tape.	83
Figure 6.2.8	Detailed analysis of error in pole pitch length	84

Figure 7.1.1	Error in pole length at pole edges written with 1.5A	86
Figure 7.1.2	Error in pole length at pole edges written with 2.5A	87
Figure 7.1.3	Error in pole length at pole edges written with 3.0A	87
Figure 7.2.1	Equivalent circuit diagram of a magnetic circuit with air gap .	89
Figure 7.2.2	Error in pole length written with 1mm air gap	89
Figure 7.3.1	Positioning error in Y-axis of KOSY3	91
Figure 7.3.2	Positioning error in linear translational stage in Y-axis	91
Figure 7.3.3	Error in pole length with Y-axis stage	92
Figure 7.3.4	Error in pole length on a standard magnetic tape	93
Figure 7.4.1	Effect of compensation step	93
Figure 7.4.2	Correction step to reduce error at pole edges (a) Beginning of write process where the electric current is supplied to the write head, placed at a distance from the tape, producing magnetic field in the circuit (b) Write head at the tape to magnetize it (c) After magnetizing a pole, the write head again moves to a distance where the polarity of the electric current is reversed (d) same process as in step (c) is repeated to magnetize another pole reverse polarity	95
Figure 7.4.3	Flowchart of error correction step	96
Figure 7.4.4	Full error range in pole pitch with comparison to the magnetic scales	97
Figure 7.4.5	Error range in the middle pole pitches	97
Figure 7.5.1	Fast Fourier transform magnitude plotted against frequency .	99
Figure 7.5.2	Harmonic analysis	99
Figure 7.5.3	Autocorrelation of signals	99

LIST OF TABLES

Table 2.5.1	Maximum permissible air gap for MLS sensor types	24
Table 5.1.1	Saturation flux densities of ferromagnetic materials	47
Table 5.1.2	Simulation results for various combinations of electric current and number of windings per coil	48
Table 5.1.3	Comparison of simulation results of G-Head and M-Head . .	59
Table 7.1.1	Effect of electric current on magnetic field intensity measured by a gauss meter	85
Table 7.1.2	Error range at pole edges for various level of electric current .	88
Table 7.2.1	Effect of air gap on the error range at pole edges	90
Table 7.3.1	Positioning error due to different stages in Y-axis	92
Table 7.5.1	Difference in the position values between two peaks of the signals from autocorrelation	100

INTRODUCTION

Data storage is one of the critical components of any information processing system. A widely used type of storage is the magnetic storage. One of the older types of magnetic storage media is the magnetic tape. The magnetic tape recorder was invented in 1928 and was primarily used for analog audio recordings. It is affordable and are capable to store large amounts of data. The data is stored by the imposing magnetic field, produced by an electrical signal, on a magnetically susceptible medium that gets magnetized. The binary information stored in terms of ones and zeros are represented by north and south magnetic polarities. One of the important features of a magnetic storage is that it provides non-volatile storage. The data encoded in the magnetic storage is not lost even when the storage device is not powered. This enables the magnetic storage devices to store a large amount of data and reuse the storage capacity by deleting older data. Hence, magnetic storage devices provide a cheap alternative to store a large amount of data and for subsequent retrieval.

The basic approach for storing data in a magnetic tape in any magnetic storage devices is similar. A write/read head moves very close to the magnetic surface. The write head modifies the magnetization of the material that results in the division of the magnetic surface into very small regions, each of which often has a uniform magnetization. Later, as the read head moves relative to the surface, the changes in magnetization from region to region are detected and recorded as zeros and ones. Different technologies used for this purpose often varies in the movement of the write/read head, relative to the surface of the media and the organization of regions on the media. However, the basic principle remains the same. Magnetic length encoding is established in various fields of industrial application as an efficient, durable and low-cost technology for position measurement. The read head usually incorporates hall or MR sensors for detecting the magnetic fields and the required position information is generated using an appropriate signal processing system. A positive aspect of this technology is that the process happens at high speeds since the scanning takes place on a totally non-contact basis. Hence, this technology can also be applied even in harsh environmental conditions.

Based on the orientation of the magnetic regions in a magnetized tape, magnetic recording methods can be broadly classified into Longitudinal Magnetic Recording (LMR) and Perpendicular Magnetic Recording (PMR) technology. In longitudinal

recording, the magnetic particles are aligned horizontally whereas in perpendicular recording, the magnetic particles are aligned vertically along the surface of the magnetic tape. The popularity of perpendicular recording, over longitudinal recording, has surged over the recent years, due to its higher storage density. The PMR system offers improved reliability and robustness. In PMR technology, the demagnetizing field in the magnetization transition can be reduced to a greater extent which results in high-density recording. Hence, perpendicular recording has the capability to extend the areal density past the limits of longitudinal recording. In both magnetic recording technologies, the write head plays a vital role. This thesis focuses on the design and construction of a structure comprising a write head and read head for producing absolute or incremental positioning magnetic scales, utilizing perpendicular magnetic recording technology for magnetizing the pole tabs. In order to evaluate the efficiency of the magnetization process, the read head is used, which consist of various magnetoresistive sensors corresponding to different pole pitch geometries. An error correction method can be incorporated for reducing the error margin on magnetic scales.

This thesis focuses on the following. Chapter 2 describes the fundamental of magnetism and the principles of magnetoresistive sensors. Chapter 3 explains the methods involved in magnetic recording. Chapter 4 reviews the basic structure and features of a magnetic tape. Chapter 5 focuses on the design and construction of the complete hardware setup along with the control program required to automate the processes involved. Chapter 6 describes the step followed to analyze the signals received from the apparatus. Various experiments performed, to evaluate the process of magnetization as well as to study the effect of different parameters involved, are explained in Chapter 7. Chapter 8 summarizes the outcomes of this thesis.

2

FUNDAMENTALS OF MAGNETISM

The story of magnetism dates back to the time of the existence of the first magnetic material known to man, i.e., magnetite (Fe_3O_4). The first truly known scientific study on magnetism was performed by William Gilbert (1540-1603), which was published in his book, *On the Magnet* in 1600. Magnetism is defined as the force of attraction or repulsion, acting at a distance between magnetic materials [CG11].

The basics of magnetism are discussed in Section 2.1. The characteristics of permanent magnet are explained in Section 2.2. The electromagnetic principles employed in the thesis work are reviewed in Section 2.3. One of the important characteristic of a ferromagnetic material is the magnetic hysteresis, which is discussed in detail in Section 2.4. The basic principles of magnetoresistive sensors that are used for evaluating the magnetization of a magnetic tape, are explained in Section 2.5.

2.1 MAGNETISM

Magnetism is defined as a class of physical phenomena that are interfered by magnetic fields. The forces of attraction and repulsion in a magnet originate at regions known as poles that are located near the ends of the magnet. That end of a magnet which points towards the geographical north pole of the earth is called the north-seeking pole or north pole. Similarly, there exist a region of south polarity towards the geographical south of the earth that is known as the south-seeking pole or south pole. The poles always appear in pairs and it is impossible to separate them. The unlike poles attract and the like poles repel. The law governing the forces between the poles were discovered independently by John Michell in 1750 and Charles Coulomb in 1785. Coulomb's inverse-square law states that the force of interaction between two poles is inversely proportional to the square of the distance between them and directly proportional to the scalar multiplication of their pole strength. The direction of the electrostatic force is along the straight line joining them. If the two poles have different polarity, then the electrostatic force between them is attractive and if the poles have the similar polarity, then the force between them is repulsive [CG11].

$$F = \frac{k_e p_1 p_2}{r^2} \quad (2.1.1)$$

where $k_e = \frac{1}{4\pi\mu_0}$ is the proportionality constant known as Coulomb's constant, p_1 and p_2 are the pole strengths of the two poles and r is the distance between them. μ_0 is the permeability of empty space which is equal to $4\pi * 10^{-7}$ Wb/Am. The force of interaction, F is measured in newtons (N).

A magnetic pole creates a magnetic field around it which produces a force on a second pole. This force is the product of the pole strength, p and the field strength or field intensity, H . It is measured in amperes per meter (A/m).

$$F = pH \quad (2.1.2)$$

where the proportionality constant is equal to 1. From this equation, the magnetic field strength, H can be defined as the field of unit strength which exerts a unit force on a unit pole. Since this field created by the magnet is capable of magnetizing an unmagnetized piece of iron when brought near to the magnet, it is also called the magnetizing force [Moro1].

$$H = \frac{p}{4\pi r^2 \mu_0} \quad (2.1.3)$$

From the Equation 2.1.3, it is clear that the magnetic field strength decreases with increase in the distance from the pole. A magnetic field can be represented by the imaginary 'lines of force'. These lines of force radiate outward from the north pole and return to the south pole [FLS13]. Figure 2.1.1 shows the direction of lines of force on a bar magnet.

The density of the magnetic field lines in an area determines the field strength. The magnetic flux (ϕ_m) can be defined as the total number of magnetic field lines passing through an area. The unit of the magnetic flux is weber (Wb). The amount of the magnetic flux passing through an unit area perpendicular to the direction of the magnetic flux, is the flux density B which is measured in newton-meters per ampere (Nm/A), also known as tesla (T). It is also called magnetic induction.

$$B = \phi_m A \quad (2.1.4)$$

where ϕ_m is the magnetic flux, B is the magnetic flux density and A is the area of the surface [FW99].

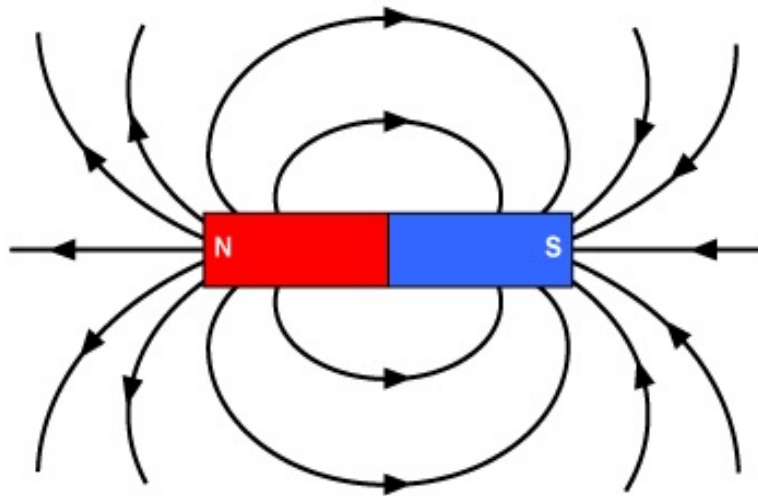


Figure 2.1.1: Magnetic field or lines of flux of a moving charged particle.

2.2 PERMANENT MAGNET

A magnet is a material or object that produces a magnetic field. Although invisible, the magnetic field is a force that attracts or repels other magnets and draws other ferromagnetic materials, such as iron towards it. A permanent magnet possesses its own persistent magnetic field. Materials that can be magnetized or strongly attracted to a magnet are called ferromagnetic (or ferrimagnetic) materials such as iron, nickel and cobalt. Although ferromagnetic (or ferrimagnetic) materials are the only ones attracted to a magnet strongly enough to be commonly considered magnetic, all other substances respond weakly to a magnetic field, by one of several other types of magnetism. A good permanent magnet should generate a high magnetic field with a low mass and it should remain stable against the influences that would demagnetize it.

2.3 ELECTROMAGNETISM

Until the 19th-century, magnetism was conceived to be a distinct phenomena. In 1820, the Danish physicist Hans Christian Oersted discovered that a wire carrying electric current produced its own magnetic field. His work, together with the works of Gauss, Faraday, Henry and others brought the magnetic field into prominence as a partner to

the electric field after which, electricity and magnetism are known to be constituents of the unified theory of electromagnetism [FLS13]. In the field of electrostatics, Coulomb's law is given as

$$F = \frac{k_e q_1 q_2}{r^2} \quad (2.3.1)$$

where $k_e = \frac{1}{4\pi\mu_0}$ is the proportionality constant, q_1 and q_2 are the two point charges at rest and r is the distance between them. μ_0 is the permeability of empty space. F is the electrostatic force.

As explained in Coulomb's law, magnetic force decreases inversely with the square of the distances between the charges. However, this is not precisely true when the charges are in motion; the forces also depends on the motion of these charges, which is one aspect of an electrical effect. The force experienced by a moving point charge or the electric current through a wire, when a magnetic field is applied, is called a Lorentz force [FLS13].

$$F = q(E + v * B) \quad (2.3.2)$$

where q is the point charge, E is the electric field, B is the magnetic field and v is the velocity of the charge. The magnetic field B can be defined from the Lorentz force and specifically from the magnetic force on a moving charge.

Faraday, in the early 1800's, showed that a magnetic field is produced by changing the electric field and vice-versa. Faraday's law of electromagnetism explains the interaction between a magnetic field and an electric circuit to produce an electromotive force (EMF). The Faraday's law of induction or the Maxwell-Faraday equation states that the electromotive force induced in a closed circuit is equal to the negative of the rate of change of the magnetic flux in the circuit [FLS13].

$$\nabla * E = - \left(\frac{\partial B}{\partial t} \right) \quad (2.3.3)$$

where E is the electric field and B is the magnetic field.

The Biot-Savart's law, is an equation that relates the magnetic field to the direction and magnitude of the electric current and to the proximity and length of the element carrying the electric current. It was named after Félix Savart and Jean-Baptiste Biot who discovered the relationship in 1820. The law states that, the magnetic flux density

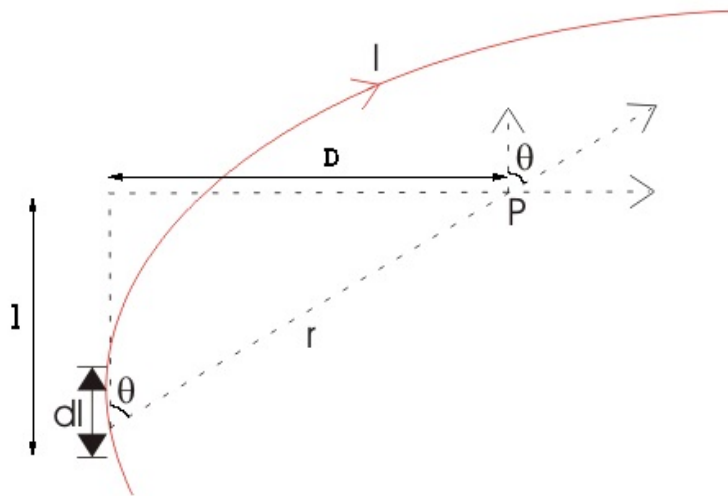


Figure 2.3.1: Figure explaining the Biot-Savart's law

dB at a given point p , is directly proportional to the current I , the length of the element dl and the sine of the angle θ between the direction of the current and the vector joining the current element and the given point p . It is also inversely proportional to the square of the distance r , between the given point p and the element dl . Figure 2.3.1 explains the Biot-Savart's law [RMCo8].

$$dB = k * \frac{Idl \sin \theta}{r^2} \quad (2.3.4)$$

where $k_e = \frac{1}{4\pi\mu_0}$ is the proportionality constant.

2.4 HYSTERESIS CURVE

The normal magnetization curve or the B-H curve shows the nonlinearity of the material permeability. The B-H curve is also known as the hysteresis loop. When a ferromagnetic (or ferrimagnetic) material is magnetized in one direction, the magnetization will not reduce back to zero when the magnetizing field is removed. It must be forced back to zero by applying a magnetic field in the reverse direction. Application of such an alternating magnetic field to the material, results in tracing out a loop called the hysteresis loop. The hysteresis is a property that is related to the existence of magnetic domains in a ferromagnetic material. Magnetizing a material

results in the reorientation of the magnetic domains and it takes some energy to turn them back again. This property of ferromagnetic materials is useful as a magnetic memory. Certain compositions of ferromagnetic materials have the capability to retain an imposed magnetization indefinitely and can be used as permanent magnets. The magnetic memory aspects of chromium oxides and iron make them beneficial for the magnetic storage of data on computer disks as well as in audio tape recording [WT99]. From the B-H curve, the following primary magnetic properties of a material can be determined.

- **Retentivity** - It is defined as a material's ability to retain a certain amount of residual magnetic field even when the magnetizing force is removed after reaching saturation. The measure of the magnetic flux density that remains in the material when the magnetizing force is brought to zero after the saturation is called the residual magnetism. The retentivity and the residual magnetism are the same when the material is magnetized to the saturation point. However, the retentivity value may be higher than the level of residual magnetism when the magnetizing force did not reach the saturation level.
- **Coercive Force** - It is defined as the amount of reverse magnetic field that must be applied to the magnetic material to bring the magnetic flux back to zero.
- **Permeability** - Property or ability of a material to establish magnetic flux within itself is defined as permeability.
- **Reluctance** - In the analysis of magnetic circuits, it is analogous to the resistance in an electrical circuit. It is defined as the opposition that a ferromagnetic material exhibits to the establishment of a magnetic field.

Figure 2.4.1 shows the stepwise formation of a B-H curve which is explained below in detail.

1. When an increasing field force is applied (current through the coils of the electromagnet), the flux density increases (go up and to the right) until it reaches the saturation level.
2. Stop the current supply. Due to the retentivity of the material, a magnetic flux persists with no applied force (no current through the coil). The electromagnet core is acting like a permanent magnet at this point.
3. Apply the same amount of magnetic field force in the opposite direction. The flux density reaches a point equivalent to that with a full positive value of field intensity (H), except in the negative direction.

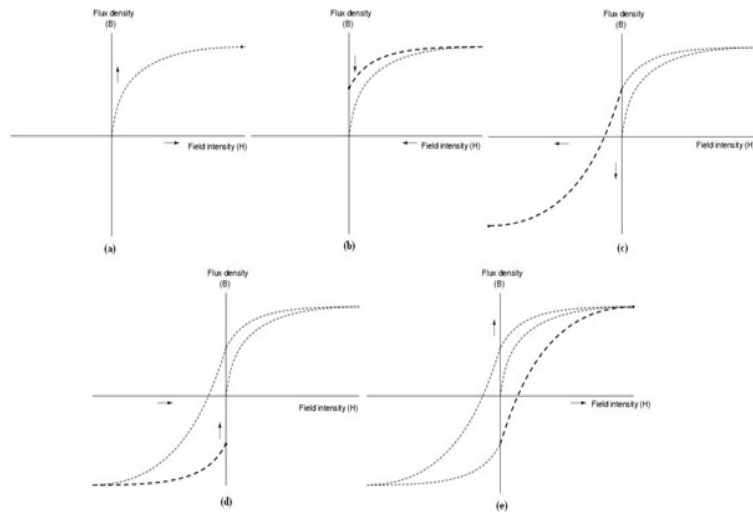


Figure 2.4.1: Figure explaining the formation of a B-H curve

4. Stop the current supply through the coil again. Due to the natural retentivity of the material, it will hold a magnetic flux with no power applied to the coil, in the opposite direction.
5. If the power is re-applied in the positive direction again, the flux density reaches its prior peak.

The 'S'-shaped curve traced by the above steps by varying the magnetic field intensity between the extremes, $+H$ and $-H$ is known as the hysteresis curve of a ferromagnetic material. Figure 2.4.2 shows the magnetic hysteresis loop in detail.

2.4.1 Magnetic hysteresis loops for soft and hard materials

The magnetic hysteresis curve shows the magnetization properties of the materials. It explains the magnetization and demagnetization properties of a material. Some materials tend to magnetize and demagnetize faster than other materials. The materials that remain magnetized even after the external magnetic field is removed, display a form of memory. The ferromagnetic materials tend to have memory because they remain magnetized even after the removal of the external magnetic field.

Those ferromagnetic materials that can be easily magnetized at low magnetic fields are called soft magnetic materials. Soft ferromagnetic materials such as silicon steel or

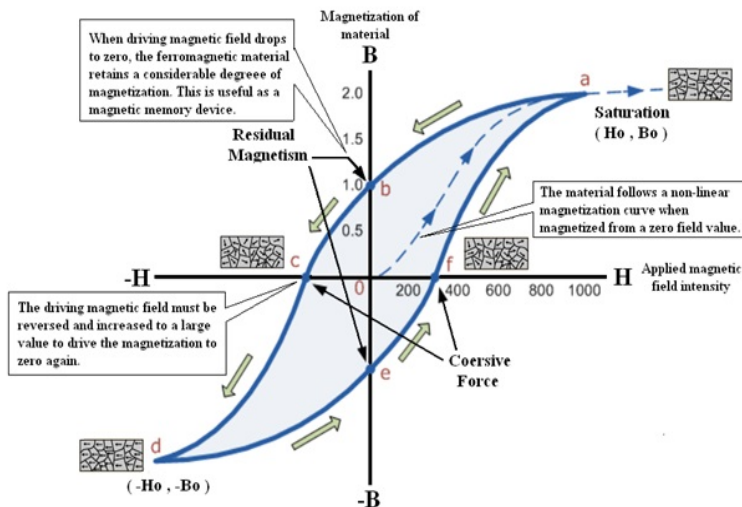


Figure 2.4.2: Hysteresis Loop

iron have very narrow magnetic hysteresis loop that results in very small amounts of residual magnetism. This property makes them ideal for use in solenoids, relays and transformers since they can be easily magnetized and demagnetized. Such materials have low coercivity and high permeability. A coercive force must be applied to overcome this residual magnetism that results in the dissipation of energy in the magnetic material, in the form of heat. This heat loss is known as hysteresis loss. For e.g., silicon has very low coercive force. Such materials with narrow hysteresis loop can be easily magnetized and demagnetized. Also, by adding silicon to iron, the coercive force of iron can be reduced.

When the magnetic domain is difficult to migrate, a high magnetic field should be applied for the magnetization of such ferromagnetic material. This type of ferromagnetic materials are difficult to magnetize, but once magnetized, it is hard to demagnetize. These materials are called hard magnetic materials. They are suitable for applications such as magnetic recording and permanent magnets. Such materials have high coercivity and low permeability. Figure 2.4.3 shows the magnetic hysteresis loop of soft and hard magnetic materials [HH89].

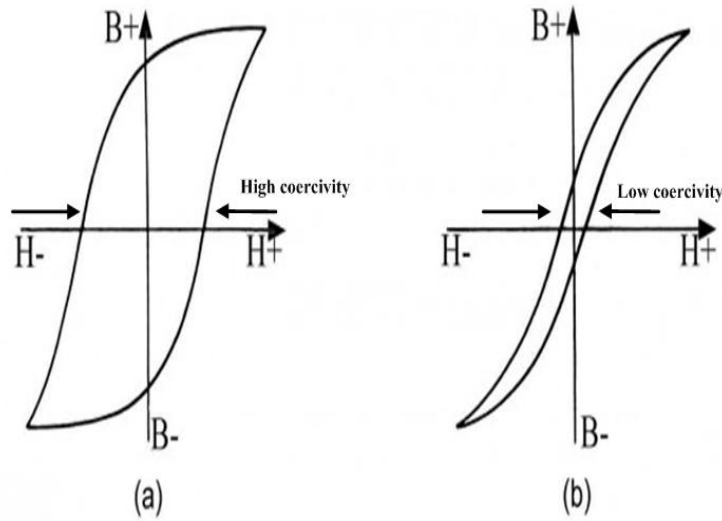


Figure 2.4.3: (a) Magnetic hysteresis loop of hard magnetic materials (b) Magnetic hysteresis loop of soft magnetic materials

2.5 MAGNETORESISTIVE SENSORS

Magnetoresistance (MR) is defined as the property of a material that results in the change of its electrical resistance when an external magnetic field is applied to it. This phenomenon occurs in all metals. The MR effect of a material depends on both the strength and the direction of the magnetic field with respect to the current[WT99].

Magnetoresistance was discovered by Lord Kelvin in 1857 when he noticed the sparse change in the electrical resistance of a piece of iron when it was placed in a magnetic field. However, it took more than 100 years for the first magnetoresistive sensor concept to be reported by Hunt in 1971. The geometry of a Hunt element that includes a magnetoresistive film with a magnetization vector (M) and a sense current (I) at a signal determining angle (α) to the current in the plane of the film is depicted in Figure 2.5.1. A magnetic field (H_y) coupled into the soft magnetic sensor material will change the resistivity of the material, which is probed by the sense current [AB12].

The change in resistivity is found experimentally to be

$$R = R_0 \left(1 + \frac{\Delta R}{R} \cos^2 \alpha \right) \quad (2.5.1)$$

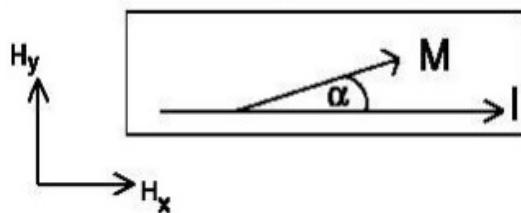


Figure 2.5.1: The geometry of a Hunt element. Image based on [AB12]

where R_0 is the resistivity of the material with magnetization perpendicular to the sense current ($\alpha = 90^\circ$). Permalloy, a nickel-iron alloy, with approximately 80% nickel content is chosen for magnetic sensors utilizing the magnetoresistance effect because of its excellent properties. The value of the MR coefficient $\Delta R/R$ is typically 1.5% – 3% for permalloy, depending on the preparation conditions and stripe geometry. An approximation between the applied magnetic field in y direction H_y and the signal determining angle α can be given for $H_y < H_{\text{eff}}$.

$$\sin \alpha = \frac{H_y}{H_{\text{eff}}} \quad (2.5.2)$$

where H_{eff} is a sensor specific constant in the order of $H_{\text{eff}} \approx 1 - 2 \text{KA/m}$

Magnetoresistive sensors can be used in high field and low field applications. In high magnetic field applications, the field strength of the applied field should be sufficiently high to saturate the soft magnetic sensor material. The magnetization vector is almost parallel to the applied field in such sensor. A common application for an MR high field sensor is a position sensor or a contact-less angular sensor [AB12].

2.5.1 Anisotropic magneto resistive effect

Anisotropic MagnetoResistance (AMR) is the property of a material in which a dependence of electrical resistance on the angle between the orientation of the magnetic field and the direction of electrical current is observed. This effect is because of the scattering of the electrons in the direction of magnetic field. Thus, the electrical resistance is maximum in the direction of applied magnetic field [Ste04].

The changes in magnetization of a Hunt element will be small if a small magnetic field is applied. A Hunt element is insensitive to low magnetic field strengths. The MR transfer curve needs to be modified to make MR sensors sensitive to low magnetic fields. Barber poles are employed to improve the low magnetic field sensitivity [Tumo1].

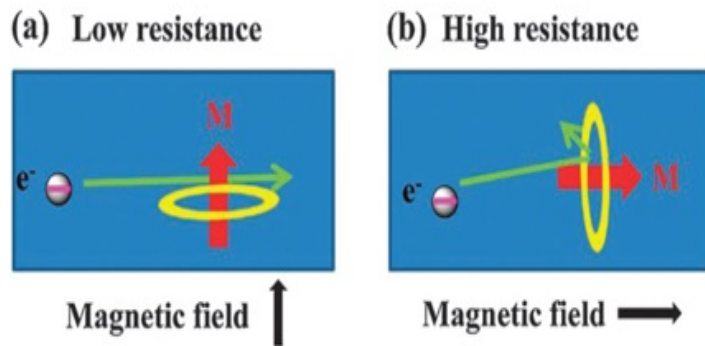


Figure 2.5.2: Physical origins of AMR (a) M is perpendicular to i and (b) M is parallel to i . The ovals represent the scattering cross-sections of the bound electronic orbits. When the orbits (and applied field) are perpendicular to the current direction, the electron scattering cross-section is reduced, giving a low resistance state. Conversely, when the orbits (and applied field) are parallel to the current direction, the electron scattering cross-section is comparatively high, giving a high resistance state.

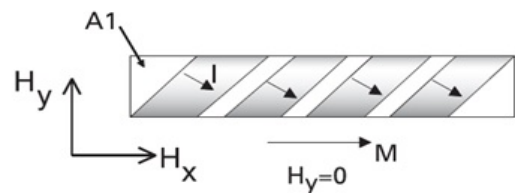


Figure 2.5.3: Barber pole construction. Image based on [AB12]

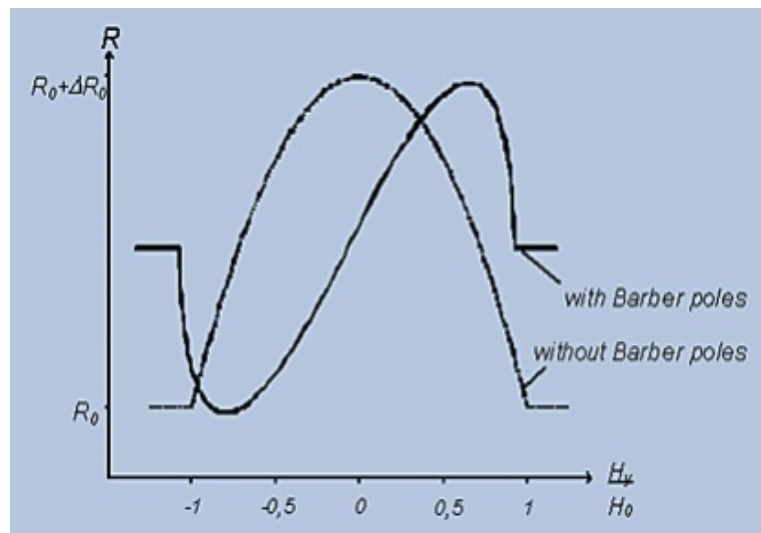


Figure 2.5.4: Characteristic transfer curves for MR elements, (a) without and (b) with barber poles. Image based on [AB12]

The geometry of a Hunt element with barber pole structure (a single AMR-Resistor) is depicted in Figure 2.5.3.

Now, with no field present, the signal determining angle will be 45° i.e. α has to be substituted by $\alpha = \alpha + 45^\circ$ which will change Equation 2.5.1 to

$$R = R_0 \left(1 + \frac{\Delta R}{R} \sin \alpha \sqrt{1 - \sin^2 \alpha} \right) \quad (2.5.3)$$

Substituting Equation 2.5.2 into Equation 2.5.3 results in

$$R = R_0 \left(1 + \frac{\Delta R}{R} \left(\frac{H_y}{H_{eff}} \right) \sqrt{1 - \left(\frac{H_y}{H_{eff}} \right)^2} \right) \quad (2.5.4)$$

which now reveals linearity with H_y for $H_y < \frac{1}{2}H_{eff}$

2.5.2 Magnetic length sensors

Magnetic Length Sensors (MLS) are AMR gradient sensors that are well suited for measuring linear displacements, movements and velocities. They are high precision

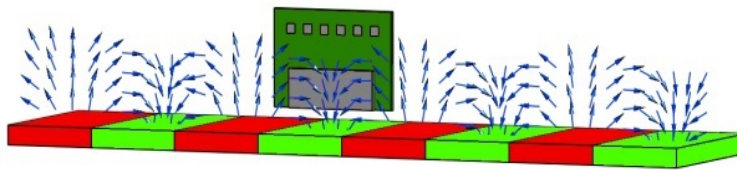


Figure 2.5.5: The MLS sensor sliding over a magnetic pole tab.

sensors available for various pole pitches (hybrid series). When the MLS Sensors are moved along a magnetic scale, a sine and a cosine output signal is produced as a function of the position. In order to achieve satisfying results, the air gap between the magnetic scale and the sensor edge should not exceed approximately half of the pole pitch. Figure 2.5.5 shows sliding an MLS sensor over a magnetic scale.

As the sensor principle is based on the anisotropic magnetoresistance effect, the amplitude of the signals are nearly independent of the magnetic field strength and therefore the variations in the air gap do not have a sound impact on the accuracy. Since the sensor detects a magnetic gradient field, it is almost insensitive to homogeneous magnetic stray fields. A sine/cosine decoder device helps in achieving precise displacement values. The maximum obtainable precision depends on the accuracy of the distance sensor and the magnetic scale. It is common to achieve values of less than 1% of the pole pitch.

The MLS sensors consists of two magnetoresistive Wheatstone bridges. The resistors of the Wheatstone bridges are placed in a way that it produces a sine and a cosine signal when used in combination with a magnetic scale. Thus, MLS sensors will only work together well with pole tabs that meet the design pole pitch. In addition, some sensor types blend over more than one pole in order to improve sensor performance. Figure 2.5.6 shows the arrangement of the Wheatstone bridges to produce sine and cosine signals from an MLS sensor.

The MLS hybrid series consist of 3 types of sensors - MLS1000, MLS2000, MLS5000. Each sensor is designed to measure a pole pitch of 1mm, 2mm and 5mm respectively. The parameters of the MLS sensors are measured in combination with the magnetic scale. The important thing to note is that the pole pitch of the scale has to match to the sensor type. Table 2.5.1 shows the maximum permissible air gap between the sensor module and the magnetic scale [Mei].

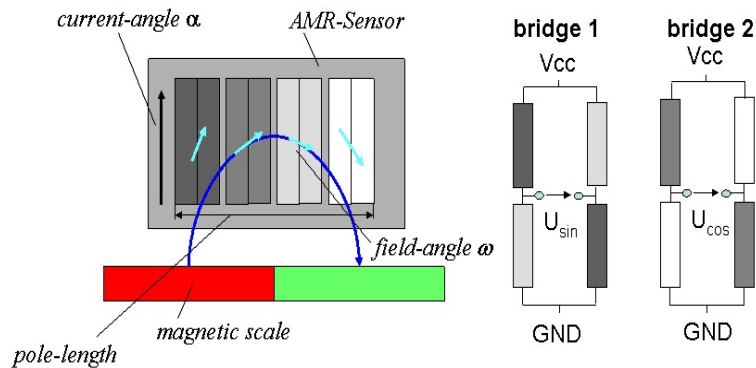


Figure 2.5.6: Principle function of the MLS sensor. Image based on [Mei]

MLS sensor type	Maximum air gap permissible (mm)
MLS1000	0.5
MLS2000	1.0
MLS5000	2.5

Table 2.5.1: Maximum permissible air gap for MLS sensor types

MLS5000 Sensor

Since the thesis work focuses on magnetic scales with pole pitch of 5mm, MLS5000 sensor was used for evaluating the magnetic scale. The MLS5000 is a magnetoresistive sensor designed to measure displacements utilizing a magnetic scale with a period (i.e. pole distance) of 5mm. In addition, rotational angles can be measured using pole wheels with similar magnetic periods. Sliding the MLS5000 along a magnetic scale, the two Wheatstone bridges will produce a sine and a cosine output signal. The distance between sensor edge and magnetic scale surface should not exceed 2.5mm. Precise displacement values will be archived by appropriate sine/cosine analysis that can be performed numerically in a micro-controller or by using a sine/cosine decoder. Figure 2.5.7 shows the working of an MLS5000 sensor.

The MLS5000 sensor has been designed for working together with a magnetic scale. These pole tabs usually consist of a thin steel back with an approximately 1 mm thick layer of plastic bound magnetic material on its front side. The permanent magnet layer generates a strong magnetic field close to its surface which decreases exponentially

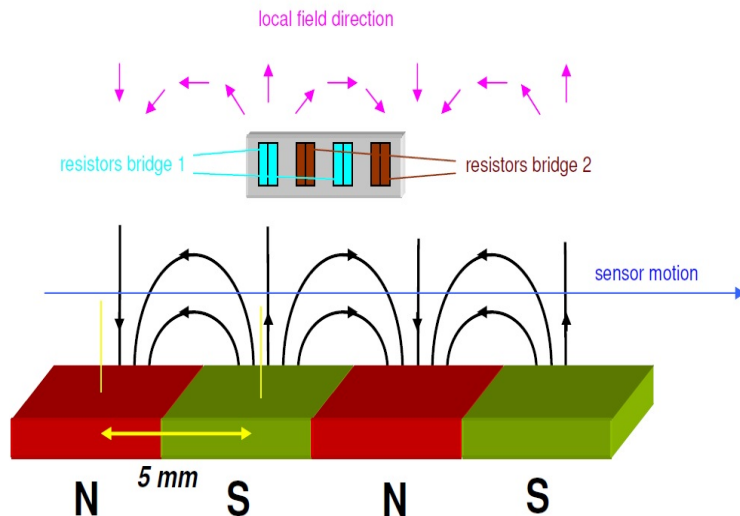


Figure 2.5.7: Principle function of the MLS5000 sensor. Image based on [Mei15]

with increasing distance. Therefore, a well defined and controlled distance between the sensor and magnetic scale has to be ensured during operation.

The magnetic layer is periodically magnetized with alternating south and north poles with a single pole length of 5 mm (periodicity = 10 mm). It is important to note that the MLS5000 sensor works properly only with a magnetic scale with a pole length of 5 mm. Using such a magnetization, the magnetic field at the sensor position will rotate when the sensor is moved along the magnetic scale. These are highly desirable conditions for the sensors using the anisotropic magnetoresistive effect because such sensors detect only the direction of the field, independent of the field strength as long as the field strength does not exceed the saturation field of the sensor material.

Therefore, a suitable pole tab should generate a strong field near its surface, which rotates proportional to the position when sliding along the scale. In order to detect the angle of magnetic field lines, both rotational sensors and special length sensors can be employed. The major advantage of special length sensors over the rotational sensors is that the rotational sensors are designed to work only in homogeneous fields whereas the special length sensors like MLS sensors are gradient type that are designed to work in both homogeneous as well as non-homogeneous fields. They are almost insensitive to external disturbing fields. In addition, even irregularities of the field rotation caused by irregularities of the pole tab are being averaged out for most of the measured data [Mei15].

3

MAGNETIC RECORDING

Magnetic recording is the process of storing data on a magnetized medium. Magnetic storage uses different patterns of magnetization in a magnetizable material to store data. It acts as a form of non-volatile memory. The information stored on a magnetic medium can be accessed using one or more read heads. In this chapter, Section 3.1 describes a typical magnetic recording system. Section 3.2 and Section 3.3 gives an overview of different types of magnetic recording.

3.1 TYPICAL MAGNETIC RECORDING SYSTEM

A magnetic recording system consists of a flexible or rigid substrate coated with a magnetically susceptible medium, which becomes magnetized when moved past a write head. The magnetic medium employed is a magnetic tape: a thin plastic ribbon with randomly oriented microscopic magnetic particles glued on the surface. A current in the winding of the write head magnetizes the head material, which creates a magnetic field in the head gap. The magnetic field imposed by the write head alters the polarization (not the physical orientation) of the miniature particles in a way that they align their magnetic domains according to the imposed field. The stronger the magnetic field applied, the more particles align their orientations. Hence, the strength of the magnetic field should be sufficient to magnetize all particles. The representation of a signal is retained with the magnetization stored in the material.

To read back the recorded information, the recorded track (magnetized medium) is moved under a read head. The fringing magnetic field from the recorded tape magnetizes the read head as it passes by the head gap, and the changing magnetization in the read head generates a signal voltage in the head winding. This voltage contains the recorded information and can be amplified to recreate the information. The basic working principle of magnetic recording is shown in Figure 3.1.1. There are two types of magnetic recording methods [Low72], [Pea67], [CC99]. They are:

1. Longitudinal Magnetic Recording (LMR)
2. Perpendicular Magnetic Recording (PMR)

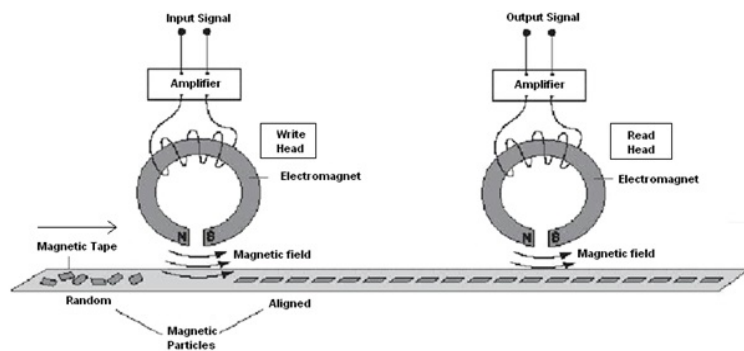


Figure 3.1.1: Principle of magnetic recording

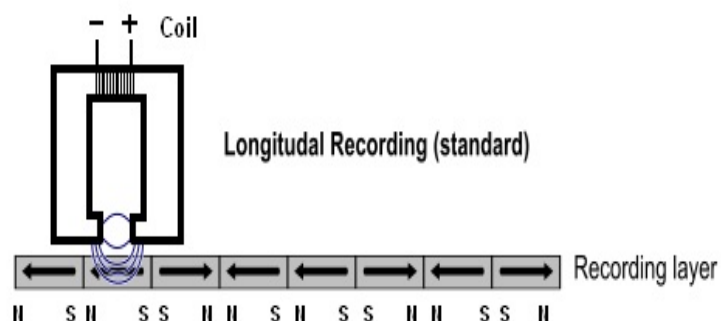


Figure 3.2.1: Longitudinal magnetic recording

3.2 LONGITUDINAL MAGNETIC RECORDING

Under longitudinal recording technology, the magnetic particles are aligned horizontally, side by side. The field from the write head switches the magnetization between the two stable states of magnetization. The magnetic fields between two adjacent poles with opposing magnetizations are separated by a transition region. The schematic representation of LMR is shown in Figure 3.2.1.

The major work in the field of longitudinal recording technology was carried out to decrease the size of the magnetic particles. The smaller the particles, the higher data that can be stored in the magnetic tape. Shrinking the magnetic particles, however, leads to a problem called superparamagnetism, which compromises the data integrity. Superparamagnetism is a form of magnetism, which appears in small ferromagnetic

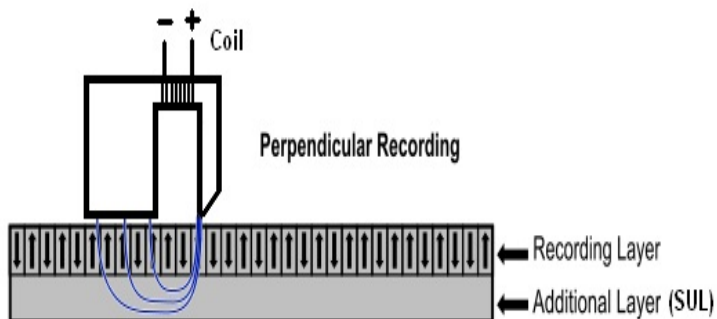


Figure 3.3.1: Perpendicular magnetic recording

or ferrimagnetic nanoparticles. In sufficiently small nanoparticles, magnetization can randomly flip direction under the influence of temperature, which would corrupt the stored data. In the superparamagnetic state, an external magnetic field is able to magnetize the nanoparticles, similarly to a paramagnet. Hence, superparamagnetism prevents from increasing the storing density of a magnetic tape [Mee86], [Pea67].

3.3 PERPENDICULAR MAGNETIC RECORDING

Under perpendicular recording technology, the magnetization in the recording surface is held in the form of perpendicular anisotropy by which the magnetic moment of the material tends to align in the perpendicular axis that forms the energetically favorable direction for spontaneous magnetization. The schematic representation of a PMR system is shown in Figure 3.3.1, where the recording head is a single pole structure. A closed path for the magnetic flux is provided through a Soft Under Layer (SUL) underneath the hard magnetic film, which is used as the recording medium [Low72], [Whi85].

The major advantages of the perpendicular recording system over the longitudinal recording are:

- Higher thermal stability can be achieved by the smaller size of the particles in the material resembling a cylindrical structure.
- A perpendicular pole head in a recording media with a SUL is capable of generating twice the magnetic field of the longitudinal recording head. This allows writing higher coercivity medium, further decreasing the grain size.

- The amplitude of the readback signals from the perpendicular medium with SUL is larger when compared to the signal from the equivalent longitudinal medium that improves the signal-to-noise ratio.
- Perpendicular media grains are strongly oriented which results in sharper recorded transition with smaller medium noise. The high orientation of the perpendicular medium improves the side-track writing and the edge noise.
- The demagnetization field in the perpendicular medium tends to be smaller at the transition region. This enables writing narrower magnetic transitions and improves the thermal stability of high-density data. Also, the non-linear transition shifts in the perpendicular medium are comparatively less critical when compared to longitudinal recording.
- The track edges in the perpendicular medium are better defined and less noisy due to the vertical pole head configuration. Sharp track edges allow smaller bit aspect ratio and higher track density.

However, as the PMR components were developed, various disadvantages were identified. Some of the disadvantages of the perpendicular system are:

- Perpendicular pole heads have a comparatively poor write gradient. Also, the pole write head geometry produces distortions when the write head is skewed relative to the direction of the magnetic track. Also, there exist the chances of exhibiting pole remanence problems at the thin pole heads caused by the magnetic domains in the pole tip.
- Perpendicular recording media with SUL also develops noise generated by magnetic domains. Hence, complicated media biasing schemes are required to eliminate the SUL domain walls.
- Due to the presence of the SUL, the readback resolution of the perpendicular recording medium is lower when compared to the longitudinal medium.
- Both write and read processes are highly sensitive to the magnetization of adjacent tracks thereby increasing the possibility of higher stray magnetic fields. This creates transition shifts in the recorded data and sensor saturation depending on the magnetization of the nearby data tracks.
- Propagation of magnetic flux through the SUL and the presence of thick return pole increase the chances of demagnetization of adjacent tracks thereby increasing the interference problem of the nearby tracks.

Apart from the above-mentioned disadvantages, numerous theoretical predictions and experimental evaluations of the perpendicular recording potential predicts the optimistic scenarios of doubling the areal density achievable with longitudinal media along with the decreasing effects of superparamagnetism. Hence, PMR technology is of interest in this thesis work.

4

MAGNETIC TAPE

A magnetic tape is a flexible scale used for recording angle and distance information. Magnetic tape with encoded pole pitches is commonly called as magnetic scales. They are used for incremental and absolute measurements. The magnetic scales also called pole tab, can be used to realize linear displacement measurements. The pole tab represents the measured magnetic field over a linear distance available. With specifically provided pole tabs for rotation angle and path length sensors, north and south poles can be detected. The magnetic tape has the following features and advantages:

- Contactless measurement using magnetic sensor and magnetic tape
- Wear-free and resistant to humidity oil, grease dust and shavings
- Non-sensitive to smoke and dirt
- Ideal for measurement in rough or harsh environments
- High accurate and repeatable measurements
- Easy and flexible installation
- Devoid of noise signals

Section 4.1 gives an overview of the structure of the magnetic tape used for magnetization. Different types of coding methodology (Section 4.2) are used to produce magnetic scales of different types. The requirements of the pole tab (Section 4.3) written on a magnetic tape depends on the applications.

4.1 STRUCTURE OF THE MAGNETIC TAPE

A magnetic scale consists of a magnetic tape bonded to a steel strip by a matrix for support. The matrix can be made either plastic bonded material or a new highly temperature and media resistive rubber bonded material, which possess different qualities. The magnetic carrier guarantees a mechanical stability. The steel carrier

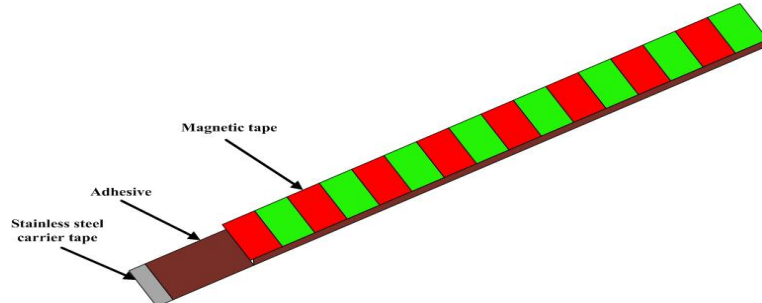


Figure 4.1.1: Structure of a magnetic tape

expansion determines the thermal expansion, which makes it optimal for use in machines made from a steel construction. By default, a pole tab consists of three layers as in Figure 4.1.1. Hard ferrite forms the uppermost layer. In the middle is the adhesive layer which connects the magnetic material with the steel strip, which forms the lower layer. Magnetic conductible and flexible stainless steel tape protects the plastic tape from mechanical damages and is a magnetic short circuit at the same time. This increases significantly the functional security under extreme magnetic influences. However, the field strengthening the effect of the pole length is dependent on the field strength that decreases with increasing altitude. The field strength of the magnetic scale is determined based on the ratio of the thickness of the material to pole length [Mee86].

In this thesis, the plastic bonded hard ferrite Tromaflex TX928 is used and coercivity (H_c) of the material is 170 kA/m [tro]. Tromaflex is an anisotropic flexible magnet. The advantage of anisotropic magnet over isotropic permanent magnets is that the oriented preferential axis is achieved, resulting in a higher magnetic energy density.

By using special ceramic oxide permanent magnet materials with plastic bonded permanent magnets and by suitable manufacturing processes, an increase in the magnetic energy density can be achieved. This also has a significant increase in adhesion compared to isotropic permanent magnets. In the preparation of anisotropic permanent magnets (usually flake shaped strontium ferrite), heated plastics are aligned mechanically in the surrounding, so that the largest possible part of their magnetic easy axis is oriented parallel to the desired direction.

In Figure 4.1.2, (a) shows the structure of isotropic permanent magnet which consists of different sized plates of barium ferrite. When magnetized, such a structure does not develop the preferred direction. It can be magnetized in any direction. Whereas anisotropic magnet (Figure 4.1.2, (b)) has its own preferred direction and can be magnetized exclusively in the specified direction (Figure 4.1.2, (c)). Magnetic

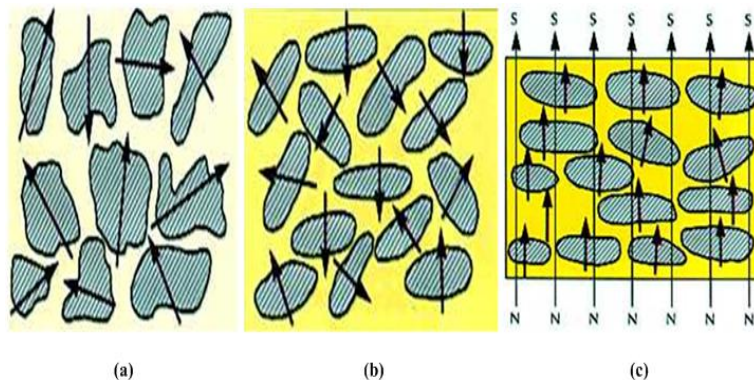


Figure 4.1.2: Comparison of isotropic-anisotropic materials (a) barium ferrite isotropy (b) strontium ferrite anisotropy (c) Magnetic domains oriented along the desired direction

Anisotropy is the dependence of a material's magnetic properties on its direction. Magnetically anisotropic materials have a tendency to align their magnetic moment along the direction of spontaneous magnetization. The two opposite directions along the axis of spontaneous direction are usually equivalent and the actual direction of magnetization can be along either of them. Unless there is an applied magnetic field, a magnetically isotropic material has no preferential direction for its magnetic moment. Anisotropic magnets have a higher adhesive force and are stronger than isotropic magnets [tro].

4.2 MAGNETIZATION OF THE MAGNETIC TAPE

Since the thesis concentration is on PMR technology, the magnetic strips are magnetized in perpendicular direction as shown in Figure 4.2.1. In this magnetization process, the magnetic flux, ϕ_m is passed through the magnetic tape forming the magnetic poles in the desired direction. By reversing the magnetic flux, the orientation of the poles is changed. The profile of the magnetic field is always from the north to the south pole of the adjacent poles and rotates by exactly 180° . In Figure 4.2.1, a simplified model of a vertically magnetized magnetic strip is shown. The arrows drawn indicate the direction of the magnetic field inside the magnetic strip as well as the flow direction as read by a rotation angle sensor.

Basically, two different kinds of magnetic tapes are available: incremental or absolute coded variants, which must be selected accordingly.

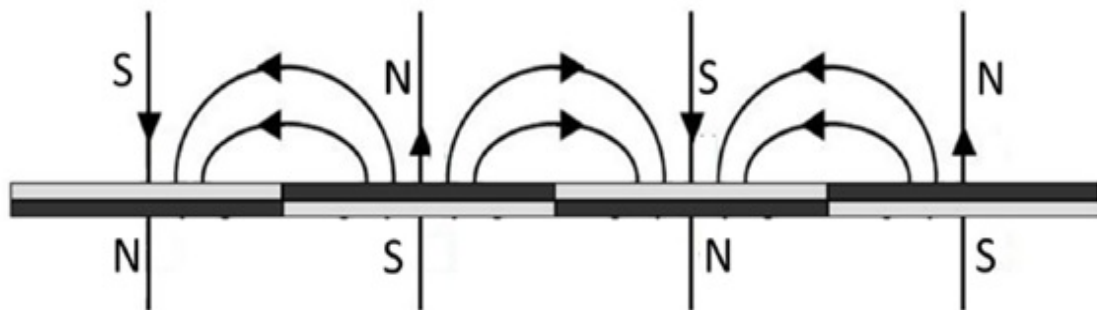


Figure 4.2.1: Perpendicular magnetization of a pole tab

Incremental coding scales

Incremental measuring systems are currently the most popular because they are produced at relatively low cost when compared to the absolute system and are easy to use. In an incremental measurement system, only a single-track magnetic tape is needed. The magnetic strip consists of equidistant pole lengths, which are lined up with alternating polarity as shown in Figure 4.2.2. In incremental systems, every measurement refers to a previously dimensioned position (point-to-point). Incremental dimensions are the distances between two adjacent points. The basis of magnetic incremental measuring systems consists of a technology, which scans the north and south poles on the coded magnetic tape. It produces a single sine and cosine wave for each pole. The complete sine and cosine signal process is interpolated electronically. The resolution of the measuring system is determined, depending on the refinement of the interpolation, together with the pole length of the magnetic tape. There are magnetic tapes with different pole pitches available, which are used correspondingly to the suitable measuring system.

Depending on the demand, magnetic tapes with different pole distances are available, that are used for various products (depending on demanded accuracy). If absolute position information is required, the measuring system should have a reference point from which traversed poles must be counted. When the system fails to operate (Power failure), then the incremental measuring system cannot identify the absolute position anymore and must be started again from the reference point, which is one of the major disadvantage of an incremental measuring system [Nyco4].

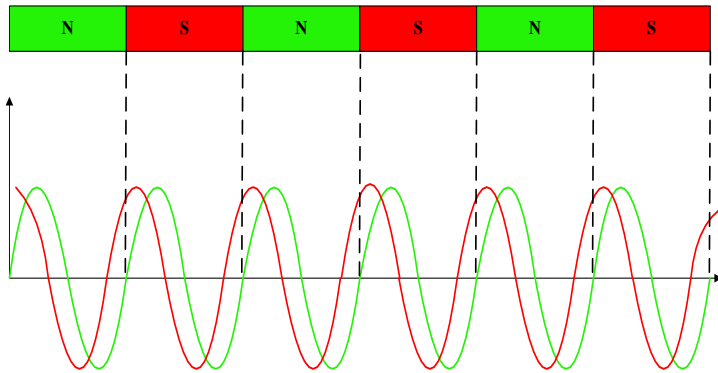


Figure 4.2.2: Incremental measuring system

Absolute coding scales

In absolute measuring system, all coordinate values are relative to a fixed origin of the coordinate system. Referencing or gauging of the evaluation unit is not necessary any longer, because an absolute measuring system supplies the correct absolute value immediately after power is on. This means that the position remains at the same point, even if the system is moved manually when the power is off. The actual position on the magnetic tape is immediately recognized in real time as soon as supply voltage is connected by the interface of the magnetic sensor and transferred to the evaluation unit. The magnetic tape that is magnetically coded as "absolute", is combined with multiple sensors in the sensor head. This displays a unique position for every step of the resolution.

In recent years, absolute measuring systems are gaining more and more importance. Over the past few years, incremental measuring systems were used more often. However, now the trend is towards the absolute measuring systems. The advantages of absolute measuring systems are obvious. The handling and programming of the system are much easier. It needs no reference point to be set, which meets the security criteria for many applications. An absolute measuring system knows the current position immediately after switching on the supply voltage. To determine this, the magnetic strip must be specially coded.

An absolute position code can be generated by using a magnetized tape having varying pole pitches. If the resulting magnetic pole pattern does not repeat itself over the whole traveling distance, it can be represented as an absolute position data. However, in order to process this code, a parallel incremental track is required. This incremental track can be used by an electronic reader as a clock signal to synchronize the sampling

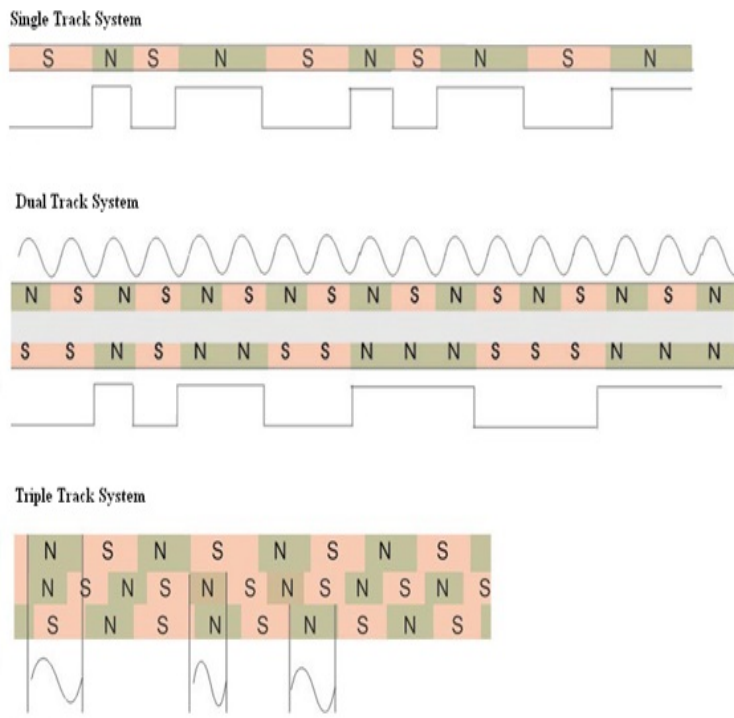


Figure 4.2.3: Track system in absolute measuring system

points. Nowadays, the dual track system is offered by various manufacturers and is one of the accepted standards [Nyco4].

The dual track magnetic tapes are used along with dual track sensor heads. The greater space requirement of the sensor and tape along with the technical criteria necessary to guarantee precise guidance of the sensor heads come at a higher price. Also, lateral displacement of the sensor head will lead to measurement errors and system failure. With absolute coded tapes, single and multiple track systems are possible as shown in Figure 4.2.3:

- Single track system (pseudo random code)
- Dual track system (fine interpolation track / absolute track)
- Triple track system (phase different measurement after the nonius principle)

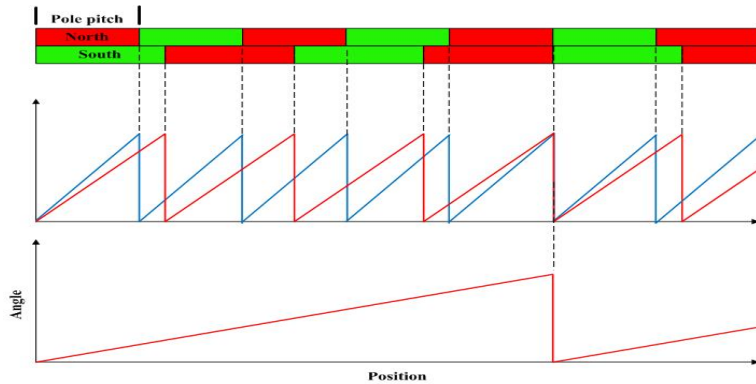


Figure 4.2.4: Vernier coding scales

Vernier coding system

A vernier coding scales, as shown in Figure 4.2.4, is a simple way by which an absolute measuring system is constructed. The encoding is performed by two adjacent tracks with constant pole length in each track. The pole length of the tracks is different from each other. The second track has slightly longer poles, so the number of poles is therefore reduced by a pole.

To measure the absolute position, the position signal of the two tracks is calculated at the same point. The measured field angle of the pole width of each track is dependent and the Pole difference of the two tracks differs in length. Subtracting the two field angles from each other, we will obtain a linear waveform at which one can determine the current position precisely. The vernier system is only suitable for very short distances measurement.

Gray coding system

The Gray-coding reading system, as shown in Figure 4.2.5, is a multi-track measuring system that contains digital information on the immediate absolute position. Each track is read by a separate sensor and can thus detect each "1" and "0". Since the tracks are arranged in parallel, the information is read as a 4-bit wide word. By the detected binary word, one can determine the absolute position. With an interpolation, the exact position can be determined. In this measuring system, the cost of longer measuring distances increases on the basis of the parallel measurement scales and sensors. Hence, this limits its application to be practical only over shorter distances.



Figure 4.2.5: Gray code measurement system

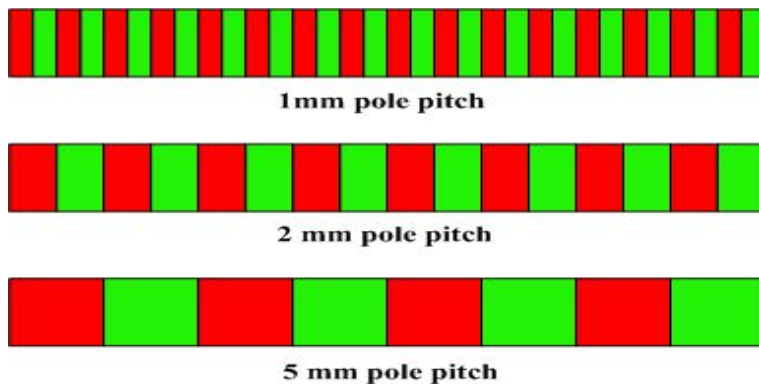


Figure 4.3.1: Different pole pitches in magnetic tape

4.3 REQUIREMENTS OF A POLE TAB

For the magnetoresistive sensors to encode the information from the chain coded magnetic tape, the field strength generated by the magnetic tape must be atleast 8 kA/m. If the field strength of the measured values is under 8 kA/m, the magnetoresistive sensors provide no more reliable information. Also, the magnetic tape needs to be examined with the sensor system at a distance in the range of 0.5mm to 2.5mm which is considered as the optimal air gap [Mei15]. The pole pitch to be written on the magnetic tape can be decided as per requirement. Usually pole pitches of 1mm, 2mm and 5mm are generally used as shown in Figure 4.3.1.

5

SYSTEM DESIGN

The major objective of the system was to magnetize a magnetic tape as per the requirements and analyze the magnetization process. This chapter gives a detailed overview of the design and construction of an apparatus to magnetize a magnetic tape. The apparatus consists of a write head (Section 5.1) that is required to perpendicularly magnetizes the magnetic tape. The magnetization process is evaluated using read head (Section 5.2). A coordinate system (Section 5.3) is required to map the movement of write and read head in 3-dimensional space. A control program (Section 5.4) is developed to control the process of magnetization and evaluation. The Figure 5.0.2 shows the block diagram of the entire system.

5.1 DESIGN OF WRITE HEAD

Requirements for write head designs

The design requirements for the write head had been analyzed and categorized into primary and secondary requirements. The ‘must do’ design criteria that are considered as the dominant constraints for designing the prototype of the write head were included in the primary requirements category. The ‘shall do’ design criteria were listed in the secondary requirements category. The primary requirements are listed below:

1. **Guided flux design:** One of the major objectives for the construction of the write head was to use a guided-flux design with an air gap. A magnetic circuit that channels the magnetic flux lines through a high permeability material can be considered as a guided-flux design as shown in Figure 5.1.1. Since the permeability of air surrounding the circuit is lower than the magnetic core, the magnetic flux lines are guided through the material. The guided flux design under consideration should contain an air gap for magnetizing the tape. An air gap is a non-magnetic part of a magnetic circuit that is connected magnetically in series with the rest of the circuit. A considerable part of the magnetic flux flows through the air gap. The air gap often accounts for almost all the reluctance seen by the magnetic field. This leads to an interesting property of practical

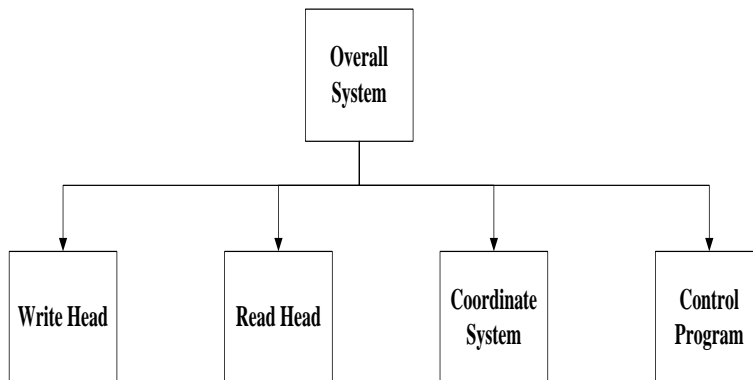


Figure 5.0.2: Block diagram of the overall system

gapped cores. This gap contains nearly all of the field energy. A comparison of the orientation of magnetic field lines across a guided flux and non-guided flux design is shown in the Figure 5.1.2.

2. **Less current:** The magnetic field intensity generated at the air gap of the guided flux design should be strong enough to magnetize the tape. The strength of the magnetic field should be attained with a minimum possible current.
3. **Less heat dissipation:** The design of the structure should be carried out in such a way that the ambient temperature of the magnetic circuit should be as minimum as possible. The increase in the coil temperature leads to the rise in the resistance of the coil. This reduces the current flow. If the current flow decreases, the magnetic field intensity generated at the air gap reduces causing an adverse effect on the magnetization process. Therefore, when considering a proper design, the temperature of the circuit needs to be considered.
4. **Reduce stray field:** Another important objective of the design was to result in narrow stray fields along the edges of the pole pitches. The guided flux design is expected to produce comparatively less stray field, as much of the magnetic field lines are focused to pass through the air gap to reach the other tip of the write head.
5. **Material selection:** The magnetic materials with magnetic susceptibilities of the higher orders are capable of producing high magnetic flux densities with comparably small currents. The material selected should also be machinable.

The secondary requirements are listed below:

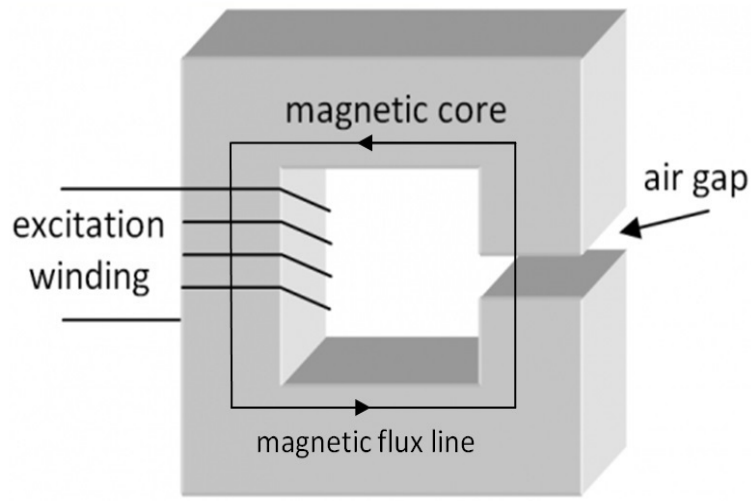


Figure 5.1.1: Guided flux design of magnetic core

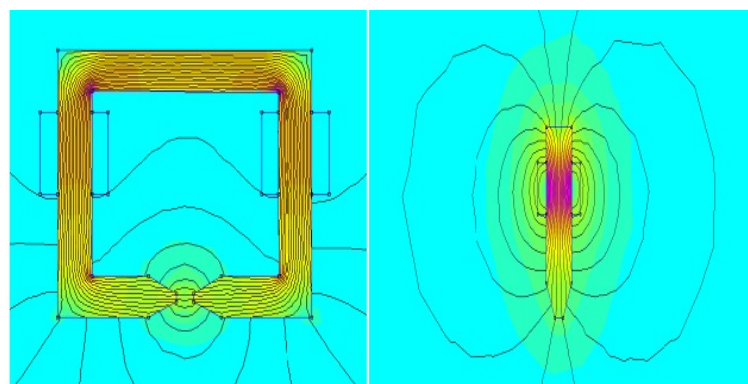


Figure 5.1.2: Comparison between guided flux and non-guided design of magnetic core (a) Guided flux design (b) Non-guided flux design

1. **Mechanical strength:** The designed part should be mechanically strong enough to withstand vibrations.
2. **Minimum parts:** Another important constraint for the design of the prototype was to have a minimum number of joints to increase strength and robustness of the structure. Since the write head has to be placed perpendicular to the magnetic tape to magnetize it, a minimum number of joints reduces the chance of producing error due to change in the alignment.
3. **Minimum cost:** The material selection and design of parts have to be carried out in such a way that it is cost-effective.
4. **Optimal air gap adjustment mechanism:** Air gap plays a significant role in the magnetic circuit. The magnetic tape to be magnetized is placed in this space. The distance between the magnetic tape and the write head tip is to be determined through experiments that depend on the current supply and the material and size of the magnetic tape used.

Experimental investigation of different write head designs

In accordance with the above-mentioned primary and secondary requirements, the following prototype designs had been taken into consideration.

1. G-Head
2. M-Head

The designs were first implemented in Finite Element Method Magnetics (FEMM) [Fin] to inspect the influence of different material types as well as the sizes of the write head parts. A detailed study of the behavior of magnetic field lines with different parameters was also conducted. Once the simulation results were in accordance with the requirements, the 3D model of the prototype was designed using SolidWorks 3D CAD design software [sol].

Magnetic field simulation

To better understand the principle and mathematically map the magnetic path length, a simulation model is required, by which the entire system analysis can be performed. The system parameters found in this way can later be incorporated in a prototype for absolute distance and position measurement. As a physical measure, the information about the strength and direction of the magnetic field at each respective position over

the employed magnetic tape has to be determined. The effect of various mechanical distortions such as the tilting of the system can also be analyzed through the spatial description of the entire system. Moreover, it is necessary to simulate and optimize electromagnetic components and systems before the manufacturing stage to avoid building multiple prototypes, thus lowering the development costs and time.

With the above-mentioned system design requirements, various approaches had been studied and analyzed through the simulation of the magnetic field generated over the magnetic pole tab. The calculation using the finite element method poses many advantages including less time calculation. Moreover, it enables the study of external magnetic field influences providing different material compositions and geometry. The major drawback of the simulation software used (Finite Element Method Magnetics) is that it allows only two-dimensional considerations.

Finite Element Method Magnetics (FEMM)

Finite Element Method Magnetics (FEMM) [Fin] is a set of programs for solving low-frequency electromagnetic problems on 2D axisymmetric and planar domains. The program discusses nonlinear/linear magnetostatic problems, nonlinear/linear time harmonic magnetic problems, steady-state heat flow problems and linear electrostatic problems. Among these, linear/nonlinear magnetostatic problems are of interest to us.

The package is composed of an interactive shell encompassing graphical pre- and post-processing, a mesh generator and various solvers. It contains a Computer Aided Design (CAD) like interface for designing the geometry of the problem that is to be solved and for defining the boundary conditions and material properties. The triangulation process breaks down the solution region into numerous triangles, a vital part of the finite element process. A powerful scripting language, Lua 4.0 [IDFCF96], is integrated with the program. The single instance of Lua can both build and analyze the geometry and it also evaluates the post-processing results by simplifying the process by the creation of various kinds of 'batch' runs.

The solver used in FEMM for magnetic problems is 'fkern'. It takes a set of data files that describe the problem and it solves the relevant partial differential equations to gain values for the required field throughout the solution domain. The magnetic pre-processor is used for drawing the problem's geometry, defining materials, and defining boundary conditions. The magnetic post-processing functionality of FEMM is used to view solutions generated by the 'fkern' solver. Figure 5.1.3 shows an example of FEMM simulation.

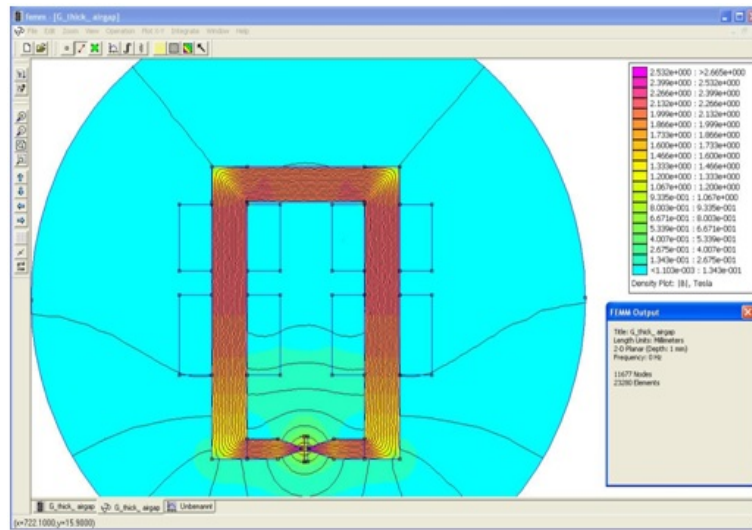


Figure 5.1.3: FEMM Simulation

5.1.1 G-Head design

One of the guided flux designs considered was 'G' shaped design. The design was constructed in such a way that the write head acted as a magnetic circuit. It consisted of a magnetic core and coils attached to the core. It also included an air gap between the tips of the write head, in which the magnetic tape to be magnetized was placed perpendicularly, as shown in Figure 5.1.4.

Simulation

The G-Head design was implemented in the simulation software and the influence of the following parameters (in accordance with the above mentioned requirements) had been analyzed.

1. **Material selection:** Various soft magnetic materials were considered as the material for the core of the write head. Mu-metal and pure iron were considered for the analysis. Mu-metal is a nickel-iron soft magnetic alloy with very high permeability. It is composed of approximately 5% molybdenum, 80% nickel and balance iron. Pure iron is a common metal with fewer impurities due to its low carbon content. Due to its small amount of impurities, pure iron has high magnetic stability, high permeability and has high saturation magnetic induction. It is used as magnetic core since it can endure high temperature and won't saturate.

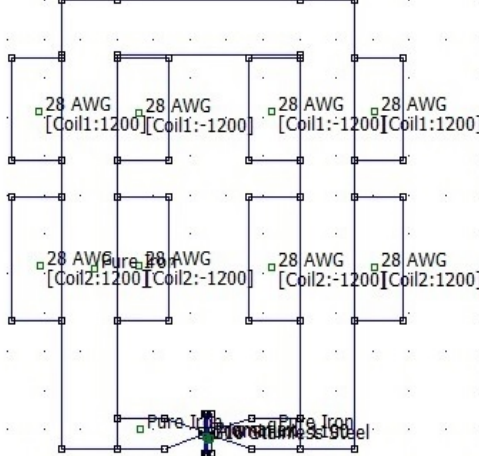


Figure 5.1.4: The geometry design of G-Head

Saturation is a characteristic of ferromagnetic and ferrimagnetic materials. It is a state reached when an increase in the applied external magnetic field cannot enhance the magnetization of the material further. Saturation flux density is an important criterion for selecting the suitable material for the magnetic core [Boz93]. An ideal candidate should possess high saturation flux density so that there is a possibility of applying higher voltage for obtaining higher magnetic fields without the material getting saturated. From the Table 5.1.1, it is clear that pure iron has a saturation flux density higher than mu-metal. Moreover, the above-mentioned properties of pure iron make it an ideal candidate for the magnetic core when compared to mu-metal.

Ferromagnetic materials considered	Saturation Flux Density, Bs (T)
Pure Iron	2.3
Mu-metal	0.8

Table 5.1.1: Saturation flux densities of ferromagnetic materials

- Length and width of the parts: The length and width of the various parts of the proposed G-Head design were experimented according to the dimensions of the standard parts used along with the design. The length and width of the legs

of the G-Head were chosen in such a way that it should match the size of the standard coil holder. The minimum pole pitch to be written on a magnetic tape was 1mm. Hence, the tip of the write head was chosen to be 1mm which also facilitated the possibility of magnetizing pole tabs with pole pitches of a higher order with a resolution of 1mm.

3. **Current supply and number of turns in each coil:** The number of windings in each coil and the current supply were experimentally determined to generate a minimum magnetic field of 170kA/m (coercivity of Tromaflex 928) in the air gap and also to limit the flux density below 2.3T. Based on the results summarized in Table 5.1.2, four coils of 1000 windings each, with a current supply of 3A were chosen as an ideal combination to generate the required magnetic field strength.

Current (A)	No. of windings/coil (4 coils used)	$ H $ at the magnetic tape (kA/m)
1.5	500	102
2.5	500	132
3.0	500	175
1.5	1000	195
2.5	1000	260
3.0	1000	365

Table 5.1.2: Simulation results for various combinations of electric current and number of windings per coil

4. **The air gap between the write tips:** Since the simulation software was incapable of showing minute changes in results due to small variations in air gap, a detailed study on the effect of air gap was carried out in real-time experiments. An air gap of 2mm was chosen in simulation study to analyze the effect of parameters mentioned above.

Considering these parameters, a simulation result was finalized as shown in Figure 5.1.5. The figure shows the magnetic flux density plot of the write head and its surrounding areas inside a defined boundary. The colour in the figure denotes the strength of the magnetic field area. From the figure, it is evident that the magnetic field lines are guided through the magnetic core. Due to the reluctance of the air gap at the write tip, the field lines are slightly dispersed.

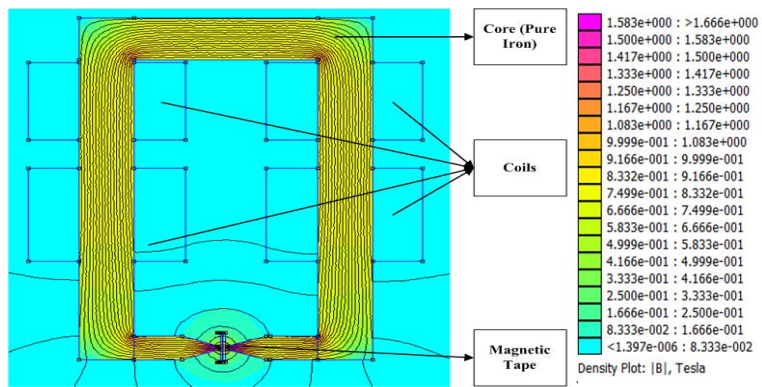


Figure 5.1.5: Simulation results of G-Head design. The figure on the right shows the magnetic flux distribution chart corresponding to the simulation result shown on the left.

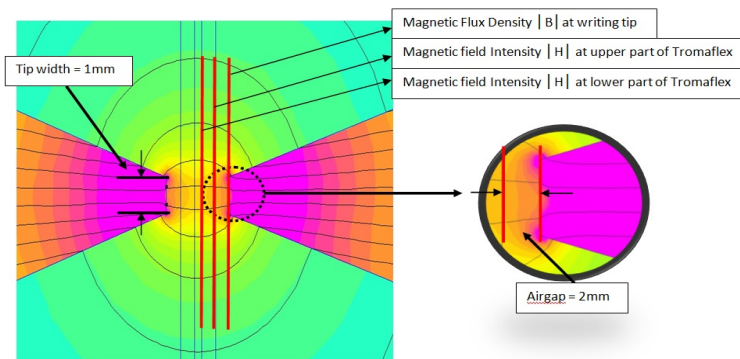


Figure 5.1.6: Detailed view of the write tip of G-Head

The Figure 5.1.6 shows a detailed view of the simulation results of the write tip of the G-Head design. The areas marked with red lines shows the three different quantities measured in the simulation. They are:

1. Magnetic flux density $|B|$ at the write tip facing the magnetic tape
2. Magnetic field intensity $|H|$ at the upper layer of the magnetic tape
3. Magnetic field intensity $|H|$ at the lower layer of the magnetic tape

An air gap of 2mm was found ideal for the above analyzed quantities to be in the satisfactory range. With the change in the current supply, the magnetic flux density at the write tip was measured and was found to be below the saturation flux density (B_s) of pure iron. The Figure 5.1.7 shows that the flux density at the write tip was found to be in the range of 1.4T with a current supply of 3A that is marked with red dotted lines in the figure. The magnetic flux at the write tip is less than the saturation flux density of pure iron ($B_s = 2.3T$). The green lines in the figure show the width of the tip (1mm). The magnetic field intensity was measured at the upper and lower layer of the magnetic tape to ensure that the tape was fully magnetized. Figure 5.1.8 shows that the magnetic field intensity at the upper layer of the magnetic tape was found to be more than the coercivity of Tromaflex 928, which is necessary for the material to get magnetized. The horizontal red dotted line marked in the figure shows the minimum magnetic field required to magnetize the tape ($H_c = 170 \text{ kA/m}$). The horizontal green dotted line marked in the figure displays the actual magnetic field intensity at the write tip. The vertical green lines indicate the width of the tip (1mm). The red vertical lines indicate the complete area on the magnetic tape that get magnetized. The area on the magnetic tape between the red and green lines are magnetized by the stray field.

Figure 5.1.9 shows the magnetic field intensity at the lower layer of the magnetic tape. It is evident that the supplied current was enough to produce a magnetic field to fully magnetize the material. The horizontal red dotted line marked in the figure shows the minimum magnetic field necessary to magnetize the tape ($H_c = 170 \text{ kA/m}$). The vertical green lines indicate the width of the tip (1mm). As per the simulation results shown above, the stray field on either side of the write head tip decreased towards the lower part of the magnetic tape.

Based on the experiments carried out in the simulation, the following design parameters were chosen. Pure iron was selected as the magnetic core material. Four coils with 1000 windings each, a current supply of 3.0A and an air gap of 2mm were also chosen. Also, from the simulation, the required magnetic field intensity was achieved with these optimum values.

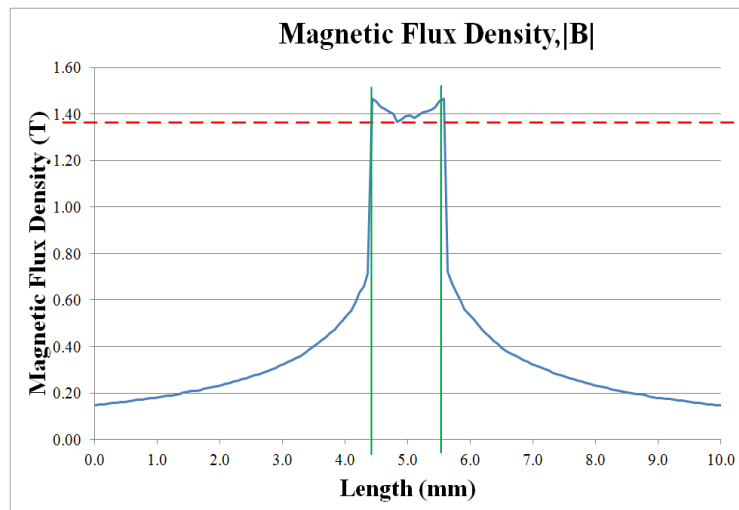


Figure 5.1.7: The magnetic flux density at the write tip of G-Head

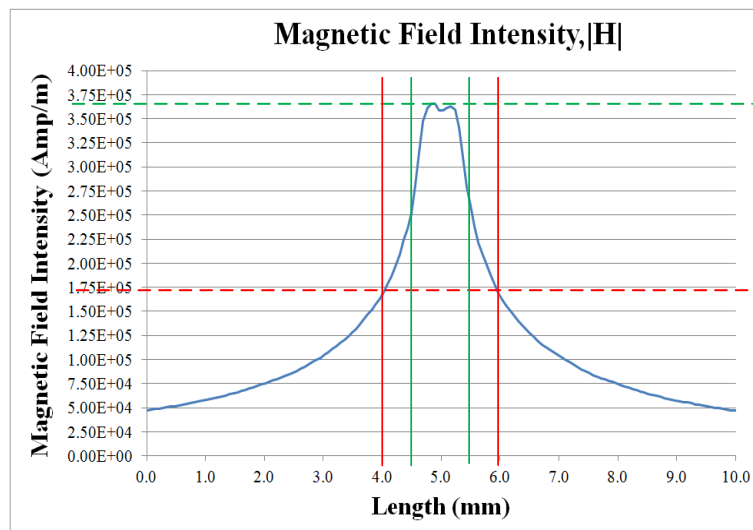


Figure 5.1.8: The magnetic field intensity at the upper layer of magnetic tape

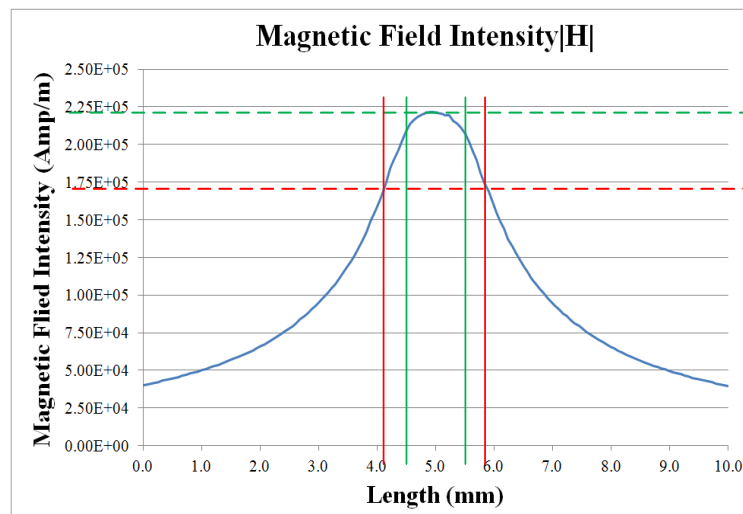


Figure 5.1.9: The magnetic field intensity at the lower layer of magnetic tape

Mechanical modeling and structure

Mechanical modeling was carried out with SolidWorks software [sol]. The SolidWorks CAD software is a mechanical design automation application that aids the designers to quickly sketch out ideas, carry out an experiment with features and dimensions and produce detailed drawings and models. A 3D design approach was used in modeling. The part was designed from an initial sketch in 2D. Later the final result was implemented as a 3D model. From this model, 2D drawings were created or individual components were mated to other parts to form assemblies or subassemblies. 2-dimensional drawings of 3D assemblies were also be created. When designing a model using SolidWorks, it is possible to visualize the model in three dimensions, to view how the model exists once it is manufactured.

The Figure 5.1.10 shows the 3D model of the G-Head design. The model of the write head was created by arranging thin metal sheets of 0.5mm width. The purpose of this design was the easy arrangement and alteration of the width of the complete part as per need. The write head was equipped with space for coils on the legs. The bottom of the G-Head design marked with green arrow shows that it can be moved to and fro for the air gap adjustment. The green structure in between the write tip is an arrangement for holding the magnetic tape in the perpendicular direction. The Figure 5.1.11 shows the write head prototype constructed with four coils and necessary components.

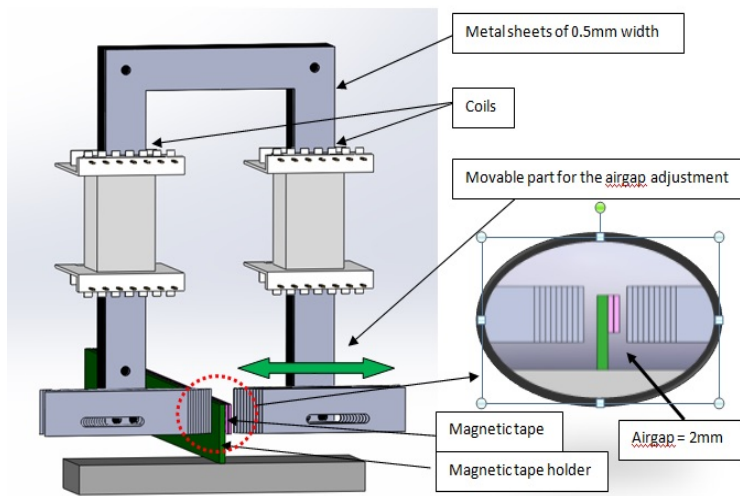


Figure 5.1.10: 3D model of the write head

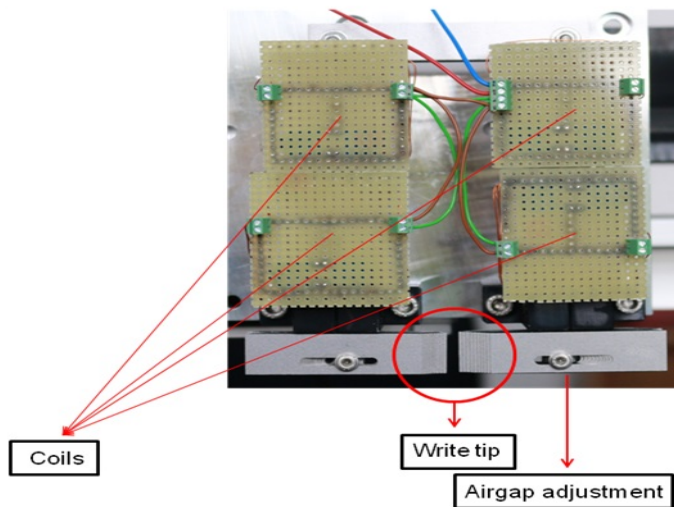


Figure 5.1.11: The prototype of the write head

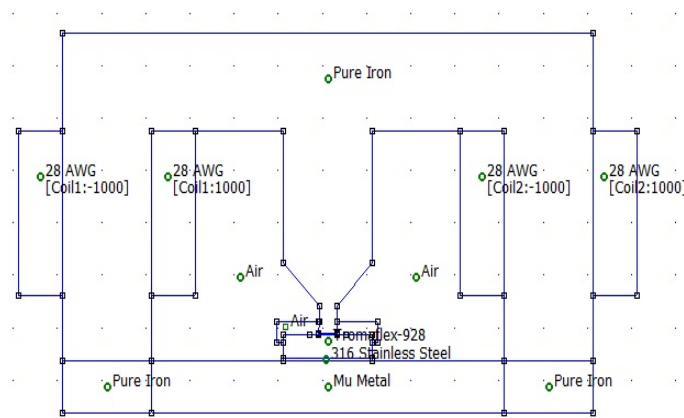


Figure 5.1.12: The geometry design of M-Head

5.1.2 *M-Head design*

An alternate guided flux design was 'M' shaped design. The design was conceived in such a way that the magnetic tape to be magnetized was placed below the middle tip of the M-Head with sufficient air gap between the tip of the write head and the tape as shown in Figure 5.1.12. An appropriate holder for the magnetic tape was also designed along with the write head.

Simulation

The parameters for the simulation study of the M-Head design was similar to that of G-Head design. Pure iron was chosen as the material for the magnetic core. The length and width of the various parts of the proposed M-Head design were experimented according to the dimensions of the standard parts used along with the design. The number of windings in each coil and the current supply were experimentally determined similarly to G-Head design. An air gap of 2mm was chosen. Considering the above parameters, a simulation result was finalized as shown in Figure 5.1.13.

The Figure 5.1.14 shows a detailed view of the simulation results of the write tip of the M-Head design. The areas marked with red lines shows the three different quantities measured in the simulation. They are:

1. Magnetic flux density $|B|$ at the write tip facing the magnetic tape

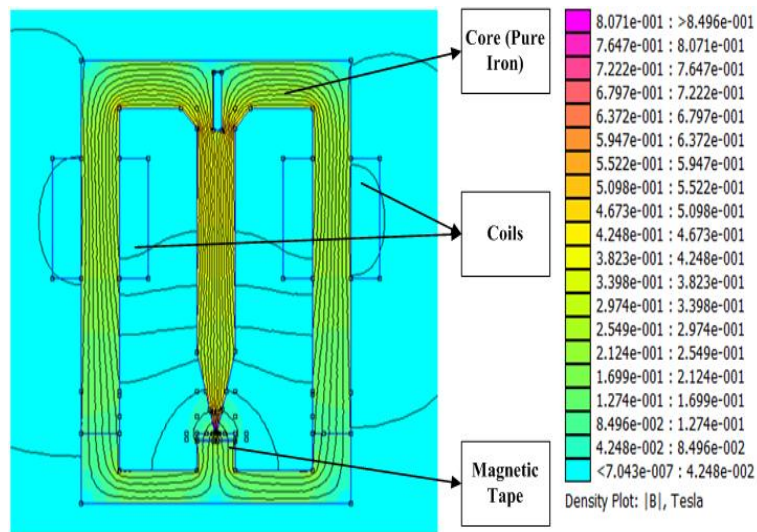


Figure 5.1.13: Simulation results of M-Head design. The figure on the right shows the magnetic flux distribution chart corresponding to the simulation result shown on the left.

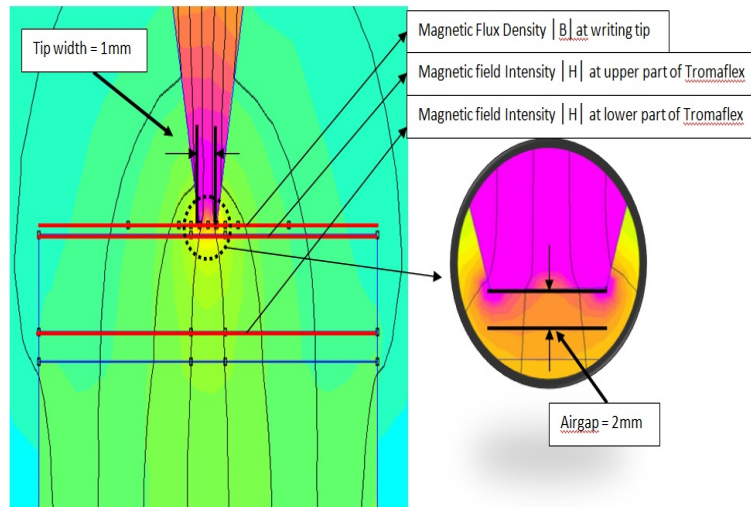


Figure 5.1.14: Detailed view of the write tip of M-Head

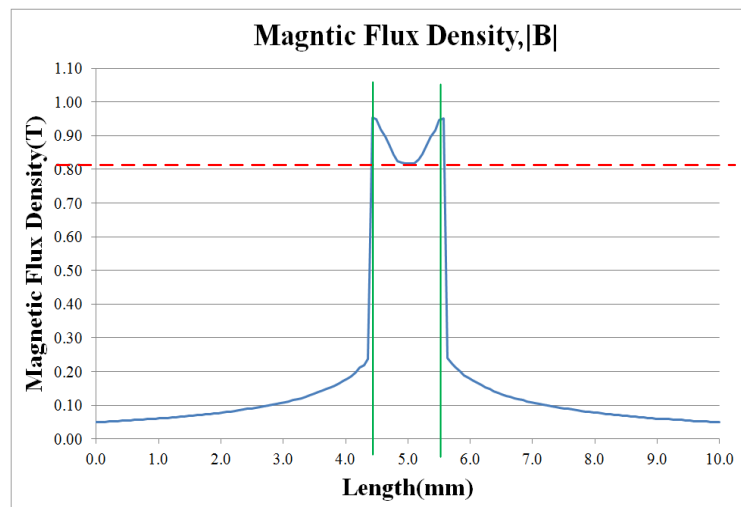


Figure 5.1.15: The magnetic flux density at the write tip of M-Head

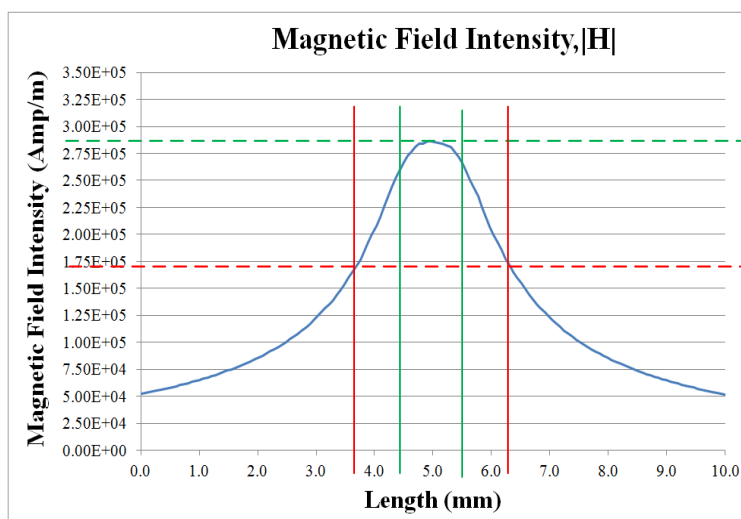


Figure 5.1.16: The magnetic field intensity at the upper layer of the magnetic tape

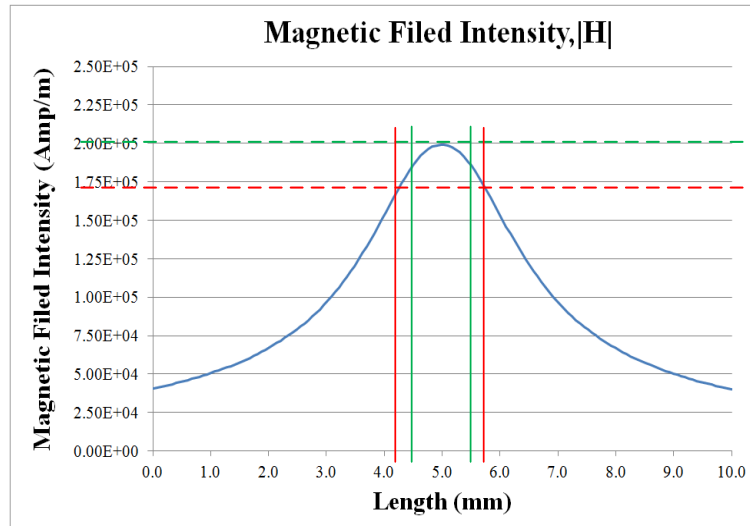


Figure 5.1.17: The magnetic field intensity at the lower layer of the magnetic tape

2. Magnetic field intensity $|H|$ at the upper layer of the magnetic tape
3. Magnetic field intensity $|H|$ at the lower layer of the magnetic tape

The air gap of 2mm was found ideal for the analyzed quantities to be in the satisfactory range. With the change in the current supply, the magnetic flux density at the write tip was measured to be a value below the saturation flux density (B_s) of pure iron. The Figure 5.1.15 shows that the flux density at the write tip was found to be in the range of 0.8T with a current supply of 3A. The green lines in the figure show the width of the tip (1mm). The magnetic field intensity was measured at the upper and lower layer of the magnetic tape to ensure that the tape is fully magnetized. The Figure 5.1.16 shows the magnetic field intensity at the upper layer of the magnetic tape was found to be more than the coercivity of Tromaflex, necessary for the material to get magnetized. The horizontal red dotted line marked in the figure shows the minimum magnetic field required to magnetize the tape ($H_c = 170 \text{ kA/m}$). The vertical green lines indicate the width of the tip (1mm). The red vertical lines indicate the complete area on the magnetic tape that get magnetized. The area on the magnetic tape between the red and green lines are magnetized by the stray field.

The Figure 5.1.17 shows the magnetic field intensity at the lower layer of the magnetic tape. It was evident that the supplied current was enough to produce a magnetic field to fully magnetize the material. The horizontal red dotted line marked in the figure shows the minimum magnetic field necessary to magnetize the tape ($H_c = 170 \text{ kA/m}$).

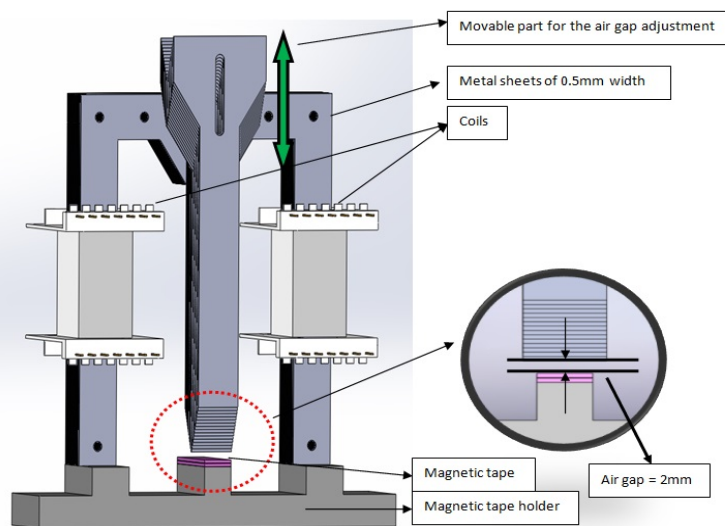


Figure 5.1.18: 3D model of the M-head

The vertical green lines indicate the width of the tip (1mm). As per the simulation results shown above, the stray field on either side of the write head tip decreased towards the lower part of the magnetic tape.

Mechanical modeling and structure

The Figure 5.1.18 shows the 3D model of the M-Head design. The model of the write head was created by arranging thin metal sheets of 0.5mm width. This was designed for the easy arrangement and alteration of the width of the complete part as per need. The write head is equipped with space for coils on the legs. The head was designed in such a manner that the middle leg was used as the write tip and the legs on either side were used to guide the flux at the write tip through both sides. The upper part of the M-Head design marked with green arrow shows that the middle leg can be moved up and down for the air gap adjustment. An arrangement was constructed to hold the magnetic tape. The holder was in 'W' shape. This acted as a mirror image of the M-head design and facilitated the magnetic field lines at the tip to be directed through the magnetic tape.

5.1.3 Comparison of G-Head and M-Head designs

The Table 5.1.3 shows a comparison between the simulation results of the G-Head and M-Head designs at a current of 3A. All the measurement values were approximated from the above-shown graphs. In G-Head design, the magnetic flux density at the write tip was in the range of 1.45T. The magnetic field intensity at the upper part of the tape was found to be in the range of 365kA/m. This was more than twice the amount of the coercive force of Tromaflex ($H_c = 170\text{kA/m}$). This facilitated the possibility of reverse magnetization in the material. The magnetic field intensity at the lower part of the tape was found to be in the range of 221kA/m.

Write head designs	$ B $ at the write tip (T)	$ H $ at the upper layer of the magnetic tape (kA/m)	$ H $ at the lower layer of the magnetic tape (kA/m)
G-Head	1.38	365	221
M-Head	0.82	286	199

Table 5.1.3: Comparison of simulation results of G-Head and M-Head

In M-Head design, the magnetic flux density at the write tip was in the range of 0.82T. The magnetic field intensity at the upper part of the tape was found to be in the range of 286kA/m. The magnetic field intensity at the lower part of the tape was found to be in the range of 199kA/m.

From a comparison between both the designs, the measured quantities showed better simulation results for G-head design. The magnetic flux density lower than the saturation flux density of pure iron for G-Head design provides the possibility of increasing current for further strong magnetic field intensity. The magnetic field intensity obtained for 3A in G-Head design is also higher than M-Head design. In the case of M-Head design, it will require an additional construction of a specialized magnetic tape holder to act as the mirror image of the write head. Moreover, in addition to the air gap between the write tip and the magnetic tape, M-Head design will have two more air gap between the two legs on either side of the middle leg at its corresponding mirror image of the magnetic tape holder. The additional air gaps in the M-Head design leads to more reluctance in the magnetic circuit. This area is prone to additional error and needs an extensive study. Since the simulation results of the M-Head was found lesser than the G-head simulation results and its requirement for

an additional construction of magnetic tape holder, it was concluded to proceed with the prototype construction and experimental analysis for G-Head design.

5.2 DESIGN OF READ HEAD

5.2.1 *Sensor system*

In this thesis work, a read head was used to evaluate the efficiency of the magnetization of the write head. This read head comprised of multiple magnetoresistive angle and position sensors and a set up to support and control the quick evaluation of the available sensors. Since the focus of experiments in this thesis was on the magnetization of a 5mm pole pitch, MLS5000 position sensor was primarily used in the sensor system. As explained in Section 2.5, the sensor was based on anisotropic magnetoresistive (AMR) sensor technology. The sensor used magnetic fields to conduct measurement information between the sensor and the physical value, i.e. angle or linear position. The contact-less operating principle allows the isolation of all moving components, making the entire sensing system robust with respect to environmental influences and mechanical wear. AMR sensors feature magnetoresistive elements arranged in a Wheatstone bridge. The direction of the magnetic field is evaluated, independent of the strength of the field. As a result, AMR sensors are very tolerant with respect to variations in field strength caused by aging of the magnet, its temperature sensitivity or mechanical fluctuations Section 2.5.

The Figure 5.2.1 shows the block diagram explaining the working of the read head. The sensor received analog signals in the form of voltage due to the variation in the resistance according to the magnetic field experienced. The weak signals were amplified using an operational amplifier and then converted into digital signals through a 12-bit ADC. These signals were fed to a general purpose board (STM32F303 Discovery) [st]. This general purpose board facilitated the quick evaluation and control of the signals from multiple sensors. It was equipped with a facility for the USB connection, through which the signals from the MLS5000 sensor was transferred to the computer for further evaluation and analysis.

5.2.2 *Mechanical modeling and structure*

The Figure 5.2.2 shows the 3D model of the read head assembly. The modeling was performed in such a way that there was enough space to arrange different sensors and the sensors could be placed in a convenient position so that it could read the magnetic

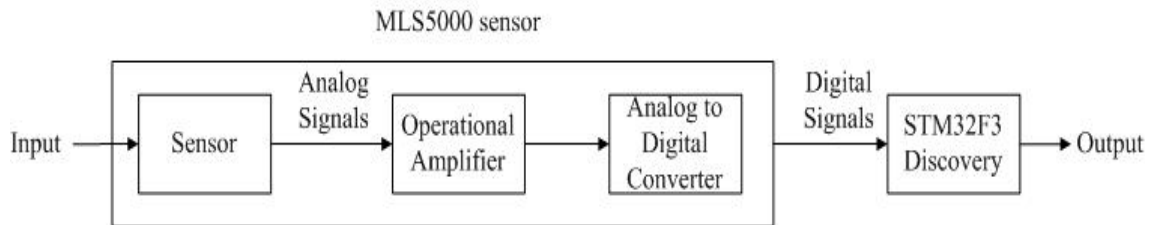


Figure 5.2.1: Block diagram showing the working of the read head

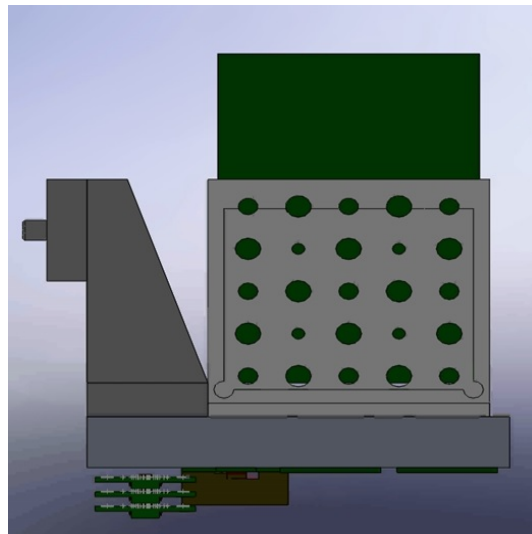


Figure 5.2.2: 3D model of the Read Head

tape that was fixed in a perpendicular direction. The Figure 5.2.3 shows the read head prototype constructed. The sensors were placed on the lower side of the holder in such a way that the sensor could be brought to the perpendicularly placed magnetic tape. The figure shows an MLS5000 sensor placed to read magnetic tapes of 5mm pole pitch.

5.3 CO-ORDINATE SYSTEM

The Coordinate system (Koordinatentisch-System) KOSY3 [kos] was used for moving and positioning in 3D space. The KOSY3 consisted of a combination of two orthogonally arranged linear plates. The vertical plate was movable in X and Z-direction and the horizontal plate could be moved in the Y-direction. This made it possible for

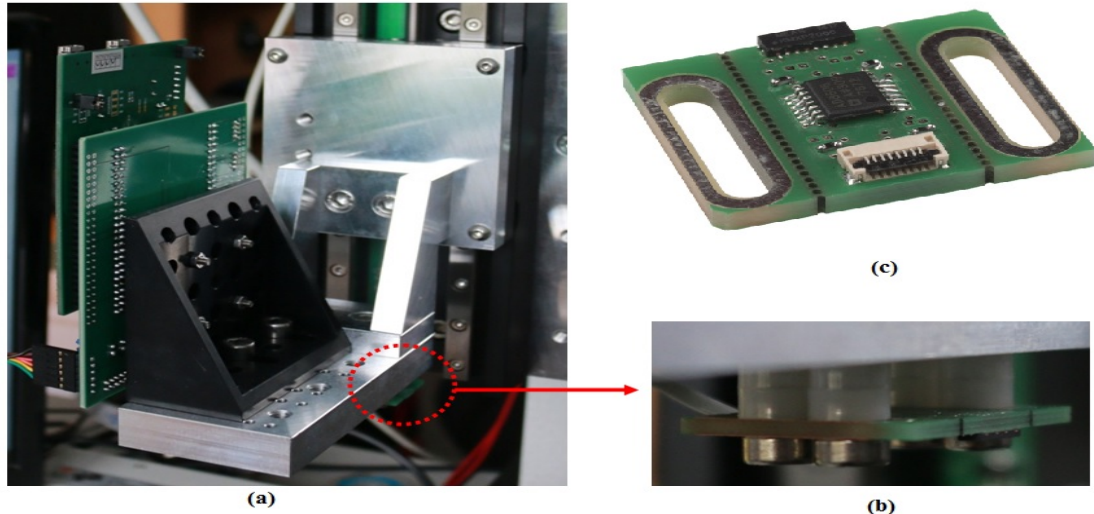


Figure 5.2.3: Prototype of the Read Head (a) Complete read head assembly (b) Arrangement of MLS5000 sensor on the read head (c) MLS5000 sensor PCB

the components attached to the vertical and horizontal plates to move in all three spatial directions relative to each other. The system was controlled using a LabVIEW program [lab]. A 3D model and an actual picture of the KOSY3 platform is shown in Figure 5.3.1.

In order to determine the accurate position on the magnetic tape, a high precision linear translational stage (M-531s.DG) was fixed on the Y-axis of the KOSY3 coordinate system which was used as the carrier of the magnetic tape. This stage is termed as the 'Y-axis stage' throughout this thesis. The translational stage has a travel range of 306mm with a maximum velocity up to 100mm/s. DC servo motor with gear-head in combination with the precision rotary encoder is used in the translational stage to ensure high resolution and repeatability. These closed-loop DC motors with shaft mounted position encoders and precision gear-heads provides minimum incremental motion to $0.1\mu\text{m}$ with velocities up to 6mm/s which enables the possibility of getting higher resolution readings. It also has a unidirectional repeatability of $0.2\mu\text{m}$. The translational stage is controlled using a LabVIEW program [hig].

In addition to the movement in Z-axis by KOSY3 coordinate system, an additional linear translational stage (M-403.6DG) was also incorporated in Z-axis for the movement of read head assembly. This stage is termed as the 'Sensor stage' throughout this thesis. This was incorporated to ensure a smooth and collision-free working of the entire system. This translational stage was also used for precise positioning with a travel

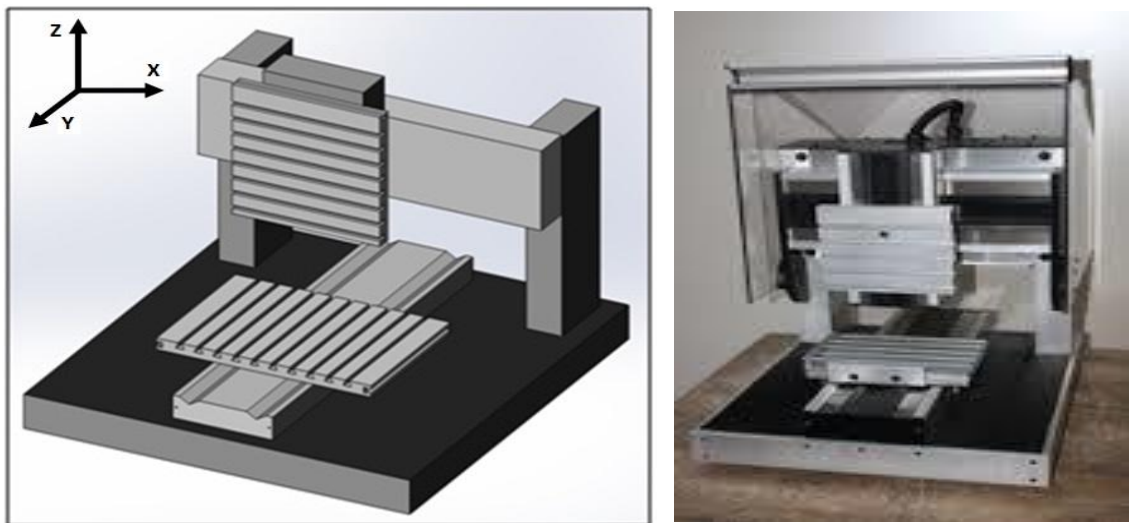


Figure 5.3.1: KOSY3 paltform (a) CAD drawing of the KOSY3 coordinate system (b) KOSY3 platform

range up to 150mm. It has a DC gear motor with a rotary encoder as the integrated sensor. The stage has a minimum incremental motion of $0.2\mu\text{m}$ and a unidirectional repeatability of $1\mu\text{m}$. The translational stage is controlled using a LabVIEW program [pre].

Both the above mentioned linear translational stages were controlled using a DC motor controller (C-863) which ensured a cost-effective and flexible positioning system. Signals from the incremental position sensors were used for axis position and feedback. A reference point was defined on each of the translational stages for determining the absolute target positions. The controller was connected to the PC through Universal Serial Bus (USB) and was controller using a LabVIEW program [mer].

5.3.1 Position reference measurement system

In order to provide a reliable standard evaluation method for the determination of the position of the magnetic tape, a position reference system was mounted on the KOSY3 platform, parallel to the horizontal moving plate in the Y-direction. Two linear encoders, a magnetic encoder, and an optical encoder, and the corresponding scales had been incorporated on the KOSY3 platform as a reference system. The scales moved along with the horizontal plate during the measurement whereas the optical

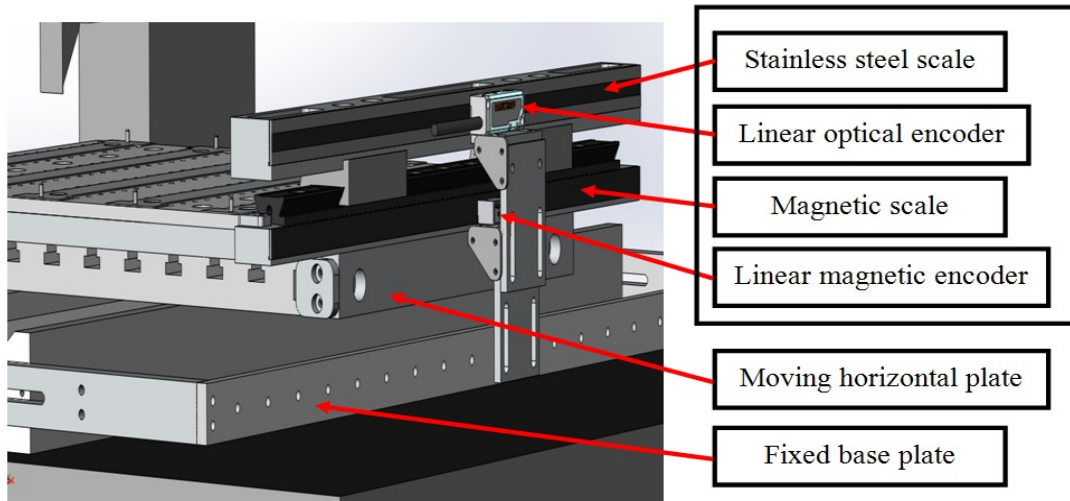


Figure 5.3.2: CAD design of the system with the position reference system comprising of two linear encoders and corresponding scales for evaluation.

and magnetic encoders remained stationary as they were mounted to the base plate of the coordinate table in a fixed position. During the movement of the stage, a relative movement between the linear encoders and the corresponding scales was evaluated and used for positional mapping of the measurement signals. The Figure 5.3.2 shows the 3D model of the position reference system on Y-axis of the KOSY3 platform.

Linear magnetic encoder with magnetic scale of 1mm pole pitch

The ED34 is an incremental linear encoder based on the magnetoresistive sensor technology. For precise incremental displacement measurement, the contact-less magnetic measuring principle is used. The encoder was used with a magnetized scale of 1mm pole pitch with alternating north and south poles. Air gaps up to 0.4mm are possible between scale and the read head. The encoder device was equipped with an internal sine/cosine interpolation unit that supported A/B quadrature output with reliable position information. The small housing could be well integrated into machinery where position feedback was needed. The contactless AMR technology is well suited for applications covered by pollution like dust or oil that could not affect the measurement. The maximum air gap between scale and encoder lower side is 0.4mm [lina]. The Figure 5.3.3 shows the linear magnetic encoder with a magnetic scale.

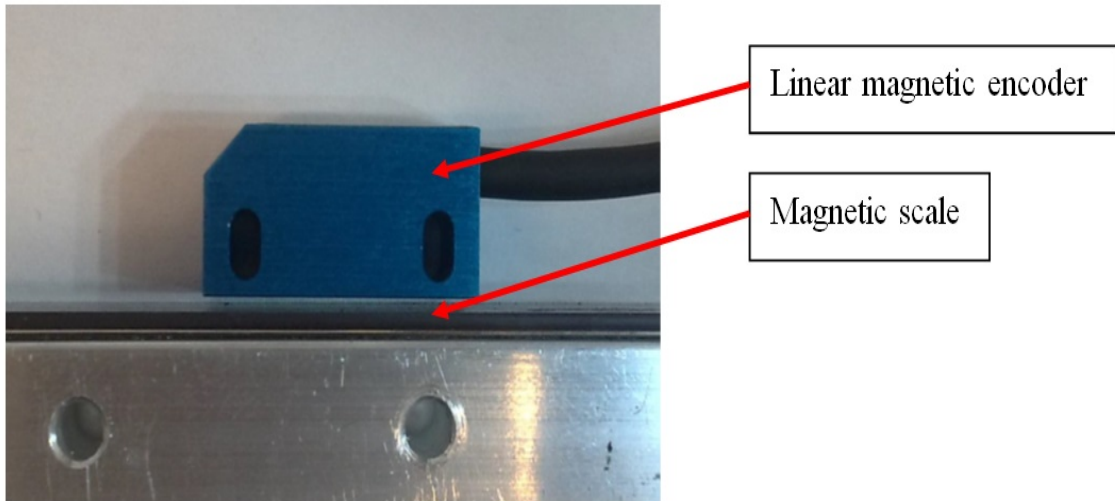


Figure 5.3.3: Linear magnetic encoder with magnetic scale

Linear optical encoder system with stainless steel scale

The linear optical encoder is compact and non-contact. It offers speeds up to 10 m/s and resolutions down to 1nm for both linear and rotary applications. It also gives improved signal stability and long-term reliability. The encoder was equipped with an infra-red LED that emits light onto the scale, which is a plane reflective metal grating of 20 μ m period. The encoder read head optics average the contributions from many scale periods and effectively filters out non-periodic features such as dirt. The system produced photo-currents in the form of four symmetrically phased signals. These are combined to remove DC components and produce cosine and sine signal outputs with low offset and high spectral purity while maintaining a bandwidth of beyond 500 kHz [linb]. The Figure 5.3.4 shows the linear optical encoder used in the position reference system.

5.3.2 Mechanical modeling and structure

The Figure 5.3.5 below shows the 3D model for the entire write and read setup. Figure 5.3.6 displays the construction and assembly of the complete system. A relay system was used to switch the direction of the current flow through the coils of the write head to produce north and south poles as per requirement. Also, two power

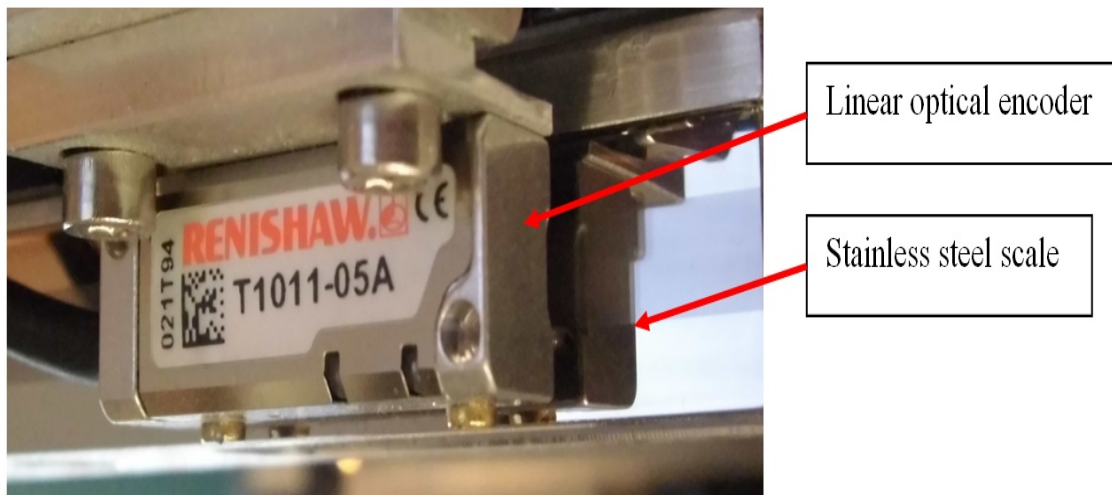


Figure 5.3.4: Linear optical encoder with stainless steel scale

supplies were used, one to power up the write head with 6V and the other to provide the required current to magnetize the magnetic tape.

5.4 DESIGN OF CONTROL PROGRAM

LabVIEW [lab] is a graphical programming language that utilizes icons instead of lines of text to create its applications. In text-based programming languages, instructions determine the program execution, whereas LabVIEW uses data-flow programming in which the flow of data determines the execution. In LabVIEW, a user interface is built with a set of tools and objects. LabVIEW consist of a front panel and a block diagram. The front panel of the LabVIEW is the user interface. In LabVIEW, the graphical representations of functions that control the objects, appear in the front panel. The program written in LabVIEW appears in the block diagram. In other way, the block diagram resembles a flowchart.

LabVIEW programs are also called Virtual Instruments (VIs) because their operation and appearance resemble physical instruments, such as multimeters and oscilloscopes. LabVIEW consist of a complete set of tools for analyzing, acquiring, displaying, and storing data, as well as the tools to debug the written program. In LabVIEW, the user interface, or the front panel is built with indicators and controls. Controls are dials, push buttons, knobs and other input mechanisms. Indicators are LEDs, graphs and

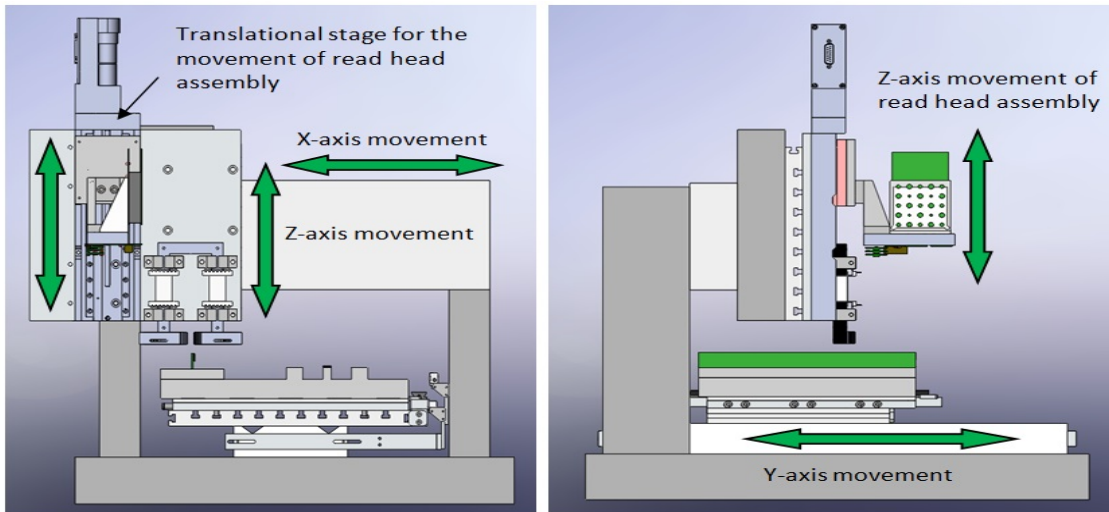


Figure 5.3.5: 3D model of the entire system. Figure on the left shows the front view and the figure on the right shows the side view of the 3D model.

other output displays. After the user interface is built, codes can be added using VIs and structures can be added to control the objects in the front panel. LabVIEW can be used to communicate or interact with hardware devices such as motion control devices, vision and data acquisition, as well as VXI, PXI, GPIB, RS485, and RS232 instruments. The Figure 5.4.1 shows the example of the front panel and block diagram in a LabVIEW program.

Control panel

The Figure 5.4.2 shows the control panel of the main program. This program facilitated the setup and control of the KOSY3 platform and the related hardware. This program was used to control the platform manually as well as automatically. The program starts with an automatic initialization of the complete hardware involved. A detailed explanation for the control panel is given below.

The Figure 5.4.3 shows the part of the control panel, where the manual control can be executed. The speed of the movement of the KOSY3 can be controlled from the keyboard with (+) and (-) keys. The corresponding speed will be displayed on the control panel (a). The movement of the three axes of the KOSY3 in either of the direction can be carried out in (b). Relative movement of a particular axis in the desired direction can be done by setting steps. Continuous movement can be executed from

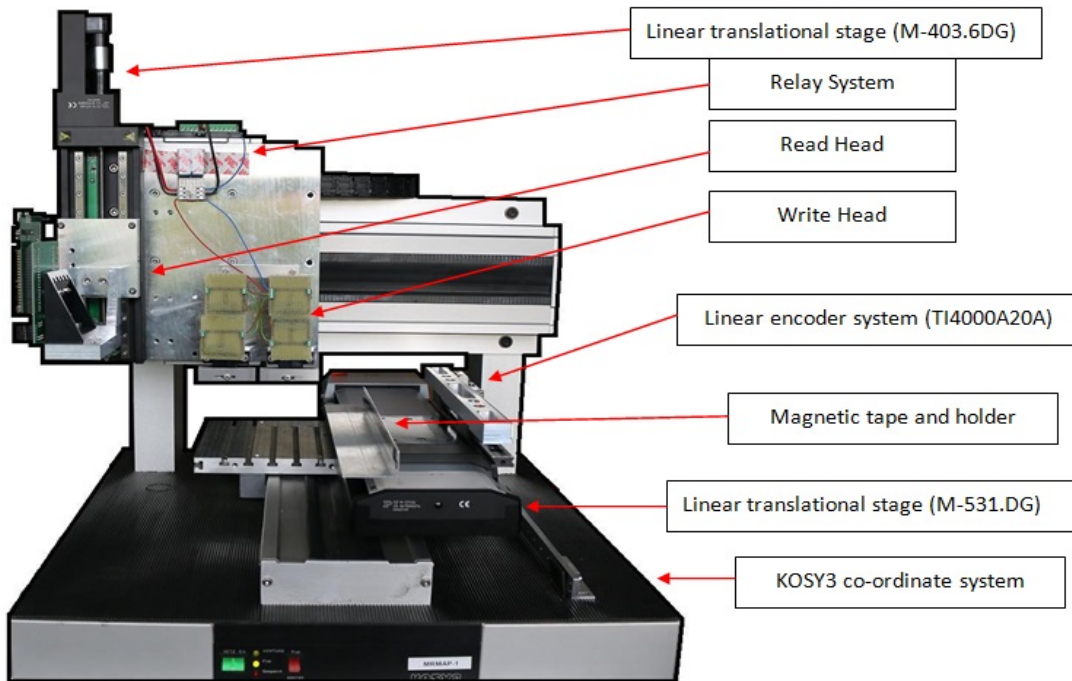


Figure 5.3.6: Apparatus used for write and read process

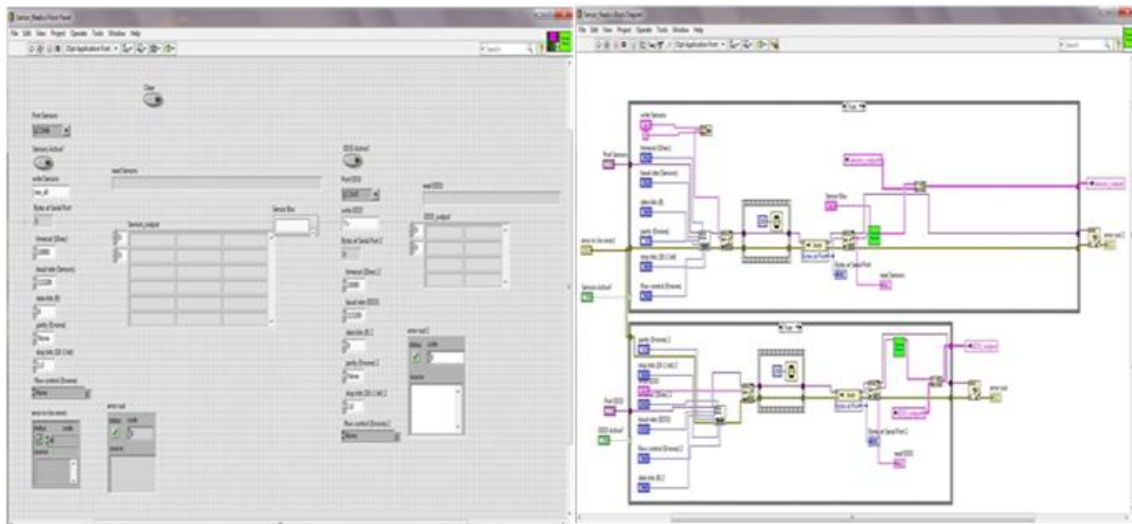


Figure 5.4.1: Front panel and Block Diagram of a LabVIEW program

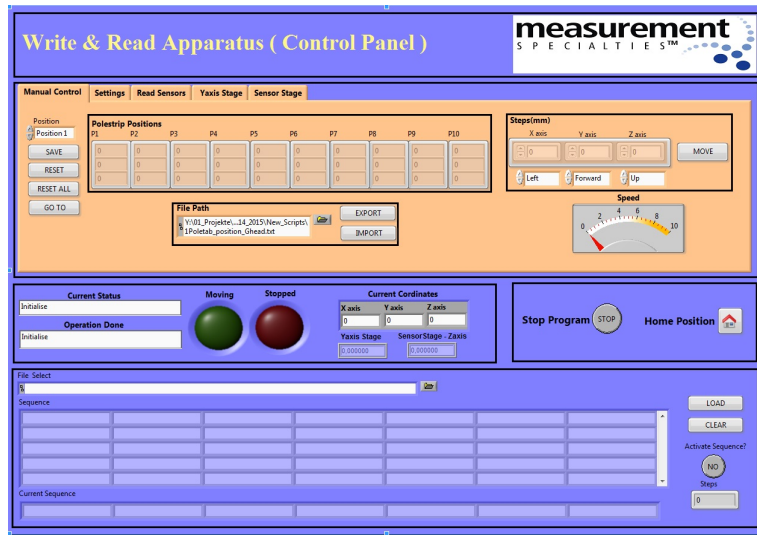


Figure 5.4.2: Control panel of the LabVIEW program

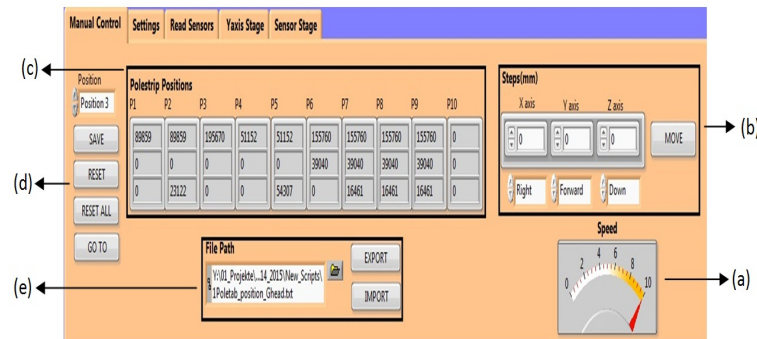


Figure 5.4.3: Manual control of the KOSY3 platform

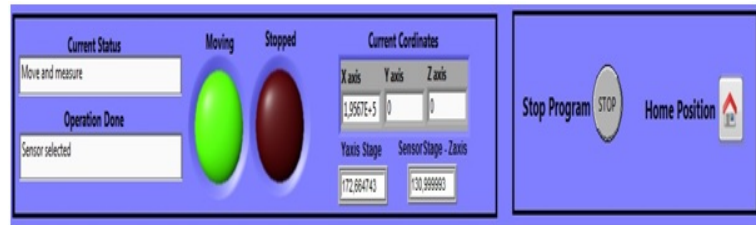


Figure 5.4.4: Information and global control

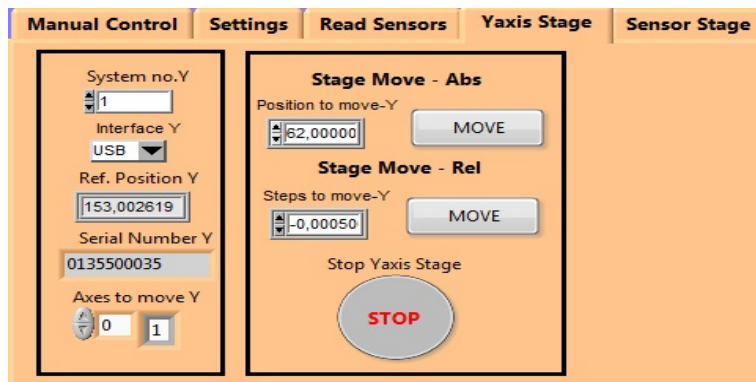


Figure 5.4.5: Control of the translational stage on Y-axis

the keyboard with arrow keys ($\leftarrow, \rightarrow, \uparrow, \downarrow$, page up, page down). Various positions can be saved for future reference using (c) and (d). Although the number of positions that can be saved at a time is limited to 10, these can be further exported to a file using (e) and later imported as per requirement.

The above Figure 5.4.4 shows the part of the control panel that gives the information about the current situation. The program gave feedback on the current status of the system, i.e., the current instruction carried out and also the previous operation done. It also provides the information about the current position of all the three axes of the KOSY3 and also the position of the translational stages on Y-axis and Z-axis. The icons 'Moving' and 'Stopped' show the motion of the platform. The movement of the different parts of the system always requires a safety measure to be taken in urgent situations. Hence, in case of emergency, 'Stop Program' can be used for the immediate termination of the program. It also provides a 'Home Position', by which the 3 axes of the KOSY3 platform moves to the co-ordinate (0, 0, 0) and the translational stages move to its corresponding defined reference positions.

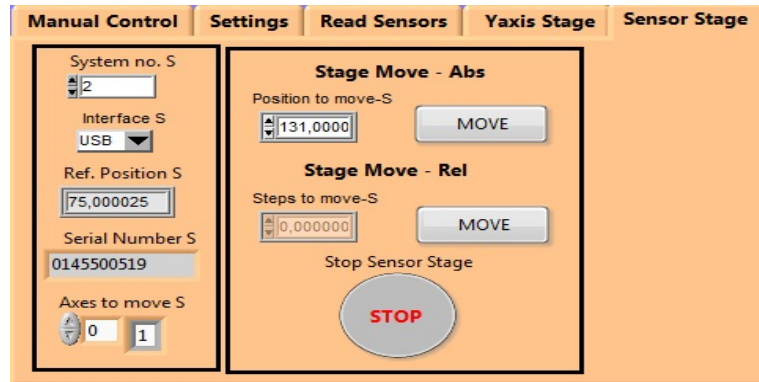


Figure 5.4.6: Control of the translational stage on Z-axis

The initial parameters for the control of the translational stage (M-531.DG) on the Y-axis of the KOSY3 platform are set by default, which can be altered as per requirement. As mentioned above, this translational stage is used for the movement of the magnetic tape with precise positioning. The translational stage can be controlled to move in either direction, either by setting relative steps or by setting the absolute position. After the movement, the current position of the stage will be updated as mentioned above. In case of emergency, the movement of the stage can be terminated anytime using the 'STOP' button. The Figure 5.4.5 shows the part of the control panel to control the translational stage (M-531.DG) on the Y-axis of the KOSY3 platform.

The initial parameters for the control of the translational stage (M-403.6DG) on the Z-axis of the KOSY3 platform are set by default, which can be altered as per requirement. As mentioned above, this translational stage is used for the movement of the Read Head with precise positioning. The translational stage can be controlled to move in either direction, either by setting relative steps or by setting the absolute position. After the movement, the current position of the stage will be updated as mentioned above. In case of emergency, the movement of the stage can be terminated anytime using the 'STOP' button. The Figure 5.4.6 shows the part of the control panel to control the translational stage (M-403.6DG) on the Z-axis of the KOSY3 platform.

The system is equipped with sensors to evaluate the performance of the process. The Figure 5.4.7 shows the part of the control panel where the sensors can be operated and the output can be viewed. The sensors used to evaluate the magnetic scale differ with the pole pitch of the magnetic scale. Hence, in order to see the output, the pole pitch (a) and the corresponding sensor (b) needs to be selected initially. An additional linear encoder system is used for position reference. The result of the sensors can be evaluated either alone (c) or along with the position reference (d).

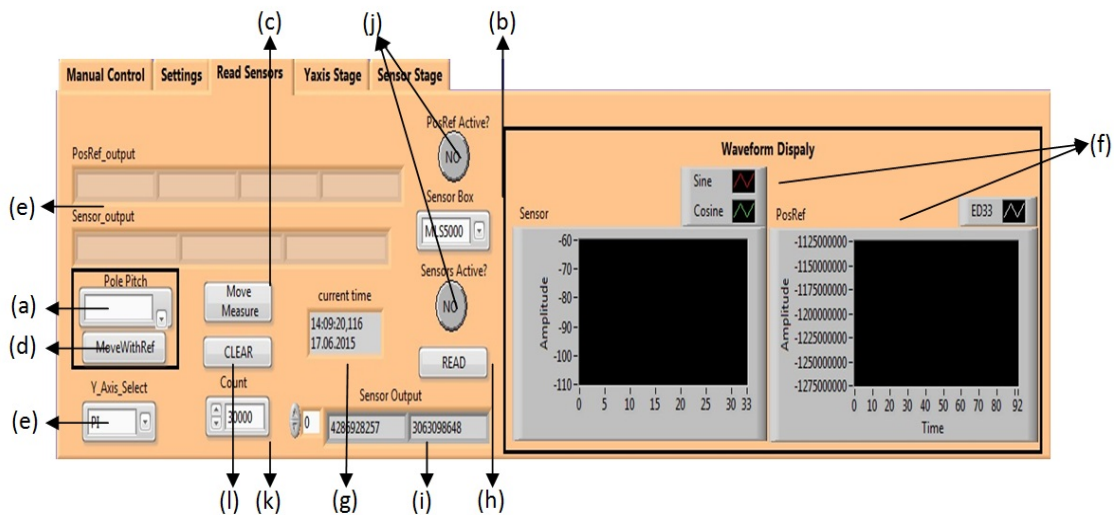


Figure 5.4.7: Sensor Output Display

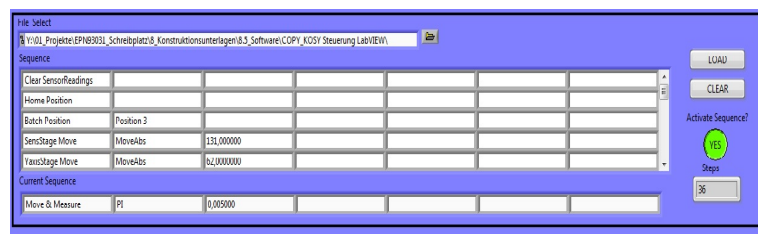


Figure 5.4.8: Automatic sequence display

The output of the sensor and the linear encoder can be viewed (e). The encoder gives two values in one reading – the position and the timer value. The sensor also gives two values – sine and cosine. The corresponding output values are plotted as graphs (f). This part also displays the current time and date (g), which can be recorded to find the time that is taken to complete a single reading or the entire run of the process. It is possible to read the current position of the sensor along with the reference position using (h), which will be displayed at (i). This requires the prior selection of the sensor (j). In order to read values by the sensor for a prescribed length or time, the program can be set to execute in a loop by selecting the sensors and setting the count (k). Once the sensor output values are displayed for a particular run, the graph and the values displayed can be erased (l).

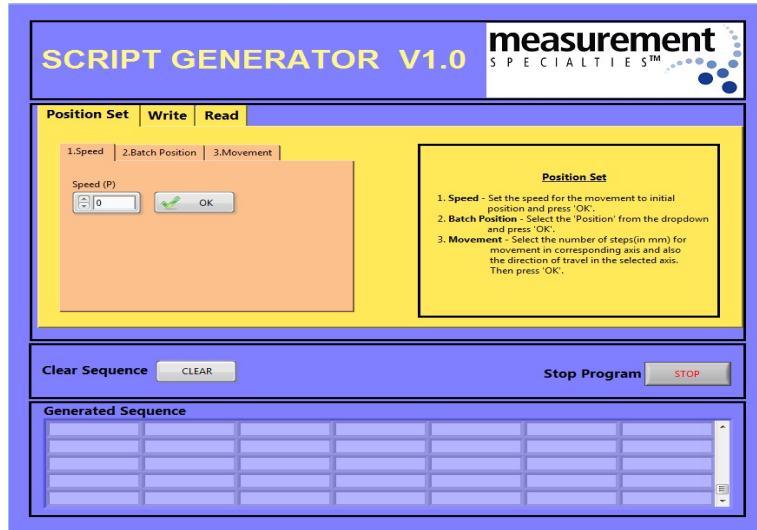


Figure 5.4.9: Script Generator

The above mentioned manual positioning and controlling of the KOSY3 platform and translational stages can be done automatically. In addition to this, the write and read process and the logging of sensor output values is also done automatically by defining the sequence structure. The Figure 5.4.8 shows the part of the control program where the sequence structure can be loaded into the program. Once the sequence is activated, the program detected the sequence one by one until it reaches the end. The count of the steps performed is also displayed. A program is used for generating the sequence structure as shown in Figure 5.4.9.

Program flow

Once the KOSY3 platform is powered, the program starts with an initialization of the complete hardware involved in the system (3 axes of the KOSY3 platform and two additional translational stages in Y and Z axis). The write and read process can be done automatically by importing the automatic sequence structure to the program. The current required for magnetizing the magnetic tape and the pole pitch to be written were initially set in the sequence structure. The automatic sequence structure starts with setting the speed for the write process. The voltage supply for the relay system and the write head should be 'ON'. The current for the magnetization is given and the positions for the write and read head are imported to the program. The program reads the reference position for the start of the write process and directs both the

write head and the translational stage on the Y-axis carrying the magnetic tape, to the corresponding position. Once the write head is in its reference position with the magnetic tape perpendicular to it, the write process starts. At the end of the writing process, the write head is moved to its home position (0,0,0). The program reads the reference position for the start of the read process and directs both the read head and the translational stage on the Y-axis carrying the magnetic tape, to the corresponding position. When the read head is in its reference position with the magnetic tape perpendicular to it, the reading process starts with mentioned resolution. At the end of the reading process, the read head is moved to its home position (0,0,0).

During the time of read process, the values read from the magnetic sensor is saved in an array in the program, which is transferred to an excel sheet at the end of the read process. The excel sheet is analyzed to determine the error at the edges of each pole pitch. If the error determined is in the range of $+/- 10\mu m$, the complete process comes to an end, else a new pole plan is generated according to the error pattern that is desirable to correct the available error. This new error correction pole plan is loaded into the program and the whole process is carried out again. This process is carried out multiple times until the error determined at the edges of each pole pitch is in the range of $+/- 10\mu m$. The program flow is shown in a flowchart Figure 5.4.10.

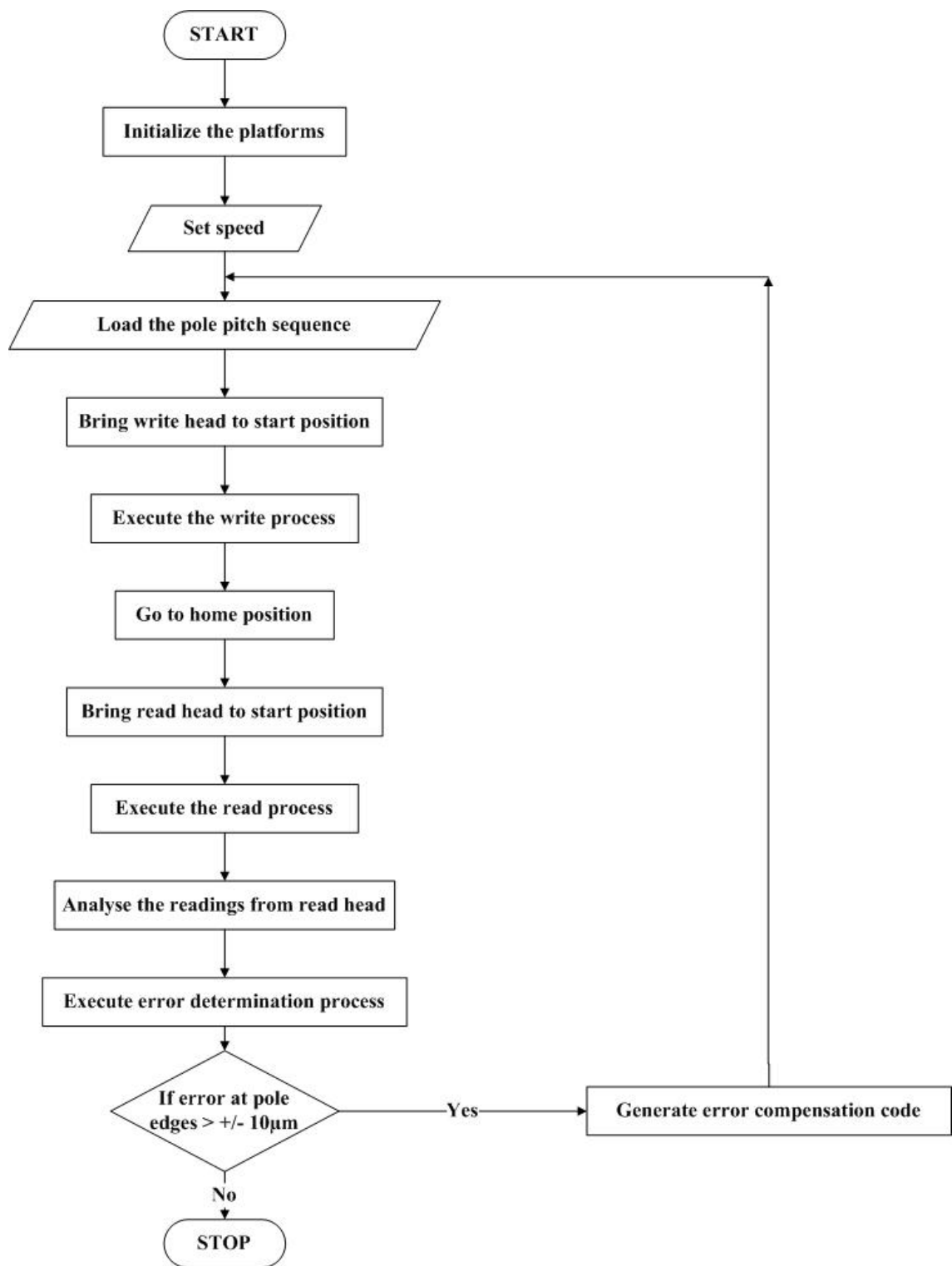


Figure 5.4.10: Flowchart of the program flow

6

SIGNAL PROCESSING AND ANALYSIS

The process of magnetizing a tape is explained in Section 6.1. The magnetization of a magnetic tape was evaluated using a read head (Section 6.2). The magnetoresistive sensor on the read head outputs sine and cosine values with respect to the corresponding position on the magnetic tape (Section 2.5). This chapter gives an overview of how the raw values from the sensor are processed and evaluated to calculate the pole length and thereby determine the error in the pole pitches.

6.1 WRITE PROCESS

The process of magnetizing the magnetic tape was performed by moving the write head over the magnetic tape that was located in between the write tips of the G-head (Subsection 5.1.1). The amount of distance moved by the write head in each iteration depends on the pole pitch to be written on the magnetic tape. This thesis focused on the magnetization of magnetic tape with 5mm pole pitch. The Figure 6.1.1 explains the steps involved in the write process. Initially, the write head was provided with a voltage that induced sufficient electric current to flow through the coil, which produced a magnetic field in the write head. Then the write head was moved over the magnetic tape for a distance of 5mm. Later, the direction of the flow of current through the coils of the write head was reversed, which caused the reversion of the polarity of magnetic field imposed by the write head. The head was again moved for a distance of another 5mm. Similarly, the magnetic tape was periodically magnetized with alternating south and north poles with a single pole pitch of 5mm (periodicity = 10mm).

Following the write process, the written magnetic tape was scanned using a read head as explained in Section 5.2 to evaluate the accuracy of the magnetization process. The sensor output values were further analyzed to determine the exact length of the written pole pitch. The analysis of the sensor output and pole pitch determination is explained below.

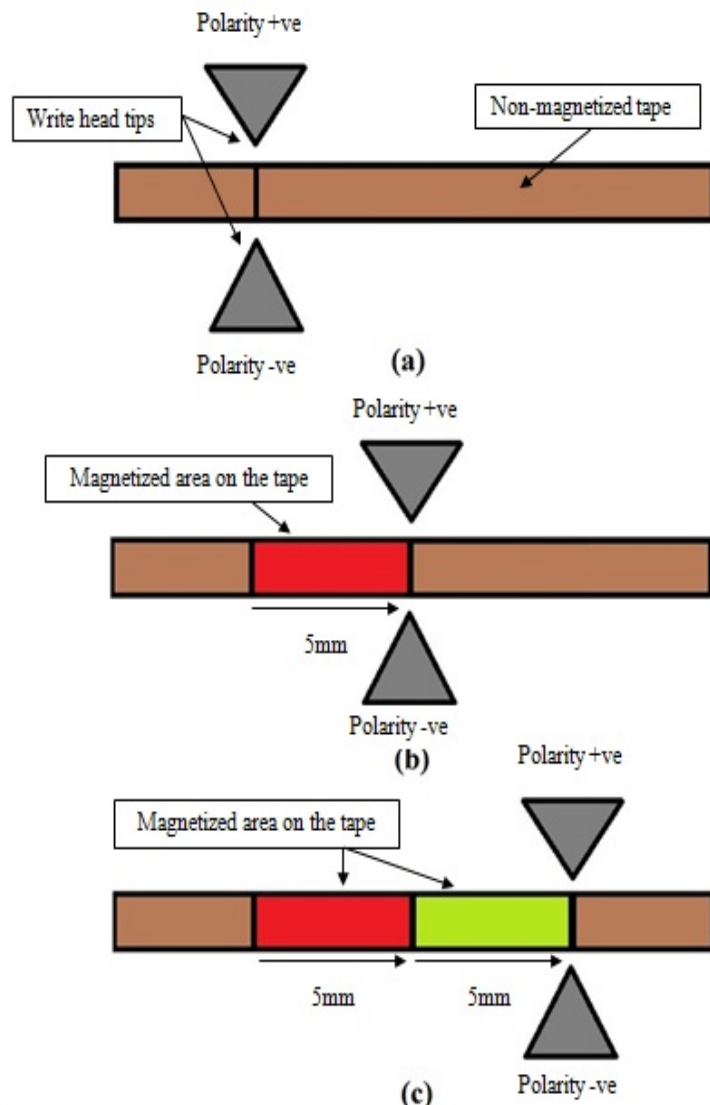


Figure 6.1.1: The write process explained in detail (a) shows the start position of the write head on a non-magnetized tape (b) shows the following stage in which the write head has written a pole pitch of 5mm with a particular polarity (denoted in red color) (c) shows the next stage in which the write head has written another pole pitch of 5mm with reversed polarity (denoted in green color)

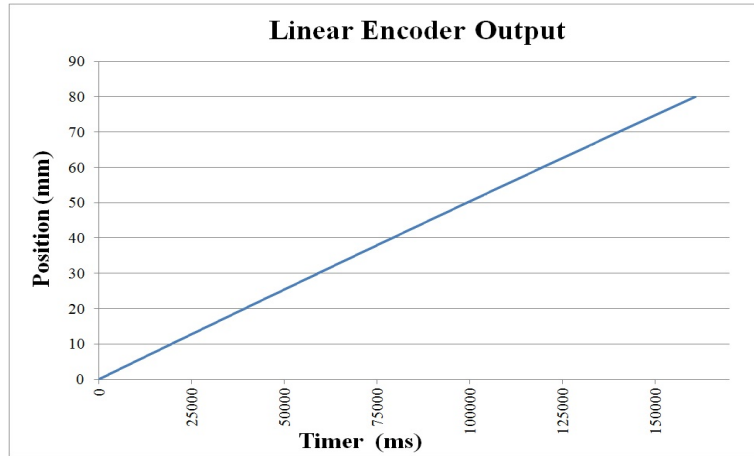


Figure 6.2.1: Output from linear encoder

6.2 READ PROCESS

As explained in Section 6.1, the write process magnetized a non-magnetic tape in required pole pitch. The performance of the magnetization procedure was evaluated by the read process. The read process involved sliding the read head across the written magnetic scale, along with a linear encoder. Two sets of values were obtained as output from the read process, position and timer values from the linear encoder (Subsection 5.3.1) and raw values from the MLS5000 sensor (Subsection 2.5.2) incorporated in the read head. The steps of the evaluation procedure are enumerated below:

Processing raw values

The linear encoder recorded the position and timer values. The position has a resolution of 5nm and the timer has a resolution of $0.05\mu\text{s}$ [linb]. The Figure 6.2.1 shows the graph drawn from the processed output of the linear encoder. The linear encoder was initialized at the beginning of the tape. Later, as the read process progressed, the encoder recorded the position and time of each reading. A resolution of $10\mu\text{m}$ was used in the control program Section 5.4 to record the values throughout the experiments in this thesis. The first recorded position value was depicted as zero and then the difference between two consecutive position values was interpreted in terms of micrometer to calculate the position on the magnetic tape.

The output of the linear encoder and the MLS5000 sensor were analyzed together to determine the pole pitch written on the magnetic tape. The Figure 6.2.2 shows

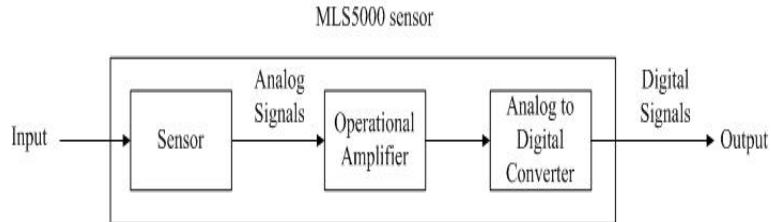


Figure 6.2.2: Block diagram showing the basic functioning of MLS5000 sensor

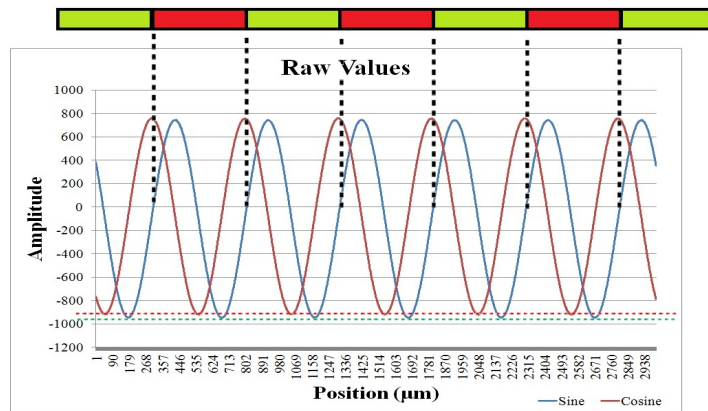


Figure 6.2.3: Raw values from MLS5000 sensor

the block diagram of the basic functioning of the MLS5000 sensor. Depending on the magnetic field in the magnetized tape, the change in the resistance of the transducer in the sensor PCB produced analog signals in the form of voltage. The weak voltage signals were amplified using an operational amplifier. The amplified voltage signals from the op-amp was fed to a 12-bit ADC where these signals were converted into digital signals. The Figure 6.2.3 shows the graph drawn from the raw digital values obtained from MLS5000 sensor. As explained before, the output signals of the sensor were in sine and cosine shapes Subsection 2.5.2. These sine and cosine signals were of different amplitude. The red and green doted lines on the graph show the difference in the amplitude. These values were used to determine the direction of the magnetic field.

The amplitude of these signals interprets the accuracy with which the magnetic angle is determined. Hence, uniform amplitude of both sine and cosine signals definitely results in better analysis of the values resulting in better evaluation. Therefore, an

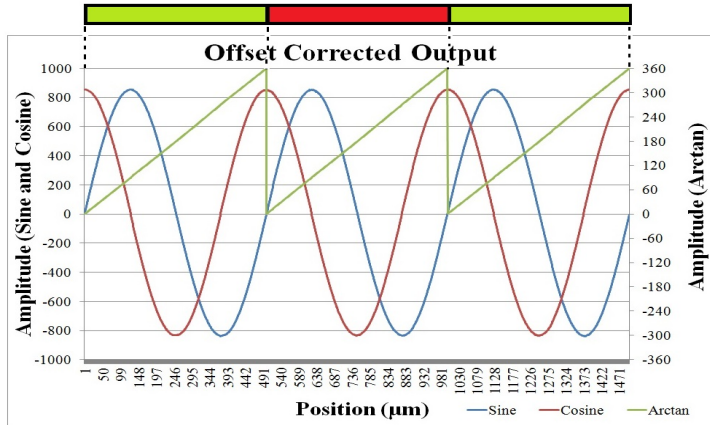


Figure 6.2.4: Offset corrected output of the MLS5000 sensor with the inverse tangent values.

offset correction was applied to the raw values to attain similar amplitude range for both signals. From the obtained sine and cosine values, the inverse tangent of these values were calculated as per Equation 6.2.1, to find the angle of the magnetic field at the corresponding position on the magnetic tape. The resultant inverse tangent values are plotted along with the offset corrected sine and cosine values in Figure 6.2.4.

$$\text{atan2}(y, x) = \begin{cases} \arctan \frac{y}{x} & x > 0 \\ \arctan \frac{y}{x} + \pi & y \geq 0, x < 0 \\ \arctan \frac{y}{x} - \pi & y < 0, x < 0 \\ +\frac{\pi}{2} & y > 0, x = 0 \\ -\frac{\pi}{2} & y < 0, x = 0 \\ \text{undefined} & y = 0, x = 0 \end{cases} \quad (6.2.1)$$

Pole length determination

When plotting the sine and cosine values in XY diagram, Lissajous figure is obtained in the form of a circle. The Figure 6.2.5 shows the XY plot of the raw sensor values as well as the offset corrected sensor values. When MLS5000 sensor was moved for a pole length of 5 mm along the magnetized pole tab, the sine and cosine channel values made one turn along the circle i.e., 360° . This angle was depicted by inverse tangent

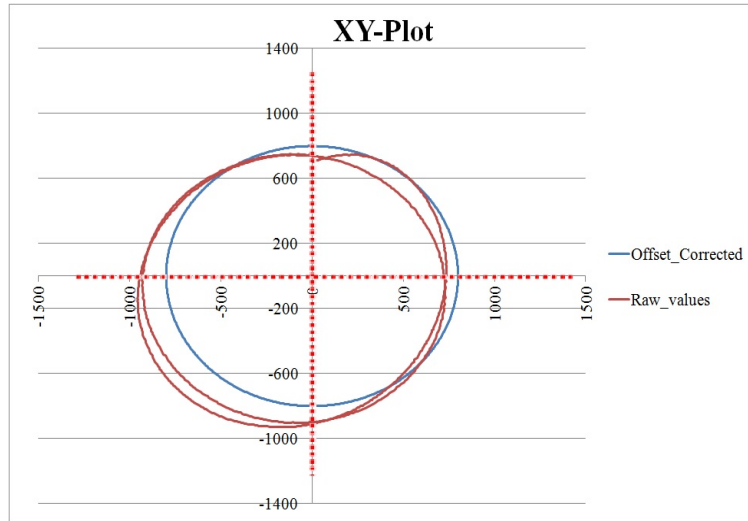


Figure 6.2.5: Lissajous figure of the sine and cosine output signals. The plot with raw sensor values does not form a perfect circle due to the difference in the amplitude of sine and cosine values. Offset corrected values gives a perfect circle.

of sine and cosine values. Therefore, measuring the difference in the position values, between two peaks in the arctangent values, results in the length of the pole tab. The Figure 6.2.6 shows the graph plotting the inverse tangent of sine and cosine values.

Since the written pole pitch is 5mm and the evaluation step size is in micrometer, the ideal pole length should be $5000\mu\text{m}$. The measured differences in the position values, at peaks in the inverse tangent values, are compared with $5000\mu\text{m}$ and are plotted to find the measured pole pitches as shown in Figure 6.2.7. This figure is an example of a magnetic tape measured from the beginning and covering a distance of 10cm. The length of the pole pitch measured was plotted in such a way that the error in the pole length was obtained at the zero position on the Y-axis. Y-axis shows the pole pitch length in micrometer and X-axis shows the corresponding position in micrometer. This way of calculation helped in analyzing the increase or decrease in the pole length in a more reliable way. From the above figure, the errors in the first two pole pitches were measurable, but the succeeding ones were not. Hence, a detailed analysis of this graph was required to determine the error in the pole pitches throughout the magnetic tape. The red dotted line in the figure at the zero position on the Y-axis is the area to be analyzed in detail.

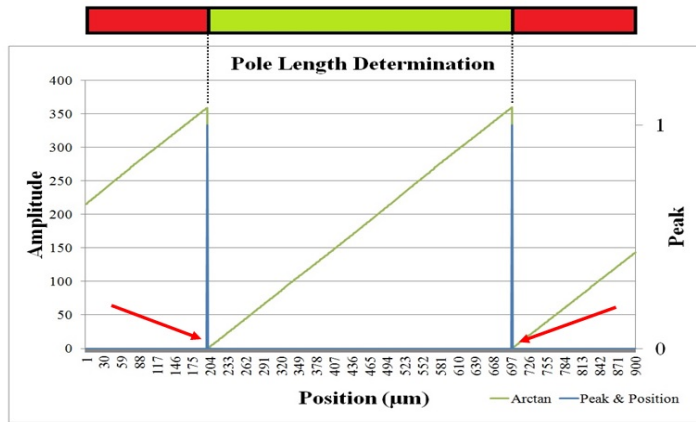


Figure 6.2.6: Pole length determination from the inverse tangent values. The red arrows in the figure shows the start and end position of the pole pitch marked in green on top of the graph.

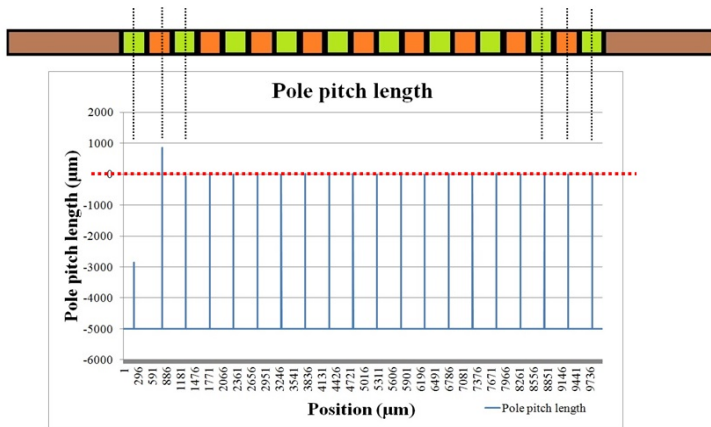


Figure 6.2.7: Pole pitches determined with respect to the alternating south and north poles in a magnetized tape.

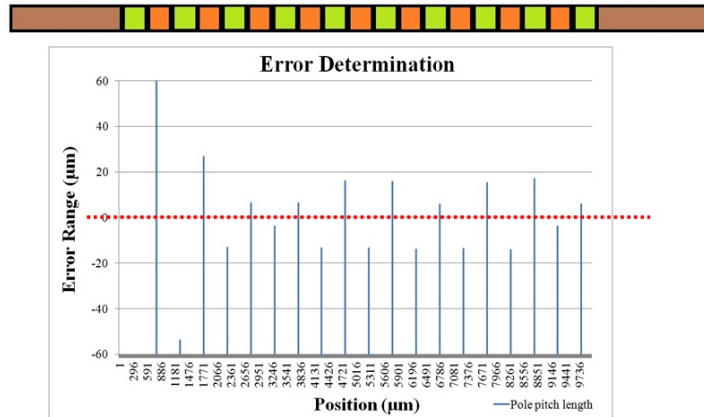


Figure 6.2.8: Detailed analysis of error in pole pitch length

Determination of error in each pole pitch

The Figure 6.2.8 shows the detailed analysis at the pole edges. The Y-axis in this graph gives the error in micrometer at the pole edges of each pole pitch. A red dotted line is drawn in the figure at the zero position on the Y-axis. The following chapter gives a detailed view of experiments that are carried out to perform a detailed study and analysis on the error at the pole edges.

7

EXPERIMENTS AND ANALYSIS

This chapter gives a detailed overview of all the experiments that were carried out to conduct a detailed study on the range and cause of errors in the pole pitch on a magnetized tape. Various parameters affecting the error at the pole edges were analyzed. Section 7.1 discusses the effect of electric current on magnetization. Section 7.2 describes an experiment to study the effect of air gap on the error at the pole pitches. Subsection 7.3.1 and Subsection 7.3.2 explains the error in the positioning of different stages used in the Y-axis movement. An error correction step that is intended to reduce the error is discussed in Section 7.4. Fourier analysis is also carried out to determine the periodicity of the pole pitches in Section 7.5.

7.1 EFFECT OF ELECTRIC CURRENT ON MAGNETIZATION

In order to determine the effect of electric current on magnetization of tape, electric current from 0.5A to 3.5A were applied. The magnetic field intensity in the air gap between the write head tips of G-Head design was measured at different levels of electric currents using a gauss meter. The corresponding values are tabulated in Table 7.1.1. With a current supply of 0.5A to 1.5A, the magnetic field intensity was measured to be 90kA/m - 120kA/m. Later, the current supply was increased and an increase in the magnetic field intensity was observed. From the observed values, a current range of 2.5A to 3.5A was necessary to produce sufficient magnetic field to magnetize Tromaflex (Section 4.1).

Current range (A)	Magnetic field intensity (kA/m)
0.5 – 1.5	90 – 120
1.5 – 2.5	120 – 160
2.5 – 3.5	160 – 350

Table 7.1.1: Effect of electric current on magnetic field intensity measured by a gauss meter

Apart from the values of magnetic field intensity observed from a gauss meter, magnetic tapes were written with current of 1.5A, 2.5A and 3.0A and with an air gap

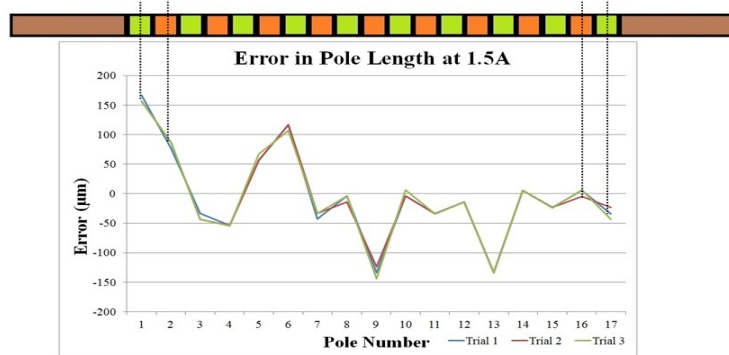


Figure 7.1.1: Error in pole length at pole edges written with 1.5A

of 2mm. The magnetic tapes were analyzed using read head (Subsection 5.2.1). The error at the pole edges were calculated and plotted as mentioned in the Section 6.2. Figure 7.1.1, Figure 7.1.2 and Figure 7.1.3 show the analysis of magnetic tapes written with 1.5A, 2.5A and 3.0A respectively. The Figure 7.1.1 shows that the error at the pole edges lies in a range of +/-200μm. Moreover, the behavior of the error was non-homogeneous. Figure 7.1.2 shows that the error at the pole edges reduced to a range of +/-100μm. Further reduction in the error at pole edges to a range of +/-60μm was observed in Figure 7.1.3. It is evident from the graphs that, increase in the current resulted in a stronger magnetic field which resulted in lesser error range at the pole pitches although the behavior of the error was still non-homogeneous.

From the results analyzed above, it is evident that a decrease in the error range was observed with increase in the current supply. As the magnetic circuit used in the experiment has a resistance of 4Ω and a 12V power supply was used to power the circuit. Increasing current above 3.0A was not a good measure, as further increase in current will result in the maximum possible limit of current supply. Hence, 3.0A was observed as the ideal current limit to obtain sufficient magnetic field intensity at the write tips of the G-head design. The results of error range observed from the magnetic tape are summarized in Table 7.1.2.

7.2 EFFECT OF AIR GAP ON MAGNETIZATION

This section explains the experiments carried out to study the effect of air gap between the write head and the magnetic tape. Previous experiments were carried out with an air gap of 2mm. This air gap was selected based on magnetic simulation results.

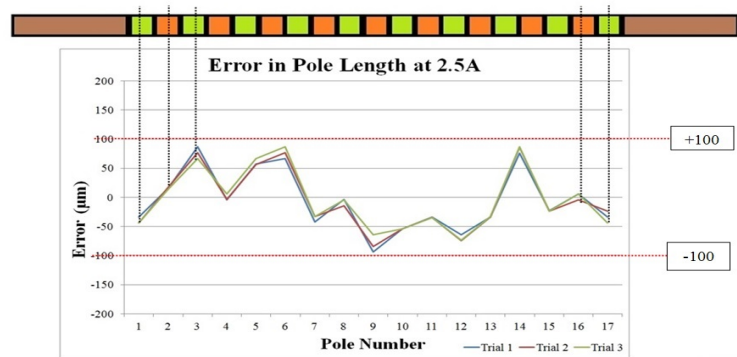


Figure 7.1.2: Error in pole length at pole edges written with 2.5A

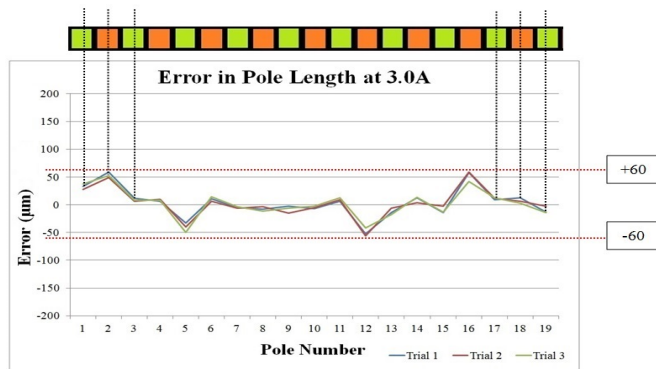


Figure 7.1.3: Error in pole length at pole edges written with 3.0A

Current (A)	Error range in pole pitch (μm)
1.5	+/-200
2.5	+/-100
3.0	+/-60

Table 7.1.2: Error range at pole edges for various level of electric current

With 2mm air gap and 3.0A current, the resulted error range was +/−60μm. The permeability of free space (a vacuum) is a physical constant equal to approximately $1.257 * 10^{-6}\text{H/m}$ (Henry per meter). It is denoted by μ_0 . Permeability, μ is a constant of proportionality that exists between magnetic flux density and magnetic field strength in a given medium. In metals like pure iron, μ is substantially greater than μ_0 . Hence, there is a possibility of acquiring stronger magnetic field with reduced air gap between write tip and magnetic tape [RMCo8]. Figure 7.2.1 shows the equivalent circuit for a magnetic circuit with air gap. In the diagram, F is the magnetizing force, ϕ_m is the magnetic flux flowing through the circuit, R_c is the reluctance in the circuit and R_g is the reluctance across the air gap. Equation 7.2.1 shows the effect of air gap on the magnetic circuit. From the equation, it is clear that an decrease in the air gap results in the decrease in the reluctance, thereby increasing the magnetic flux flowing through the circuit. Hence, an experiment was carried out with decreased air gap.

$$\phi_m = \frac{F}{R_c + R_g} \quad (7.2.1)$$

The experiment in this section was carried out with 1mm air gap and 3.0A current. The resultant graph is given in Figure 7.2.2. From the graph, it is evident that the error at the pole edges reduced to a range of +/−50μm. Hence, from the experiments conducted, the ideal air gap was found to be 1mm and ideal current supply to be 3.0A. The results are summarized in Table 7.2.1.

7.3 ANALYSIS OF MAGNETIZATION EFFECTS ON 5MM POLE PITCH

The above sections explained the experiments conducted to analyze the effect of various parameters on the magnetization of magnetic tape. All the experiments were carried out on 5mm pole pitches and analyzed using MLS5000 sensor. The results were summarized in graphs and were discussed in detail. Changing the values of the

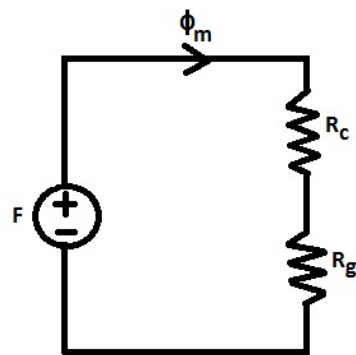


Figure 7.2.1: Equivalent circuit diagram of a magnetic circuit with air gap

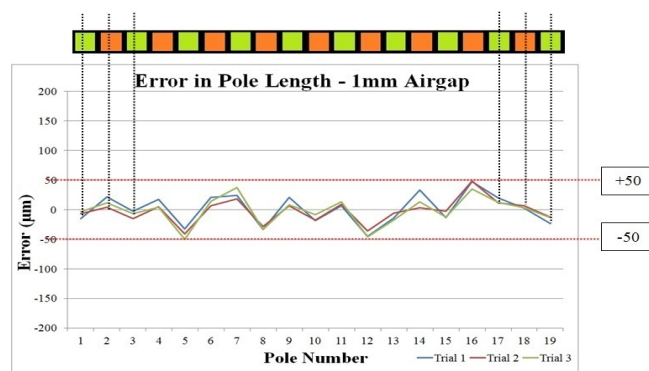


Figure 7.2.2: Error in pole length written with 1mm air gap

Air gap (mm)	Error range in pole pitch (μm)
2	+/-60
1	+/-50

Table 7.2.1: Effect of air gap on the error range at pole edges

parameters in a particular range showed increase and decrease in the error caused at the pole edges in the written pole tab. Hence, these experiments gave an overview of the accuracy that can be attained at the pole pitches with the optimum values for the parameters.

This section involves conducting an extensive study on the cause of the error at the pole edges. The pole tab written on the magnetic tape is evaluated by comparing the sine and cosine signals obtained from the sensor with reference to the corresponding position on the magnetic tape. Hence, in this evaluation method, determination of accurate precision is highly important. The evaluation process involves setting a particular step size for the Y-axis movement which holds the magnetic tape and the readings of the sensor at each step size is recorded and assessed. Error in positioning may cause error in pole length. This incorporates the need of measuring the accuracy and repeatability of the platform in Y-axis.

7.3.1 *Effect of positioning error by KOSY3 stage*

The positioning error in the Y-axis movement of the KOSY3 platform can be measured with reference to the linear encoder system attached to the Y- axis of the KOSY3 platform (Subsection 5.3.1). The Y-axis of the KOSY3 platform moves according to the step size given and the linear encoder records the position in steps after each movement. With a resolution of 5nm [linb], the difference between two recorded positions of the linear encoder is compared to the step size of the KOSY3 platform and the error in positioning is measured.

Figure 7.3.1 shows the positioning error in the Y-axis of KOSY3 platform at each step. The KOSY3 platform was moved with a step size equivalent to $10\mu\text{m}$ to a distance of 80mm (8000 steps) and the corresponding position values from the linear encoder were recorded. The difference between the position values at each step was calculated and compared with $10\mu\text{m}$ to find the positioning error. The error ranges between $+/-5\mu\text{m}$. Therefore, one of the causes for the error at the pole edges was the positioning error caused by the KOSY3 platform.

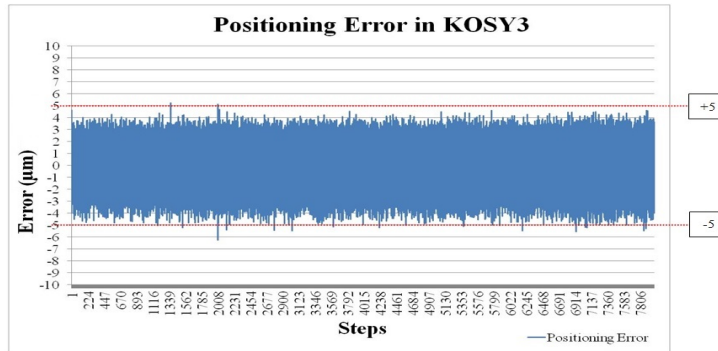


Figure 7.3.1: Positioning error in Y-axis of KOSY3

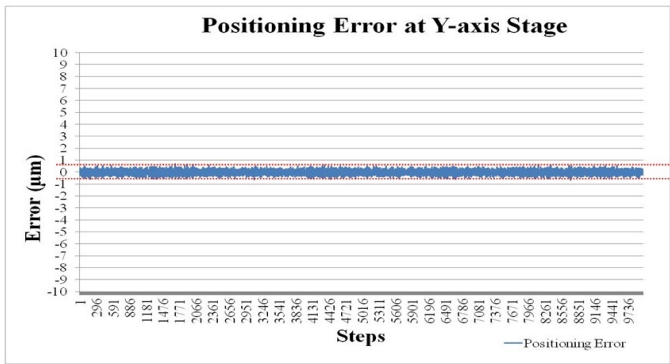


Figure 7.3.2: Positioning error in linear translational stage in Y-axis

7.3.2 Effect of positioning error by PI stage

In order to rectify the positioning error caused by the Y-axis of the KOSY3 platform, the linear translational stage (M-531.DG) was adhered to the Y-axis and this was used as the movement in the corresponding axis. Similar experiment was carried out with translational linear stage moving with a step size equivalent to $10\mu\text{m}$ to a distance of 100mm (10,000 steps) and the corresponding position values from the linear encoder were recorded. The difference between the position values at each step was calculated and compared with $10\mu\text{m}$ to find the positioning error.

The Figure 7.3.2 shows the positioning error in the linear translational stage at the Y-axis of KOSY3 platform at each step. The error range was $\pm 0.5\mu\text{m}$. The comparison of the positioning error caused by various stages is tabulated in Table 7.3.1. From the

Y-axis movement	Positioning error range (μm)
KOSY3	+/-5
Linear Translational Stage	+/-0.5

Table 7.3.1: Positioning error due to different stages in Y-axis

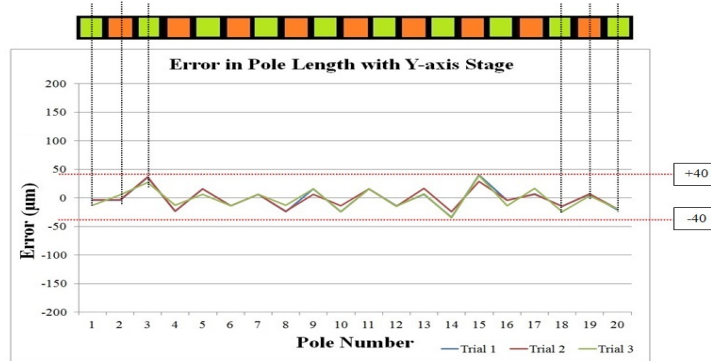


Figure 7.3.3: Error in pole length with Y-axis stage

Figure 7.3.2, it is clear that replacing the Y-axis movement of the KOSY3 platform with the linear translational stage has resulted in a decrease in the positioning error. With the linear translational stage on Y-axis on which the magnetic tape and the holder were fixed, the write and read process were carried out with optimum parameter values (1mm air gap and 3.0A). Figure 7.3.3 shows the resultant graph from the experiment that shows an error range of +/-40 μm . Decrease in the positioning error has resulted in a decrease in the error at the pole edges. Moreover, the behavior of the error appeared to be homogeneous i.e., an increase in a pole length was followed by a decrease in the next pole length.

In the above sections, experiments were carried out to determine the error at the pole pitches and an acceptable range of error at the pole edges was obtained which was comparable with other standard magnetic tapes available in market. The magnetic scales from Bogen Electronics were used for comparison and the standard accuracy of the magnetic scales were claimed to be in the range of +/-40 μm as shown in Figure 7.3.4 [mag]

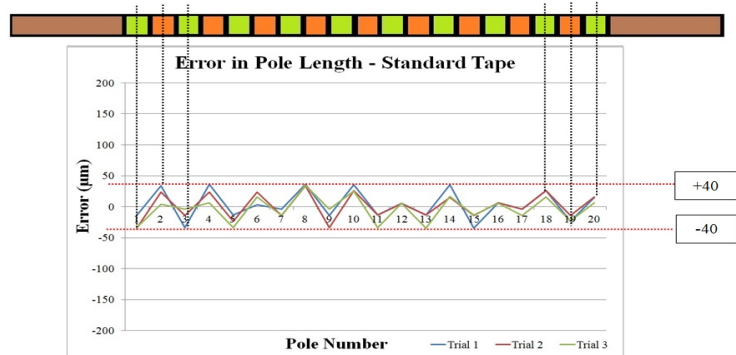


Figure 7.3.4: Error in pole length on a standard magnetic tape

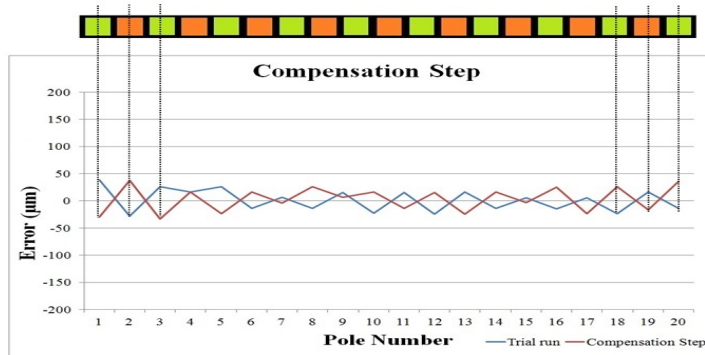


Figure 7.4.1: Effect of compensation step

7.4 ANALYSIS OF ERROR CORRECTION ON 5MM POLE PITCH

Apart from the acceptable range of error at the pole edges, further studies and analysis were executed to determine the possibility of further reduction in the error at the pole edges. Various trial runs were carried out to correct the error at the pole edges. From the first step of write and read process, the error in each pole pitch was calculated and a new correction pole pitch code was generated. This correction code was re-written on the same magnetic tape as an error compensation step. It was then evaluated using MLS5000 sensor and the error at the pole edges were calculated.

Figure 7.4.1 shows the comparison of error in the pole length before and after incorporating the error compensation step on the same magnetic tape. The graph shows a reverse behavior in the polarity of the error at the pole edges after error

correction, without much decrease in the magnitude of the error. Multiple trial runs were carried out that resulted in a similar behavior. The results from these experiments emphasized on the fact that the error compensation step did not favor in reducing the error at the pole edges but resulted in a shift of error to either side. The reason for this was assumed to be the sudden change in the direction of the current flow in the magnetic coils during the write process that causes the error at the pole edges to remain in the range of $+/-40\mu\text{m}$.

Further analysis was carried out by conducting an experiment to remove the effect of reversing of the direction of the current flow from the magnetic tape as shown in Figure 7.4.2. Figure 7.4.3 shows the step by step execution of the error correction step carried out in this experiment. In the experiment, the write process was carried out in such a way that the direction reversal of the current flow in the magnetic coils, to write alternate poles on the magnetic tape, was performed at a distance of 20mm to the top of the magnetic tape. This distance was chosen to ensure that the direction reversal takes place at safe distance from the magnetic tape. Figure 7.4.4 shows the error at each pole pitch on a completely written magnetic tape in comparison to a pictorial representation of the magnetized tape. From the figure, it is evident that, other than the first and last two pole pitches, the rest of the pole pitches in the middle of the magnetic tape have a stable lesser error ranges at the pole edges. Since the read head did not have a reference position to detect the beginning of the magnetic tape, the sensor read the magnetic tape at an ambiguous position other than the exact start position of the first pole written on the magnetic tape. Hence, the first pole pitch cannot be detected accurately. Similarly, the last pole written on the magnetic tape is supposed to have left the shades of the last written pole on the non-magnetic part of the magnetic tape.

Figure 7.4.5 shows a detailed view of the error at the middle pole pitches given in Figure 7.4.4. The error at the pole edges are in the range of $+/-20\mu\text{m}$. The error in the pole lengths on the magnetic tape, written without the effect of reversing of the direction of the current flow, has resulted in a lesser error. The error behavior was homogeneous and was stable over a much longer range of the magnetic tape.

7.5 FOURIER ANALYSIS OF SIGNALS

Joseph Fourier showed that a periodic signal can always be expressed as a sum of sinusoids (sines and cosines or sines with angles). Hence, this representation is called a Fourier Series in his honor [Wal96]. Since the received signal from the read head is periodic with respect to distance, Fourier analysis was performed on the received

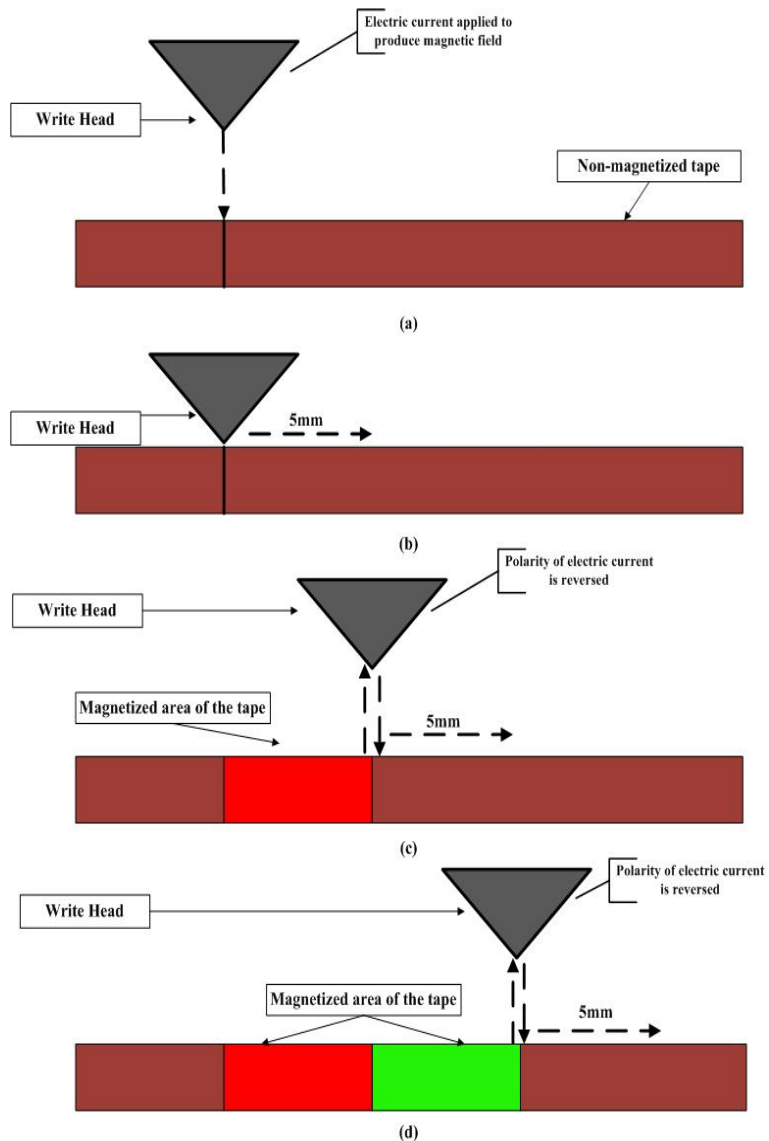


Figure 7.4.2: Correction step to reduce error at pole edges (a) Beginning of write process where the electric current is supplied to the write head, placed at a distance from the tape, producing magnetic field in the circuit (b) Write head at the tape to magnetize it (c) After magnetizing a pole, the write head again moves to a distance where the polarity of the electric current is reversed (d) same process as in step (c) is repeated to magnetize another pole reverse polarity

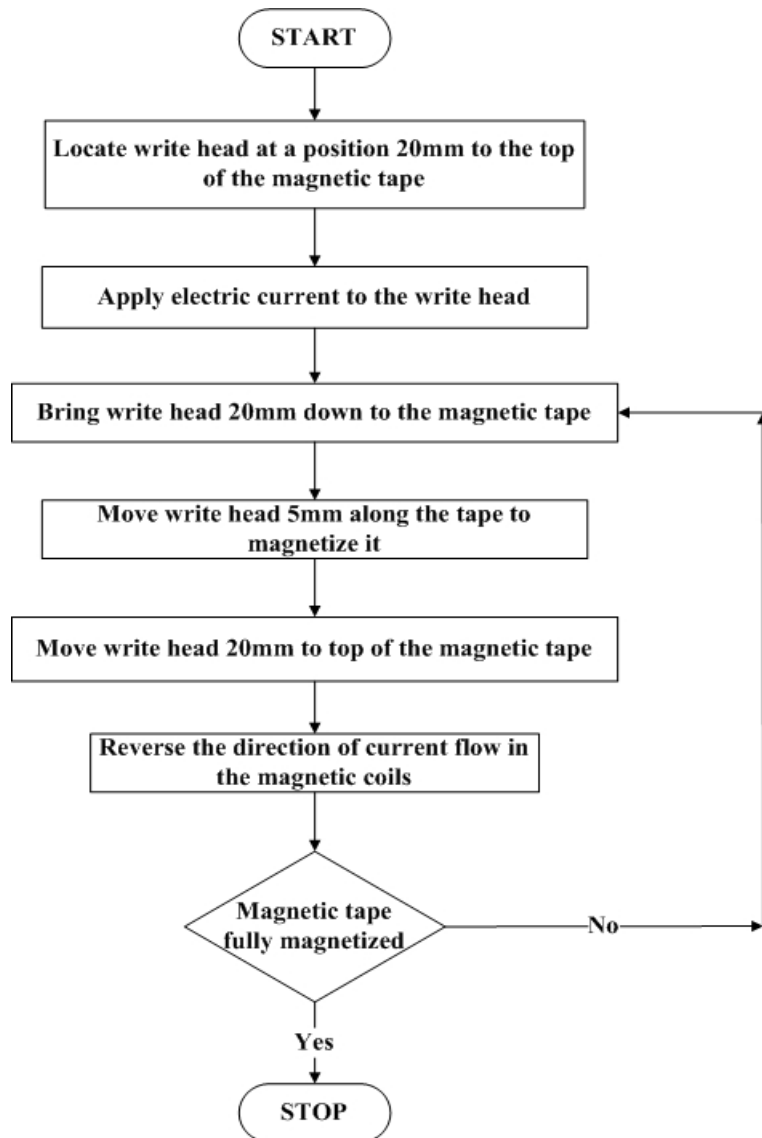


Figure 7.4.3: Flowchart of error correction step

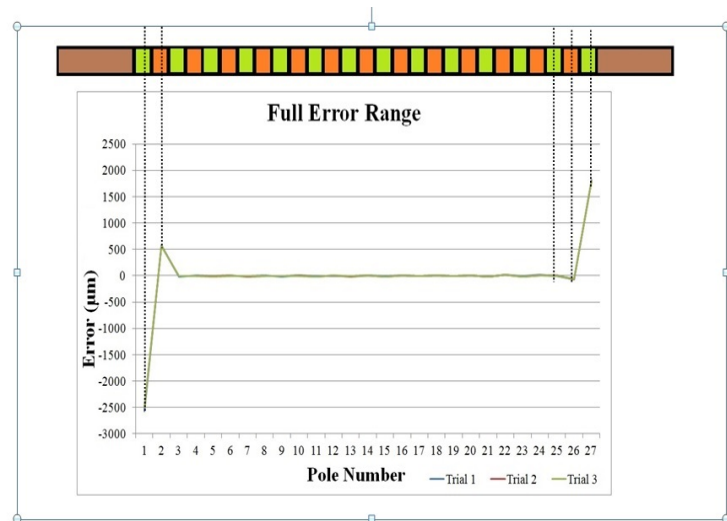


Figure 7.4.4: Full error range in pole pitch with comparison to the magnetic scales

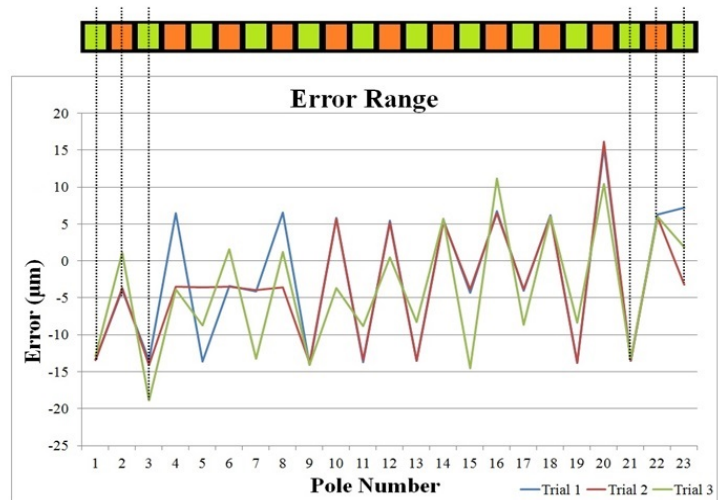


Figure 7.4.5: Error range in the middle pole pitches

signal in order to obtain the periodicity of signal with respect to distance. Fourier analysis was carried out as a comparison to the method of determining the length of pole pitch written on a magnetic tape (Section 6.2). In this thesis, distance dependent signals were considered instead of time-dependent signals. Hence, the term 'Frequency' denotes the reciprocal of distance.

The Fast Fourier transform (FFT) was computed with the signals to reduces the number of computations needed for N points from $2N^2$ to $2N\lg N$, where \lg is the base-2 logarithm [Wal96]. $4096(2^{10})$ number of samples were used to compute FFT in MATLAB [MAT10] that yielded FFT complex values using Equation 7.5.1. The FFT magnitude of the complex values were calculated. Sampling frequency was calculated using Equation 7.5.2 and was found to be 0.1998. The step value to determine the interval in the frequency values were calculated by Equation 7.5.3 and was found to be $4.8779 * 10^{-5}$. Figure 7.5.1 shows the graph plotting FFT magnitude versus frequency. The dominant or the fundamental frequency was determined from the graph to be 0.000195116. The period of the signals analyzed were determined using Equation 7.5.4 to be $5125.165\mu\text{m}$. Figure 7.5.2 shows the plot of even and odd harmonics till 7th harmonic calculated from the signals of the MLS5000 sensor. The figure shows that the signals have only a single dominant frequency. This is because of the arrangement of the resistors in the Wheatstone bridge in the sensor hardware, that results in the cancellation of further harmonic signals [A.M15].

$$F(x) = \sum_{n=0}^{N-1} f(n) e^{-j2\pi(x\frac{n}{N})} \quad (7.5.1)$$

$$\text{Samplingfrequency} = \frac{\text{Number of samples}}{\text{Last position} - \text{First position}} \quad (7.5.2)$$

$$\text{Stepvalue} = \frac{\text{Sampling frequency}}{\text{Number of samples}} \quad (7.5.3)$$

$$\text{Period} = \frac{1}{\text{Dominant frequency}} \quad (7.5.4)$$

The results from the Fourier analysis showed that the periodicity of the signals from the sensors was 5125.165 . Hence, an error of $+125.165\mu\text{m}$ resulted from the signals. This is due to the fact that in n-point FFT, the harmonic analysis of the frequencies

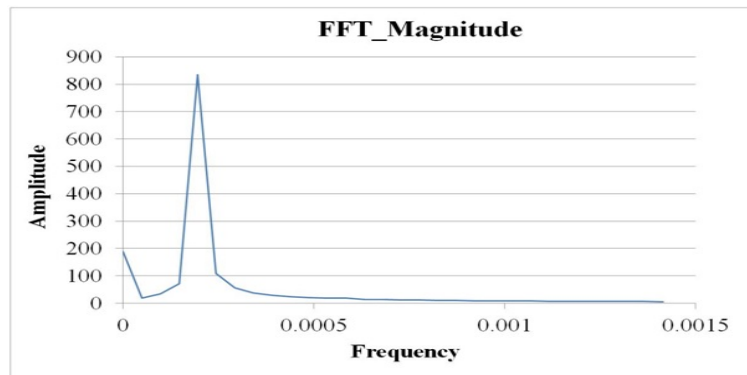


Figure 7.5.1: Fast Fourier transform magnitude plotted against frequency

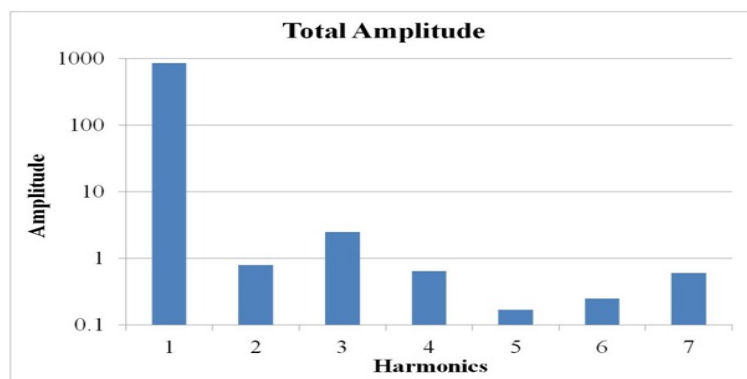


Figure 7.5.2: Harmonic analysis

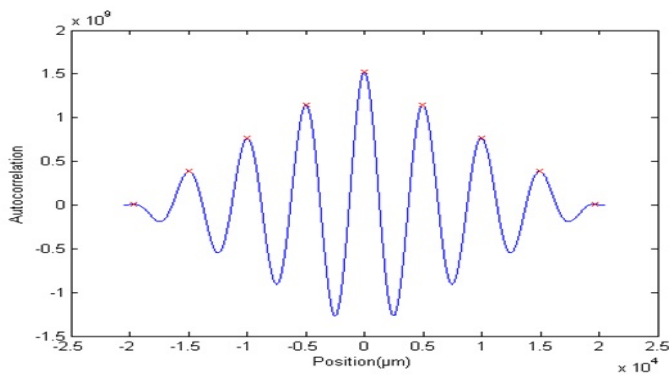


Figure 7.5.3: Autocorrelation of signals

Difference in position between two peaks (μm)	Error (μm)
5019	+19
4986	-14
4985	-15
4980	-20
5013	+13
4985	-15
4995	-5
5005	+5

Table 7.5.1: Difference in the position values between two peaks of the signals from autocorrelation

is dependent on the number of samples, N and they are the integer multiples of the fundamental frequency. Hence, when the number of samples is not a multiple of the signal period, there may be harmonic components whose frequencies are not expressible in the N-point FFT spectrum. This causes a “leakage” of such frequencies in the spectrum [SR12]. Hence, the periodicity found from the Fourier analysis was not the exact one. As an alternative, autocorrelation was performed on the signals from the sensor. Autocorrelation sequence of a period signal has the same cyclic characteristics as the signal. Hence, autocorrelation can help in verifying the presence of cycles and determine their periodicity. Figure 7.5.3 shows the graph of autocorrelation on the signals, carried out in MATLAB [MAT10]. The difference in the positions between every two peaks were calculated and tabulated in Table 7.5.1. Analyzing the results in the table, it is clear that the periodicity of the signal lies between $4980\mu\text{m}$ and $5019\mu\text{m}$ on an average.

8

CONCLUSION

Magnetic measurement technology has been successfully applied in various industries for decades. Depending on the specific requirements involved, this technology provides a basis for the derivation of suitable products. Magnetic tapes are extensively used as an information recording medium. Position and angular information storage in harsh environments utilize magnetic tapes since they are highly resistant to smoke,dirt,humidity etc. Also, they are wear-free. Hence, magnetic tapes are widely used in applications like drive technology, level measurements, valve actuators,automation and handling and feedback system in hydraulic axes. The widely used methods for recording information on a magnetic tape are longitudinal and perpendicular magnetic recording. Longitudinal recording technology was widely used for data recording in commercial applications. Recently, perpendicular recording technology gained popularity due to its capability to deliver higher storage density when compared to traditional longitudinal recording.

This thesis focused on the design and construction of an apparatus to produce multi-pole tab magnetic scales, using perpendicular magnetic recording technology, with the robust performance for any linear position sensing application. Initially, the requirement analysis was performed to build a setup with a write head to magnetize the magnetic tape and a read head to evaluate the written magnetic scales. Different guided flux write head designs were analyzed using magnetic field simulation among which a G-Head design with a pure iron core and 4 coils of 1000 windings each was chosen to be constructed based on the simulation results. The 3D modeling of proposed head design was carried out and subsequently a prototype was constructed. In order to assess the efficiency of the write head, a read head was designed. The read head was designed in such a way that it could accommodate multiple sensors to evaluate different types of magnetic scales written. To automate the complete process, a control program was developed in LabVIEW. Hence, a complete apparatus was developed to magnetize tapes.

In order to evaluate the efficiency of the process of magnetization, various experiments were carried out. These experiments focused on the study of effect of electric current and air gap on the error at the pole edges. A position reference system with an additional linear encoder system was used to calculate the accuracy of the magnetization process. The optimum values of the above-mentioned parameters. With 1mm

air gap and 3.0A current supply, the error in the pole length was found to be in the range of $+/- 40\mu m$, which was in a comparable range with the accuracy of standard magnetic tapes available in the market [mag]. Further analysis of the error range led to a correction step that nullified the effect of reversing the direction of current flow on the magnetic tapes. This resulted in the reduction of error in pole length to a stable range of $+/- 20\mu m$ over the middle poles on a fully written magnetic tape. One of the most important outcome of this thesis work is that the designed apparatus could achieve an accuracy of $+/- 20\mu m$ on the magnetic tape, which is comparable to the accuracy of a high resolution magnetic tape available in the market [mag].

Furthermore, as an extension of the experiments carried out in this thesis with the available hardware setup, different pole pitches of 2mm and 1mm can be written and evaluated using MLS2000 and MLS1000 sensors respectively. A similar set of experiments can be conducted to assess the performance of M-Head design on 5mm, 2mm and 1mm pole pitches. As an improvement to the current G-Head design, the width of the write tip can be reduced from 1mm to 0.5mm and a detailed study can be conducted to evaluate the effect of thinner write tip on magnetization and the magnitude of error caused at the pole edges. The effect of magnetic history due to re-writing on the magnetic tape can also be considered as a topic for further investigation. The possibility of further reduction in the error range needs to be analyzed. This requires much more sophisticated and precise components in the hardware setup. Also, the trials need to be carried out in a completely controlled environment since a minute change in the environment like temperature differences can have a drastic impact on the magnetization process. Therefore, further investigation in error minimization using the suggested improvements can be an interesting research topic.

BIBLIOGRAPHY

- [AB12] AXEL BARTOS, Amin M.: MR Basics : An introduction into MR Sensor Applications. (2012). http://www.meas-spec.com/downloads/MR_Basics.pdf
- [A.M15] A.MEISENBERG, A.Bartos A.Voss: Measurement Specialities : Modern Scale Based Magneto Resistive Sensor Systems. (2015)
- [Boz93] BOZORTH, Richard M.: Ferromagnetism. In: *Ferromagnetism, by Richard M. Bozorth, pp. 992. ISBN 0-7803-1032-2. Wiley-VCH, August 1993.* 1 (1993)
- [CC99] COMSTOCK, R L. ; COMSTOCK, Lawrence R.: Introduction to magnetism and magnetic recording. (1999)
- [CG11] CULLITY, Bernard D. ; GRAHAM, Chad D.: *Introduction to magnetic materials.* John Wiley & Sons, 2011
- [Fin] *Finite Element Method Magnetics: Reference Manual. : Finite Element Method Magnetics: Reference Manual*, <http://www.femm.info/Archives/doc/manual42.pdf>
- [FLS13] FEYNMAN, Richard P. ; LEIGHTON, Robert B. ; SANDS, Matthew: *The Feynman Lectures on Physics, Desktop Edition Volume I.* Bd. 1. Basic Books, 2013
- [FW99] FEYNMAN, Richard P. ; WEINBERG, Steven: *Elementary particles and the laws of physics: The 1986 Dirac memorial lectures.* Cambridge University Press, 1999
- [HH89] HOROWITZ, Paul ; HILL, Winfield: *The art of electronics.* Cambridge Univ. Press, 1989
- [hig] PI (Physik Instrumente) GmbH & Co. KG. : *M-531 High-Precision Linear Translation Stage, Datasheet.* : PI (Physik Instrumente) GmbH & Co. KG. : *M-531 High-Precision Linear Translation Stage, Datasheet*, http://www.physikinstrumente.com/download/PI_Datasheet_M-511--M-521--M-531_20150121.pdf
- [IDFCF96] IERUSALIMSCHY, Roberto ; DE FIGUEIREDO, Luiz H. ; CELES FILHO, Walde-mar: Lua-an extensible extension language. In: *Softw., Pract. Exper.* 26 (1996), Nr. 6, S. 635–652

- [kos] *MAXcomputer GmbH : KOSY3 Co-ordinate Systems, Datasheet.* : MAXcomputer GmbH : KOSY3 Co-ordinate Systems, Datasheet, <http://www.max-computer.de/x5e/kosy-overview.html>
- [lab] *National Instruments : LabVIEW System design Software, Manual.* : National Instruments : LabVIEW System design Software, Manual, <http://www.ni.com/manuals/>
- [lina] *Measurement Specialities : Linear Encoder - ED 34, Datasheet.* : Measurement Specialities : Linear Encoder - ED 34, Datasheet.
- [linb] *Renishaw GmbH : TONiC linear encoders, Datasheet.* : Renishaw GmbH : TONiC linear encoders, Datasheet, <http://resources.renishaw.com/en/details/data-sheet-tonic-encoder-system--57501>
- [Low72] LOWMAN, Charles E.: Magnetic Recording. (1972)
- [mag] *Bogen Electronic GmbH : Magnetic Scales, Datasheet.* : Bogen Electronic GmbH : Magnetic Scales, Datasheet, http://www.bogen-electronic.com/downloads/Datenblaetter/Technisches_Datenblatt_Magnetband.pdf
- [MAT10] MATLAB: *version 7.10.0 (R2010a).* Natick, Massachusetts : The MathWorks Inc., 2010
- [Mee86] MEE, C D.: *The physics of magnetic recording.* North-Holland Publishing Co., 1986
- [Mei] MEISENBERG, Armin: Measurement Specialities : Position Sensors - MLS Magnetic Length Sensors, Datasheet.
- [Mei15] MEISENBERG, Armin: Measurement Specialities : MLS5000 - Application Note. (2015)
- [mer] PI (*Physik Instrumente*) GmbH & Co. KG. : *C-863 Mercury Servo Controller, Datasheet.* : PI (*Physik Instrumente*) GmbH & Co. KG. : *C-863 Mercury Servo Controller, Datasheet*, http://www.physikinstrumente.com/download/PI_Datasheet_C-863_20150120.pdf
- [Moro01] MORRISH, Allan H.: The physical principles of magnetism. In: *The Physical Principles of Magnetism*, by Allan H. Morrish, pp. 696. ISBN 0-7803-6029-X. Wiley-VCH, January 2001. 1 (2001)

- [Nyco4] NYCE, David S.: *Linear position sensors: theory and application*. John Wiley & Sons, 2004
- [Pea67] PEAR, Charles B.: *Magnetic recording in science and industry*. Reinhold Publishing Corporation, 1967
- [pre] PI (Physik Instrumente) GmbH & Co. KG. : M-403 Precision Translation Stage, Datasheet. : PI (Physik Instrumente) GmbH & Co. KG. : M-403 Precision Translation Stage, Datasheet, http://www.physikinstrumente.com/download/PI_Datasheet_M-403_20150121.pdf
- [RMCo8] REITZ, John R. ; MILFORD, Frederick J. ; CHRISTY, Robert W.: *Foundations of electromagnetic theory*. Addison-Wesley Publishing Company, 2008
- [sol] Dassault Systems SOLIDWORKS Corp. : Solidworks 3D design, Datasheets. : Dassault Systems SOLIDWORKS Corp. : Solidworks 3D design, Datasheets, https://www.solidworks.com/sw/docs/Student_WB_2011_ENG.pdf
- [SR12] SYSEL, Petr ; RAJMIC, Pavel: Goertzel algorithm generalized to non-integer multiples of fundamental frequency. In: *EURASIP Journal on Advances in Signal Processing* 2012 (2012), Nr. 1, S. 1–8
- [st] ST Microelectronics : STM32F3DISCOVERY, Datasheet.
- [Ste04] STEINER, Marcus: *Micromagnetism and Electrical Resistance of Ferromagnetic Electrodes for Spin Injection Devices*. Cuvillier Verlag, 2004
- [tro] Max Baermann GmbH : Tromaflex 928, Datasheet. : Max Baermann GmbH : Tromaflex 928, Datasheet, <http://www.max-baermann.de/uk-index-gmbh.htm>
- [Tumo01] TUMANSKI, Slawomir: *Thin film magnetoresistive sensors*. CRC Press, 2001
- [Wal96] WALKER, James S.: *Fast fourier transforms*. Bd. 24. CRC press, 1996
- [Whi85] WHITE, Robert M.: *Introduction to magnetic recording*. IEEE, 1985
- [WT99] WANG, Shan X. ; TARATORIN, Alex M.: *Magnetic Information Storage Technology: A Volume in the Electromagnetism Series*. Academic press, 1999